UNIVERSIDADE D
COIMBRA

Daniel Jorge Silva Bento

ORAL FILMS BASED ON LIPID NANOPARTICLES FOR DRUG ADMINISTRATION: A COMPUTATIONAL AND EXPERIMENTAL APPROACH

Dissertação de Mestrado em Química Medicinal,
orientada pelo Professor Doutor Alberto Canelas Pais
e pela Professora Doutora Carla Sofia Pinheiro Vitorino,
apresentada ao Departamento de Química da Faculdade de Ciências e Tecnologia
da Universidade de Coimbra

Setembro de 2018

Faculdade de Ciências e Tecnologia
da Universidade de Coimbra

Oral films based on lipid nanoparticles for drug administration: a computational and experimental approach

Daniel Jorge Silva Bento

Dissertação no âmbito do Mestrado em Química Medicinal, orientada pelo Professor Doutor Alberto Canelas Pais e pela Professora Doutora Carla Sofia Pinheiro Vitorino e apresentada ao Departamento de Química da Faculdade de Ciências Tecnologia da Universidade de Coimbra.

Setembro 2018

UNIVERSIDADE D
COIMBRA

Agradecimentos

A Coimbra, cidade do conhecimento e dos estudantes. Desde cedo apaixonado por esta cidade e por tudo o que oferecia, rapidamente me apercebi que seria o local indicado para crescer enquanto pessoa e para ser a rampa de lançamento para o futuro. Foi a partir de 2013 que começou a ser escrito um dos capítulos mais ambicionados a nível pessoal, a formação académica. Passados 5 anos, e em fase de conclusão deste projeto científico, não posso deixar de agradecer a quem contribuiu para que tudo isto fosse possível.

O meu sincero reconhecimento e agradecimento aos meus orientadores. Ao Professor Doutor Alberto Canelas Pais, gostava de agradecer todos os ensinamentos, atenção ao detalhe e ao rigor, todo o apoio, motivação, confiança e disponibilidade transmitida neste último ano. À Professora Doutora Carla Vitorino pela valiosa orientação na Faculdade de Farmácia da Universidade de Coimbra (FFUC), por conectar-me à prática laboratorial e por toda a ajuda e conselhos ao longo deste trabalho.

Um agradecimento especial à Doutora Tânia Firmino por todo o apoio e imensa disponibilidade para ajudar em qualquer tipo de tarefa, pela constante preocupação e por todos os conselhos. Agradecer também toda a ajuda na programação em R, sem dúvida essencial.

A todos os elementos e funcionários do Laboratório de Tecnologia Farmacêutica da FFUC agradeço o fantástico acolhimento e auxílio prestado. Um agradecimento muito especial à Maria Mendes, principalmente por toda a paciência em explicar cada detalhe da parte experimental, por vezes, repetidamente. Pelo acompanhamento constante no laboratório e por toda a sua disponibilidade empregue neste trabalho.

Aos da terrinha, nomeadamente à Mocidade e amigos, essencialmente agradeço pela preocupação demonstrada e pela motivação transmitida nestes últimos tempos. Por todos os momentos de descontração e companheirismo. Aos de Coimbra, que fizeram a passagem por esta cidade tão bela, com excelentes memórias para recordar, desde o primeiro dia até hoje. Pelo apoio e preocupação constante, pelos momentos de descompressão, desabafos constantes quando as coisas não corriam tão bem e pela partilha de bons momentos.

À Rita que sempre estendeu a mão para me ajudar e por arranjar sempre alguma paciência extra para me ouvir e, ainda no fim, transmitir uma palavra amiga. Pela

demonstração da pessoa forte que é e por sempre me incentivar a ser uma pessoa capaz de atingir os objetivos.

Por último deixar uma palavra de apreço aos meus pais e a todos os meus familiares que me acompanharam ao longo de toda esta etapa. Tenho plena consciência que a ajuda dos meus pais, todo o apoio e ânimo transmitidos, tornaram todas as adversidades numa mera formalidade. À minha irmã Vera pela confiança e por todo o incentivo desde o primeiro dia da minha vida académica, a sua preocupação constante foi notável, tornando-se, também, numa inspiração.

A todos agradeço, essencialmente, a compreensão e o apoio. Espero que tenham um orgulho tão grande como o esforço e o prazer que tive em desenvolver este projeto que agora também vos dedico. Obrigado!

Table of contents

Resumo

Este trabalho tem como foco o desenvolvimento de uma plataforma computacional para tratar e analisar de uma forma generalizada perfis de dissolução. Diversos programas concebidos em R exploram modelos matemáticos, análises de similaridade, bem como o tempo de latência. Na contrapartida experimental, numa abordagem farmacêutica, foi estudado o comportamento *in vitro* de filmes orais resultantes da mistura de hidrogéis com nanopartículas lipídicas co-encapsuladas com fármacos. Posteriormente, a abordagem computacional desenvolvida foi utilizada para analisar os perfis de dissolução obtidos experimentalmente.

Os perfis de dissolução resultantes foram examinados através de métodos independentes e métodos dependentes do modelo. Da primeira abordagem, um programa integrado, seguindo diretrizes específicas, foi desenvolvido. O cálculo dos fatores de ajuste, tempo de dissolução médio e a Distância de Mahalanobis são apresentados de uma forma simplista, bem como a visualização gráfica dos dados, facilitando a interpretação ao utilizador. Nas abordagens dependentes do modelo, diversas ferramentas foram desenvolvidas atendendo a diversas necessidades. Os índices correspondentes ao critério de informação de Akaike e ao coeficiente de determinação ajustado foram utilizados para definir e verificar a qualidade do melhor modelo de ajuste aos pontos de dissolução. O estudo do tempo de latência também foi incorporado na abordagem computacional, identificando e quantificando a sua presença.

A nanotecnologia foi explorada usando nanopartículas lipídicas carregadas com fármacos, caracterizados por diferentes propriedades químicas, para a produção de filmes orais. A proposta é aumentar a biodisponibilidade dos fármacos em estudo, que possuem baixa solubilidade aquosa, bem como ultrapassar outras limitações associadas aos comprimidos convencionais. Os filmes orais são caracterizados por promoverem uma maior aceitabilidade para o paciente, ostentando uma forma apelativa para a administração de fármacos com forte incidência na população geriátrica e pediátrica. Foram produzidas nanopartículas lipídicas co-encapsuladas com olanzapina e sinvastatina que apresentaram tamanho de partícula, índice de polidispersão, potencial zeta, eficiência de encapsulação e capacidade de carga, de acordo com os valores pretendidos. Foram testados hidrogéis com diferentes graus de hidroxipropilmetilcelulose

que após misturados com as nanopartículas lipídicas, resultaram numa dispersão homogénea promissora para a produção de filmes orais. De uma forma geral, todos os filmes apresentaram propriedades adesivas atrativas. A adição de plastificante, PEG 400, na preparação dos hidrogéis combinou uma melhor aparência dos filmes orais, mostrando, também, aumentar a flexibilidade e a facilidade de remoção do filme do suporte.

Nos testes *in vitro* com saliva simulada não foram detetadas diferenças significativas entre os filmes orais, pelo que, não mais de 10% de cada fármaco foi dissolvido durante este ensaio. Por outro lado, o comportamento de cada fármaco foi distinto quando as condições do trato gastrointestinal foram mimetizadas. Para a olanzapina, toda a quantidade de fármaco foi libertada nas duas primeiras horas, não existindo qualquer efeito no controlo da libertação. Para os perfis de dissolução da sinvastatina identificaram-se diferenças entre o grau do polímero utilizado. Deste modo, verificou-se uma maior quantidade de sinvastatina libertada nos filmes orais produzidos com o polímero de menor peso molecular. A inclusão de PEG 400 mostrou, também, aumentar a exposição dos fármacos na libertação.

A abordagem experimental desenvolvida demonstrou ser uma ferramenta importante para caracterizar e analisar os perfis de dissolução obtidos com os filmes orais. Conclui-se assim, que os métodos independentes e dependentes do modelo produziram facilmente resultados coerentes e objetivos para a racionalização da análise dos sistemas em estudo.

Palavras chave: linguagem R, métodos independentes e dependentes do modelo, nanopartículas lipídicas, co-encapsulação, olanzapina, sinvastatina, filmes orais.

Abstract

This work focuses on the development of a computational platform able to provide a comprehensive analysis of dissolution profiles, exploring mathematical models, similarity analysis, and lag time using R programming. Also, a pharmaceutical approach conducting the study of the *in vitro* behavior of oral films, based on hydrogels and lipid nanoparticles co-encapsulating drugs with distinct physicochemical characteristics was performed. Subsequently, the computational approach developed was used to analyse the dissolution profiles experimentally obtained.

Two general approaches for comparing dissolution profiles were examined: model independent and model dependent approaches. In the former approach, an integrated program following regulatory specifications was developed. Values of fit factors (f_1 and f_2), mean dissolution times (MDT), Mahalanobis Distance (D_M) and the graphical data visualization are presented, providing an easy interpretation for the user. For model dependent approaches, several tools were developed taking into account different situations. Akaike information criterion (AIC) and adjusted coefficient of determination $R^2_{adjusted}$, are used to define the model that better fits the dissolution points. An approach to identify the presence and quantify the lag time was also explored.

Nanotechnology was explored using loaded lipid nanoparticles (LLN) co-encapsulating drugs for the production of oral films. The drugs possess a low aqueous solubility, and the purpose is increasing the bioavailability, and overcoming other limitations associated to conventional dosage forms. Oral films promote patient compliance, and provide a very appealing system for the administration of drugs in the geriatric and paediatric populations. Specifically, LLN for co-delivery of olanzapine (OL) and simvastatin (SV) were developed and characterized, showing appropriate values of particle size, zeta potential, encapsulation efficiency and drug loading. Hydrogels containing different hydroxypropyl methylcellulose (HPMC) grades were tested after mixing with LLN, to provide a promising method to obtain a homogeneous formulation for oral films. In general, all films presented attractive adhesive properties. The addition of plasticizer, PEG 400, on the hydrogels showed an improvement on the final appearance of the oral films, such as an enhanced flexibility and an easier detachment from the support.

In the *in vitro* tests with simulated saliva, no substantial differences were detected between the oral films, in which no more than 10% of each drug was released during the test. Conversely, the behavior of each drug in situations mimicking the human gastrointestinal tract conditions was distinct. For OL, the whole amount was released within 2 hours, thus no significant control was detected. For SV, the impact of the polymer grade on the release was apparent, with a larger amount of drug being released when the lower molecular weight HPMC was employed. Also, the inclusion of PEG 400 increased the extent of drug release.

The computational approach developed demonstrates to be an important tool to characterize the dissolution profiles obtained with the oral films. It is also concluded that model independent and several model dependent approaches yielded numerical results that can serve as objective and quantitative metrics for comparing the dissolution profiles.

Key-words: R language, independent and model dependent methods, lipid nanoparticles, co-encapsulation, olanzapine, simvastatin, oral films.

Motivation and aims

Exploring the *in vivo* behavior of an oral drug product by performing *in vitro* dissolution studies has gained particular interest in the last decade. Current compendial dissolution methods are not always reliable to predict the *in vivo* performance, especially in case of Biopharmaceutics Classification System (BCS) class 2/4 drugs, resulting from their low aqueous solubility. In addition, the suitability of dissolution specifications employed to support marketing authorisation procedures has been subject of debate, as demonstrated by the recent reflection paper on the dissolution specification for generic solid oral immediate release products with systemic action, released by the European Medicines Agency. Similarly, there is an increasing interest in the application of computational frameworks to provide a comprehensive understanding of the dissolution behavior. Developing an integrated and predictive dissolution test computational platform able to provide reliable, cost-effective and less time-consuming interpretation, as long as the predictive power of the test is thus highly desirable.

Motivated by this issue, this work envisioned the development of a computational toolbox to provide support in the statistical analysis of dissolution profiles, taking into account the requirements released by the regulatory entities.

In this context, the objectives of the present dissertation are:

• To develop an integrative computational approach able to provide a comprehensive analysis of dissolution profiles, in terms of modelling, similarity analysis, lag time using R environment as template;

• To qualify the developed tools using data already reported in the literature;

• To develop and optimize innovative oral film based on co-encapsulating lipid nanoparticles;

• To characterize the developed formulations in terms of particle size, zeta potential, encapsulation efficiency and drug loading, mechanical properties and *in vitro* dissolution;

• To rationalize the dissolution behavior using the developed computational tools, so as to ensure the validation of the system.

Structure of the Dissertation

In what follows, the sequence and contents of the different chapters in this dissertation are presented. Chapters 1 and 2 possess an essentially introductory nature, while the remaining describe, analyze and extract conclusions from the work performed.

In the first Chapter, a general introduction elucidates on the purpose of *in vitro* dissolution tests, and presents the approaches used to evaluate dissolution data, resorting to both model independents and dependent methods. Chapter 2 reports the scripts developed using the R language, and also includes several approaches that are suggested and discussed. This Chapter is complemented by Appendices I and II, in which a small tutorial on R code, useful for the construction of scripts, is also provided.

In Chapter 3, a literature survey on lipid nanoparticles for drug administration and the advantages of oral films is presented. Several topics such as the evolution of lipid nanoparticles, respective production methods, therapeutic applications, and the relevance and use of oral films are approached. It also discusses the strategy used in this work. Chapter 4 describes all materials and methods employed for the experimental tasks.

The development of the pharmaceutical form is reported in Chapter 5, from the initial steps concerning lipid nanoparticles production and loading, to the assessment of the oral films. This Chapter also displays the respective *in vitro* release studies for the oral films, and analyzes the impact of the different hydroxypropyl methylcellulose (HPMC) grades and plasticizer on the respective properties. The relevant dissolution data are analyzed resorting to the developed R scripts.

Chapter 6 summarizes the work contained in this dissertation, gathering the more relevant conclusions.

Abbreviations

AIC	Akaike information criterion
API	Active pharmaceutical ingredient
CR	Confidence region
CV	Coefficient of variation
DL	Drug loading
DLS	Dynamic light scattering
D_M	Mahalanobis Distance
EE	Entrapment efficiency
EMA	European Medicines Agency
f_1	Difference factor
f_2	Similarity factor
FDA	Food and Drug Administration
GIT	Gastrointestinal tract
HDL	High-density lipoproteins
HPH	High-pressure homogenization
HPLC	High Performance Liquid Chromatography
HPMC	Hydroxypropyl methylcellulose
IDE	Integrated development environment
IR	Immediate release
LDL	Low-density lipoproteins
LLN	Loaded lipid nanoparticles
MDT	Mean dissolution time
NLC	Nanostructured lipid carriers
OL	Olanzapine
OTF	Oral thin film
PDMS	Polydimethylsiloxane
PEG 400	Polyethylene glycol 400
PI	Polydispersity index
PS	Particle size
$R^2_{adjusted}$	Adjusted coefficient of determination
RSD	Relative standard deviation
SD	Standard deviation
SDC	Self-diffusion coefficient
SLN	Solid lipid nanoparticles
SR	Sustained release
SV	Simvastatin
SVA	Simvastatin acid
USP	United States Pharmacopeia
ZP	Zeta potential

Chapter 1

General Introduction

Dissolution tests are used for many purposes in the pharmaceutical industry being an important element in the development and quality control of pharmaceutical drugs. The dissolution data are obtained by measuring the amount of active substance released in the dissolution medium at different time points. The *in vitro* dissolution test requires, generally, a reference and a test batch have to be compared with each other.

To evaluate these data several methods, independent or dependents of a model, have been described.

1.1. Dissolution

The importance of studying the phenomenon of dissolution and relating to physiological bioavailability was relatively recently uncovered in the scientific community. Dissolution is a process in which a solute (solid, liquid or gas) is dissolved in a solvent to create a solution. It refers to the action and effect of separating what was previously bonded and subsequently homogenously mixing all the molecules of a substance into a liquid. Thermodynamically, this process is described as solubilization, and the existence of a concentration gradient between the particle surface and the solution, act as the driving force of the dissolution[1].

In 1897 Noyes and Whitney[2] have studied the effect of the concentration on the rate at which a solid substance dissolves in its own solution. Benzoic acid and lead chloride, two substances with different chemical nature and physical properties were used to reach an equation that describe the dissolution rate,

$$\frac{dC}{dt} = k(C_S - C) \tag{1.1}$$

According to this equation the dissolution rate is proportional to the difference between the instantaneous concentration, C at time t and the saturation solubility, C_S, and k is a constant. The mechanism of dissolution results in the formation of a thin diffusion layer around the solid surface through which molecules diffuse into the solvent phase.

Other work have demonstrated that parameters such as the amount of exposed surface, stirring speed, temperature, and apparatus also impact on the dissolution rate. Another equation considers

$$k = k_1 S \tag{1.2}$$

producing,

$$\frac{dC}{dt} = k_1 S(C_S - C) \tag{1.3}$$

where S is the surface area. In an attempt to better correlate these constants, the Nernst-Brunner equation was defined[3]

$$\frac{dC}{dt} = \frac{DS}{Vh}(C_S - C) \tag{1.4}$$

being D the diffusion coefficient, h the thickness of the diffusion layer and V the volume of the dissolution medium. This equation allows predicting the diffusion coefficient, that in turn can be related to the viscosity of the solvent. Therefore, with an increase in the viscosity of the solvent, the dissolution rate decreases. Also, the dissolution rate is higher in formulations containing smaller particle sizes, as the surface area increases with decreasing particle size. Often, the type of stirring in the dissolution process increase the diffusion gradient, by the rapid removal of molecules on the surface of the pharmaceutical form, thus increasing the dissolution rate. It is also possible to identify if another additional parameter for example pH, affect the amount of drug released, and depending on the characteristics of solvent and solute, the way this change could increase or decrease C_S[4].

The physicochemical properties of the drug have a strong impact, as assessed by the Noyes-Whitney equation[5], since the solubility and dissolution rate can be affected by the particle size, the surface properties and by the surrounding medium[1].

Other mathematic expressions can be derived by the above mentioned approaches, but these involved a limiting step for the dissolution process, corresponding to the diffusion of the molecules through the solvent around the solid surface[3].

More recently, *in vitro* dissolution tests have been used in the pharmaceutical area. Previous studies, were only based in disintegration tests, ignoring thus the dissolution process. More realistic conditions, including the gastric fluids and simulated artificial stomach (with the respective pH value) were introduced to mimic the behavior of pharmaceutical forms in the human body.

Dissolution tests are a measure in the quality control of the production of pharmaceutical products following good manufacturing practice. They are a simple, inexpensive and useful indicator in the early stages of drug development and can anticipate future developments[6]. Specifically, data from the dissolution tests are often used to study *in vitro-in vivo* correlations, to reduce the development time of a new pharmaceutical form and optimize the formulation. These correlations, apart from being an economically feasible method, have other advantages, such as the optimization of dosage in humans with fewer tests, and the study of bioequivalence, being also recommended by the regulatory authorities[7].

Additionally, dissolution tests provide the respective profile for each pharmaceutical form, allowing addressing different formulations, drugs and parameters. Statistical analysis can be performed to address differences between formulations or variations promoted by different imposed conditions. Several pharmacokinetic parameters can be extracted from the dissolution profiles allowing the respective comparison and analysis. The area under the concentration time curve (AUC); the maximum plasma concentration time curve (C_{max}), the time corresponding to the maximum concentration (t_{max}); or the time corresponding to 50% of drug dissolved ($t_{1/2}$) are some important parameters to be explored in the pharmaceutical field.

1.1.1. *In vitro* dissolution apparatus

In the next section, a brief overview of some devices used in drug dissolution will be presented. The different apparatus and techniques are regulated primarily by the United States Pharmacopoeia (USP), in which each dissolution test is identified by the abbreviation USP followed by a number. It is necessary to understand that each apparatus has a specific function, and for each one it is necessary to include a medium, mimicking *in vivo* conditions.

The basic dissolution test (USP General Chapter <711> Dissolution[8]) describes the apparatus, the dissolution procedure, and the product specifications. The focus is on USP apparatus 1 (baskets) and 2 (paddles) because these systems provide the majority of the dissolution tests in the pharmaceutical industry. These two devices are used preferentially in tablets, capsules, suspensions, modified drug products, suspensions and for evaluation of immediate release (IR) and modified release (MR) oral formulations[9]. The other apparatus also mentioned by the USP were designed for the assessment of transdermal products.

1.1.1.1. USP Apparatus 1

The apparatus consists of a metal basket coupled to a rotating metal shaft and placed inside a glass beaker or other transparent inert material (Figure 1.1 (A)). The vessel is partially immersed in a water bath at constant temperature, usually 37°C, to keep the bath fluid in a constant motion. It is important to note that there is no interference with the instrument, and the same conditions are maintained throughout the test and without movements that can be affect the rotation of basket. The baskets can have various sizes (10 up to 100 or 150 Mesh), are made of stainless steel, being the standard size of 40 Mesh (40 openings per linear inch). The distance between the bottom of the vessel and the bottom of the basket must be maintained at 25 ± 2 mm during the test. They must rotate freely under a specific rotation precisely in the centre of the vessel so as to avoid errors related to the oscillation. Other errors associated with this method including blocking of the holes in the basket due to certain excipients, rapid release or the existence of air bubbles. It is also important to cover the top of the vessel to avoid evaporation of the medium and collect the sample always in the same point.

1.1.1.2. USP Apparatus 2

For this test the conditions are similar to those of the previous test, except that instead of the rotating baskets a paddle is used as the stirring element (Figure 1.2 (B)). Both the paddle and the shaft must be a single part and must remain in the same position throughout the test without the risk of significant oscillations. The distance of 25 ± 2 mm between the bottom of the paddle and the inside bottom of the vessel should be maintained throughout the test.

1.1.1.3. Sink conditions

Sink conditions are a necessary requirement in *in vitro* assays to quantify the drug when it is released and dissolved in a dissolution medium. When a dissolution test is performed, it is required to use a volume of dissolution medium sufficient for dissolving the entire amount of drug, and ensure that the presence of an already dissolved drug does not affect the efficiency of the remainder to dissolve. That is, it must be ensured the necessary conditions for the entire drug to dissolve, avoiding the respective precipitation in the volume of the dissolution medium.

There are some limitations in some classes of drugs, for example in compounds with low aqueous solubility. In these cases, maintaining sink conditions can be

problematic. Apart from adjusting the dissolution medium volume, several solubility modifiers can be used, such as surfactants, inorganic salts and organic co-solvents[10].

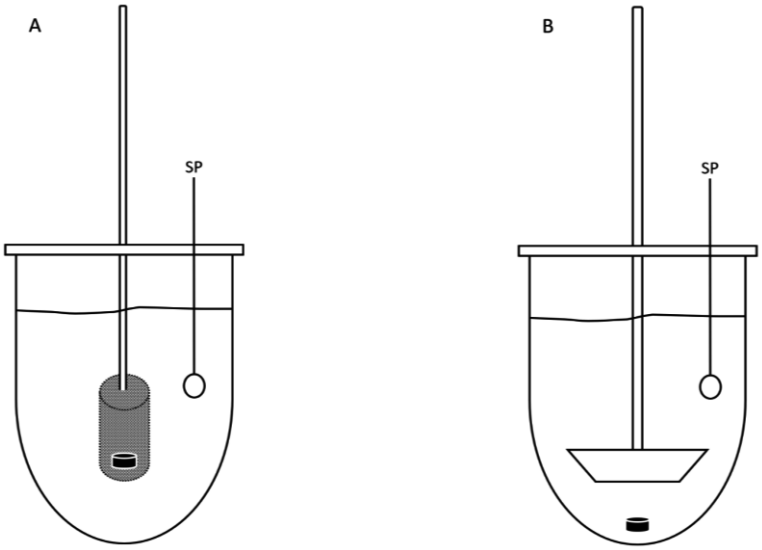

Figure 1.1 – Simplified scheme of USP apparatus 1 (A) with dosage form inside the basket, and USP apparatus 2 (B) where dosage form is on the bottom of vessel. SP is the sampling point. Schematic representation adapted from USP General Chapter <711> Dissolution[8].

1.1.2. Dissolution classification systems

A scheme that correlates *in vitro* drug dissolution and *in vivo* bioavailability has been proposed and defined, classifying drug substances based on their aqueous solubility and intestinal permeability[11]. A primary analysis is important for estimating drug absorption *in vivo* to illustrate the importance of solubility and permeability in drug absorption. The Biopharmaceutical Classification System (BCS) defines the classes of drugs as follow:

Class I: High Solubility – High Permeability

Class II: Low Solubility – High Permeability

Class III: High Solubility – Low Permeability

Class IV: Low Solubility – Low Permeability

From this classification, it is possible to establish correlations between analysis of dissolution profile and *in vivo* process behavior. This procedure should be based essentially on the physiological and physicochemical properties that control the absorption of the drug. This analysis indicates the conditions that can be expected in *in vitro-in vivo* correlation, to evaluate, for example low release immediate permeability drugs[12].

1.1.2.1. Immediate release

Most conventional oral drug products are formulated to release the active pharmaceutical ingredient (API) immediately following administration, featuring an immediate release (IR). In the production of these conventional medicaments no attempt is made to modify the dissolution rate of the drug.

An immediate release is considered in a drug product when at least 85% of the amount of drug present is dissolved within the first 30 minutes. When for an IR product, 85% or more is dissolved in the first 15 minutes, it is classified as very rapidly dissolving[13]. For bioequivalence studies in pharmaceutical forms with an immediate release dissolution profile, the new pharmaceutical form is automatically considered equivalent, if it complies with the above condition.

1.1.2.2. Modified-release

The alteration of the release pattern from the conventional dosage formulation, is performed for improving the therapeutic effect the patient compliance. The term "modified release" is used to describe products which alter various pharmacokinetic properties, especially the time it takes to reach the maximum concentration and dissolution rate.

Several types of modified-release oral drug products are recognized[14]. These are the

- Extended-release drug products – allows the reduction of the dosing frequency, the release of the drug is prolonged over time and having a prolonged action which normally releases the API at periods every 8 hours.
- Delayed-release drug products – an initial release does not occur, so there is an initial time in which the drug release is delayed for a defined time. These products are advantageous in that they can be coated to prevent and protect, for example, the release into the stomach.
- Targeted-release drug products – release the drug at the intended site of action or directs it to a location near the action site.

With the purpose of simplification, hereafter modified-release will be identified as sustained release (SR) and defined by altering the dissolution rate, releasing the same amount of drug, but in a longer period of time assuming the minimum of side effects when transposed to *in vivo* conditions.

1.1.2.3. Burst release

Burst release occurs primarily in controlled release drugs, immediately thereupon placement of a formulation in the dissolution medium, and corresponds to a large amount of drug being released before a stable profile is attained. This release occurs in a short period of time and is characterized by an unpredictable behavior, with the consequence of reducing the lifetime of the drug[15,16]. The burst release can be understood in two ways: as a negative consequence for controlled release or beneficial for pharmaceutical forms that needs to have high initial rates of delivery (immediate release)[16]. This phenomenon is little studied and mostly ignored in mathematical models for the description of release profiles.

Burst release can be a consequence of the presence of reservoir systems, injectable hydrogel systems, matrix systems, synthesis/manufacture conditions, effect of drug properties, percolation limited diffusion, triggered burst[16]. In this way the matrix is no longer in a heterogeneous state, whereby a surface layer of the drug matrix is rapidly dissolved. Another reason for this phenomenon may be the existence of pores or fracture in the matrix.

Several studies have been developed to avoid this rapid initial release. For example, one of the solutions for avoiding the burst release is the microencapsulation of nanoparticles[17] with the preparation temperature become an important factor[18].

1.2. Analysis of the dissolution profile

The procedure for the evaluation and comparison of *in vitro* dissolution profiles can be classified into two groups: independent and dependent of the model.

1.2.1. Independent approaches

Independent approaches allow comparing dissolution profiles without using complex mathematical tools and relies on methods that are independent of models.

These methods take into account each dissolution time point individually, without describing the dissolution curve. For calculations, data of the original dissolution are used and compared, yielding a single value, which defines the similarity between the profiles. This can be evaluated by determining several parameters, including the fit factors, mean dissolution time (MDT) and the Mahalanobis Distance (D_M).

1.2.1.1. Fit factors

Fit factors provide a direct measure of difference between the percentage of drug dissolved per unit of time between test and reference. A single value is produced that is exactly the same regardless of whether the reference point curve is below or above the test[19]. However, the value is associated to the lack of sensitivity to variations between different batches of production, and to dissolutions above 85%, interfering in the analysis of the similarity of the profiles[20]. On the other hand, fit factors are commonly used for bioequivalence studies, since they provide a simple approach.

Fit factors are denoted by f_1 (difference factor) and f_2 (similarity factor) and are defined by[21]

$$f_1 = \left\{\frac{\sum_{t=1}^{n}|R_t - T_t|}{\sum_{t=1}^{n} R_t}\right\} \times 100 \tag{1.5}$$

$$f_2 = 50 \times \log\left[\frac{100}{\sqrt{1 + \frac{\sum_{t=1}^{n}[R_t - T_t]^2}{n}}}\right] \tag{1.6}$$

where n is the sample size, and R_t and T_t are the percent dissolved for the reference and test products at each time point *t*.

The factor f_1 is proportional to the mean difference between the two profiles and is a measure of the relative error in relation to the two curves, while f_2 is inversely proportional to the mean quadratic difference between the two profiles. To ensure uniformity and equivalence between the profiles it is necessary that the values of f_1 do not exceed 15 (0-15) and that the values of f_2 are larger than 50 (50-100).

In an ideal situation, the expected f_2 value would be 100 or very close. An average difference of 10% at any time point in the samples is the acceptable value for analysis[20]. Assuming this value,

$$f_{2,10} = 50 \times log\left[\frac{100}{\sqrt{1 + \frac{\sum_{t=1}^{n}[10]^2}{n}}}\right] \tag{1.7}$$

and thus, equivalence between reference and test formulation is assumed when f_2 is larger than 50.

According to the bioequivalence of EMA[22] and FDA[23] to compare two drugs, it is required that assays are performed under certain conditions. Specifically, these guidelines

require that at least twelve individual values must be produced for each formulation, with at least three time points (excluding zero) and the samples have to be collected at the same time in both formulations. To proceed with the calculation, the relative standard deviation or coefficient of variation must be less than 20% for the first point, and less than 10% for the remaining points. Finally, not more than an average dissolution value higher than 85% can be used for any of the formulations.

1.2.1.2. Mean dissolution time

The mean dissolution time (MDT) is defined as the arithmetic mean value of any dissolution profile[24]. This dissolution ratio test considers the area under the curve and the mean times between each dissolution following the trapezoidal rule[25]. The mean dissolution time can be calculated by

$$MDT = \frac{\sum_i^n t_i \, \Delta M}{\sum_i^n \Delta M} \tag{1.8}$$

where n represents the number of time points, t_i is the time at the midpoint between i and $i-1$, and ΔM is the amount of drug that has been released in that period.

The variance of the dissolution times (VT) can also be calculated using

$$VT = \frac{\sum_i^n (t_{med} - MDT)^2 \, \Delta M}{\sum_i^n \Delta M} \tag{1.9}$$

as well as the relative dispersion of dissolution times (RD)[26]

$$RD = \frac{VT}{MDT^2} \tag{1.10}$$

1.2.1.3. Mahalanobis Distance

The Mahalanobis Distance (D_M) is one of the most widely used distance in chemometrics. D_M has been used for comparing different data sets, measuring standard deviation, evaluate similarity or identify outliers, whether a particular method follow the same control conditions or to assign a sample to a defined group.

This measure was proposed in 1936 by Mahalanobis for establishing an equivalence between two objects[27].

By definition, D_M takes into account the correlation of the data, since it encompasses the inverse of the variance-covariance matrix and the difference between the vectors of the two samples. A mathematical definition can be given by

$$D_M = \sqrt{(R_t - T_t)^T S_{pooled}^{-1} (R_t - T_t)} \quad (1.11)$$

where $S_{pooled} = (S_R + S_T)/2$ is the sample variance-covariance matrix pooled across both batches, reference (S_R) and test (S_T). R_t is the sample mean dissolution of the reference and T_t the dissolution values for the test. The exponent T denotes the transposed matrix of the resulting vector.

The calculation of D_M focuses on measuring the difference between groups and their subsequent interpretation[28]. Tsong et al.[20,29–32] has described the use of D_M to establish the similarity between dissolution profiles of drugs, and to identify changes that modify the quality of the drug.

To make a statistical comparison between two datasets of dissolution profiles, it is necessary to comply with some principles. Firstly, it is necessary to establish a well-defined similarity limit, resulting in a tolerable upper limit of difference, and a minimum limit resulting in an acceptable range, to assume similarity between the profiles. Other aspects stem from common sense. There should not exist a significant disparity between the profiles, that is, data cannot vary significantly to be comparable. Data must be obtained under the same conditions, time points and number of tests for each dissolution.

Dissolution data are obtained at various times, and each time point can be considered a variable, in which the dissolution value increases over time. This results in a set of variables that are correlated.

The confidence region (CR) is used to describe the variation of D_M estimates. Conclusions about similarity are extracted by the appropriate comparison of the 90% confidence limits, which can be obtained from the multivariate confidence region of the expected values for the reference and test vectors.

The region of confidence for the differences, y, must satisfy

$$RC = K\big(y - (T_t - R_t)\big)^T S_{pooled}^{-1}((y - (T_t - R_t)) \leq F_{P,2n-P-1,.90} \quad (1.12)$$

where $K = [(n^2)/(2n)](2n - p - 1)/[(2n - 2) \times p]$ and $F_{P,2n-P-1,.90}$ is the 90th percentile of F-distribution with degrees of freedoms P and $2n - P - 1$, where $2n$ must be larger than $P + 1$.

The confidence interval of the D_M, for the lower limit (D_M^l) and for the upper limit (D_M^u), is calculated using the Lagrange multiplication method,

$$D_M^u = \max\left(\sqrt{y_1^{*T}\left(S_{pooled}\right)^{-1}y_1^*}, \sqrt{y_2^{*T}\left(S_{pooled}\right)^{-1}y_2^*}\right) \quad (1.13)$$

$$D_M^l = \min\left(\sqrt{y_1^{*T}\left(S_{pooled}\right)^{-1}y_1^*}, \sqrt{y_2^{*T}\left(S_{pooled}\right)^{-1}y_2^*}\right) \quad (1.14)$$

where,

$$y_1^* = \left(x_{test} - x_{ref}\right)\left\{1 + \sqrt{F_{p,2n-p-1,0.9}/\left[K\left(x_{test} - x_{ref}\right)^T\left(S_{pooled}\right)^{-1}\left(x_{test} - x_{ref}\right)\right]}\right\} \quad (1.15)$$

$$y_2^* = \left(x_{test} - x_{ref}\right)\left\{1 - \sqrt{F_{p,2n-p-1,0.9}/\left[K\left(x_{test} - x_{ref}\right)^T\left(S_{pooled}\right)^{-1}\left(x_{test} - x_{ref}\right)\right]}\right\} \quad (1.16)$$

The overall similarity should be assessed through a calculation in the 90% confidence interval, representing the tolerable difference between the two dissolution profiles,

$$\Delta D_M = \sqrt{(m)^T S_{pooled}^{-1}(m)} \quad (1.17)$$

where m takes the value of 10%. Recall that this value also represents a limit of f_2 higher than 50, assuming that this is the minimum value to consider that two dissolution profiles are similar[33].

Thus, dissolution profile similarity is concluded if

$$D_M^u < \Delta D_M \quad (1.18)$$

1.2.2. Model dependent approaches

1.2.2.1. Zero order

The zero order model is represented by a simple linear equation, and corresponds to a constant amount of drug being released along the time. It is expressed by

$$f(t) = c_1 t \quad (1.19)$$

where f is the drug fraction released at time t and c_1 is the apparent rate of dissolution or zero order release constant.

In this way, the profile corresponding to the fraction of drug released as a function of time will be linear. This ideally describes pharmaceutical forms where a constant amount of drug is dissolved over time. This model is generally associated with controlled release, as exemplified by some transdermal systems, osmotic or coated form systems[34].

1.2.2.2. First order

This kinetic model was initially proposed by Gibaldi and Felman (1967)[35] and later by Wagner (1969)[36]. The dosage forms following this dissolution profile, release the drug depending on the remaining content. The percentage of drug dissolved decreases over time. The first order model can be described by

$$f(t) = c_2(1 - \exp(-c_1 t)) \tag{1.20}$$

where, c_1 represents the dissolution constant, compatible with the type of release of the system.

For high values of c_1, the release is assumed as immediate, because the exponential has a value close to zero and the asymptotic value is quickly attained. The opposite occurs for lower c_1 values, representing a controlled release. A new parameter, c_2, is added to prevent errors related to the dosage or to incomplete dissolution (e.g. drug trapped in the matrix). These errors can be avoided or minimized when the total amount of drug dissolved is used as an additional parameter. Even when not indicating the true asymptotic value, it will improve the quality of the fitting, and will act as a normalization constant[37].

1.2.2.3. Higuchi

Higuchi has proposed a simple equation that is often used to describe the rate release of a drug in a matrix system[38–40]. Generally, this model is translated by the following equation that relates the so-called Higuchi dissolution constant (c_1) with time

$$f(t) = c_1\sqrt{t} \tag{1.21}$$

This assumes that the dissolution of a drug occurs by a process based on the Fick's law[38], dependent on the square root of time.

However, to describe dissolution by this model it is necessary to consider some parameters. To follow Fick's law, the diffusion of the drug must be constant, ideally occurring in one-dimensional arrays, to avoid the border effect. It also presents limitations in pharmaceutical systems, making it difficult to interpret in controlled release mechanisms[41].

This model can be applied with accuracy to matrices that are not swellable, in which a very soluble drug is incorporated[42].

1.2.2.4. Korsmeyer-Peppas

Korsmeyer and Peppas[43–47] developed a simple model based on a semi-empirical equation that relates the release of a drug with time

$$f(t) = c_1 t^{c_2} \quad (1.22)$$

where c_1 is a constant that incorporates structural and geometric characteristics and c_2 is the diffusional exponent, which, according to its value, characterizes the mechanism of dissolution of the drug. It establishes whether the drug follows diffusion according to Fick's law, or if it follows a non-Fickian model, which involves the transition from a semi-rigid state to a more flexible one (Case II transport). Table 1.1 describes the limits of the c_2 values for each type of drug geometry[47].

To determine the value of c_2, one should only perform the curve adjustment for the time points where the percentage released is less than 60%. In order to follow this model, which is similar to Higuchi's but possesses an additional parameter, it is also necessary that the release is unidimensional and that the width/thickness or length/thickness ratio is at least 10.

Table 1.1 – Diffusion exponent values and the corresponding solute release mechanism.

Diffusion exponent (c_2)			**Mechanism**
Film	**Cylinder**	**Sphere**	
0.50	0.45	0.43	Fickian diffusion
$0.50 < c_2 < 1$	$0.45 < c_2 < 0.89$	$0.43 < c_2 < 0.85$	Anomalous transport
1	0.89	0.85	Case-II transport

This model is generally useful for analysing the dissolution profiles of polymeric dosage forms when the mechanism is not fully known, or when more than one mechanism contribute.

1.2.2.5. Weibull

Weibull described the so-called Weibull distribution, using probabilities and statistics[48]. Currently, the range of applications of this distribution is very wide, covering practically all areas of science. In 1972 Langenbucher[49] adapted this model to describe a dissolution profile, and since it is frequently the best fit model, it is largely used today.

The Weibull equation can be defined by

$$f(t) = c_2\left(1 - exp\left(-\frac{t}{c_1}\right)^{c_3}\right) \tag{1.23}$$

In this equation, c_2 remains an additional normalization parameter (see above, first order function) and c_1 is the scaling parameter, which is related to the time dependence. c_3 represents the shape parameter, which defines the curvature of the profile. For low values of c_3, the curve will grow fast (almost linearly) in the beginning, attaining shortly the exponential limit. For high values of c_3 assume an S-shape with the upward curvature. For intermediate values the curve is an exponential (see Figure 1.2 for an illustration).

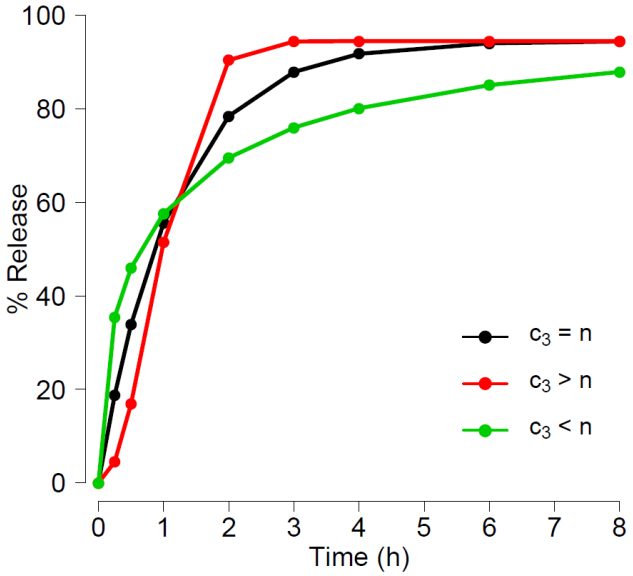

Figure 1.2 – Dissolution profile $f(t)$ for the Weibull model with a fixed value c_1 and variations in c_3. With $c_3 = n$, a reference number value. When c_3 is lower than n occurs a rapid initial growth, if c_3 is larger than n assume an S-shape form

For a linear relation, the equation can also be transformed into

$$log\left[-\ln\left(1 - \frac{f(t)}{c_2}\right)\right] = c_3 \log t - log\ c_1 \tag{1.24}$$

In this equation, the shape parameter (c_3) is easily obtained through the slope. For the scale parameter, this is estimated by the ordinate value $1/c_3$, for $t = 1$. It is common to resort to the dissolution time (T_d), since c_1 can be substituted in the equation $c_1 = (T_d)_{c_3}$. The value of T_d is obtained from the graph in which the time corresponds to $-\ln\left(1 - \frac{f(1)}{c_2}\right) = 1$, and $f(1) = 0.632$. This value represents the time interval required to dissolve 63.2% of the drug[49].

1.2.2.6. Fitting process and evaluation

The models described above provide useful approxes for the interpretation of the values obtained in the dissolution tests, but the respective usefulness depends on the actual profile. For selecting which equation provides the best fitting, two indices are commonly used.

Note that, when the number of parameters is the same, in a linear fit, one can use the coefficient of determination, R^2. Since these are non-linear fitting models with different number of parameters, an alternative is to use the adjusted coefficient of determination

$$R^2_{adjusted} = 1 - \frac{(n-1)}{(n-p)}(1 - R^2) \tag{1.25}$$

where n is the number of sampling points and p represents the number of parameters in the model. The advantage of this index over the simple calculation of R^2 is that it is also useful when the number of parameters is not the same in two (or more) models being compared. A higher value of $R^2_{adjusted}$ indicates the best model.

It is expected that a better fit is obtained when the number of parameters increases, although, in general, overfitting situations should be avoided. In the same context, another widely used index is Akaike's information criterion (AIC)

$$AIC = n\ln(RSS) + 2p \tag{1.26}$$

where, n is the number of sampling points, RSS is the residual of squares of fitted model and p the number of parameters. The model with the smallest AIC value provides the best fit for the data set[50].

1.3. References

(1) Misra, S. K.; Dybowska, A.; Berhanu, D.; Luoma, S. N.; Valsami-Jones, E. The Complexity of Nanoparticle Dissolution and Its Importance in Nanotoxicological Studies. *Sci. Total Environ.* **2012**, *438*, 225–232.

(2) Noyes, A. A.; Whitney, W. R. The Rate of Solution of Solid Substances in Their Own Solutions. *J. Am. Chem. Soc.* **1897**, *19*, 930–934.

(3) Dokoumetzidis, A.; Macheras, P. A Century of Dissolution Research: From Noyes and Whitney to the Biopharmaceutics Classification System. *Int. J. Pharm.* **2006**, *321*, 1–11.

(4) Smith, B. T. *Remington Education: Physical Pharmacy*; **2015**.

(5) Mittal, B. *How to Develop Robust Solid Oral Dosage Forms from Conception to Post-Approval*; **2017**.

(6) Hanson, W. A. *Handbook of Dissolution Testing*; **1991**.

(7) Cardot, J. M.; Beyssac, E.; Alric, M. *In vitro–in vivo* Correlation: Importance of Dissolution in IVIVC. *Dissolution Technol.* **2007**, *14*, 15–19.

(8) USP General Chapter <711> Dissolution. The United States Pharmacopeial Convention. Rockville, MD, **2011**.

(9) Gray, V.; Kelly, G.; Xia, M.; Butler, C.; Thomas, S.; Mayock, S. The Science of USP 1 and 2 Dissolution: Present Challenges and Future Relevance. *Pharm. Res.* **2009**, *26*, 1289–1302.

(10) Phillips, D. J.; Pygall, S. R.; Cooper, V. B.; Mann, J. C. Overcoming Sink Limitations in Dissolution Testing: A Review of Traditional Methods and the Potential Utility of Biphasic Systems. *J. Pharm. Pharmacol.* **2012**, *64*, 1549–1559.

(11) Amidon, G. L.; Lennernäs, H.; Shah, V. P.; Crison, J. R. A Theoretical Basis for a Biopharmaceutic Drug Classification: The Correlation of *in vitro* Drug Product Dissolution and *in vivo* Bioavailability. *Pharm. Res. An Off. J. Am. Assoc. Pharm. Sci.* **1995**, *12*, 413–420.

(12) Dressman, J. B.; Amidon, G. L.; Reppas, C.; Shah, V. P. Dissolution Testing as a Prognostic Tool for Oral Drug Absorption: Immediate Release Dosage Forms. *Pharm. Res.* **1998**, *15*, 11–22.

(13) Guidance for Industry: Waiver of *in vivo* Bioavailability and Bioequivalence Studies for Immediate Release Solid Oral Dosage Forms Based on a Biopharmaceutics Classification System. FDA Center for Drug Evaluation and Research (CDER). Silver Spring, MD, **2015**.

(14) Shargel, L.; Wu-Pong, S.; Yu, A. *Applied Biopharmaceutics and Pharmacokinetics*; **2005**.

(15) Yeo, Y.; Park, K. Control of Encapsulation Efficiency and Initial Burst in Polymeric Microparticle Systems. *Arch. Pharm. Res.* **2004**, *27*, 1–12.

(16) Huang, X.; Brazel, C. S. On the Importance and Mechanisms of Burst Release in Matrix-Controlled Drug Delivery Systems. *J. Control. Release* **2001**, *73*, 121–136.

(17) Hasan, A. S.; Socha, M.; Lamprecht, A.; Ghazouani, F. El; Sapin, A.; Hoffman, M.; Maincent, P.; Ubrich, N. Effect of the Microencapsulation of Nanoparticles on the Reduction of Burst Release. *Int. J. Pharm.* **2007**, *344*, 53–61.

(18) Yang, Y. Y.; Chia, H. H.; Chung, T. S. Effect of Preparation Temperature on the Characteristics and Release Profiles of PLGA Microspheres Containing Protein Fabricated by Double-Emulsion Solvent Extraction/Evaporation Method. *J. Control. Release* **2000**, *69*, 81–96.

(19) Costa, P. An Alternative Method to the Evaluation of Similarity Factor in Dissolution Testing. *Int. J. Pharm.* **2001**, *220*, 77–83.

(20) Shah, V. P.; Tsong, Y.; Sathe, P.; Liu, J. P. *In vitro* Dissolution Profile Comparison - Statistics and Analysis of the Similarity Factor, f2. *Pharm. Res.* **1998**, *15*, 889–896.

(21) Moore, J. W.; Planner, H. H. Mathematical Comparison of Dissolution Profiles. *Pharm. Technol.* **1996**, *20* (6), 64–74.

(22) Guideline on the investigation of bioequivalence. EMA Committee For Medicinal Products For Human Use (CHMP). London, UK, **2010**.

(23) Guidance for Industry: Dissolution Testing of Immediate Release Solid Oral Dosage Forms. FDA Center for Drug Evaluation and Research (CDER). Rockville, MD, **1997**.

(24) Podczeck, F. Comparison of *in vitro* Dissolution Profiles by Calculating Mean Dissolution Time (MDT) or Mean Residence Time (MRT). *Int. J. Pharm.* **1993**, *97*, 93–100.

(25) Tanigawara, Y.; Yamaoka, K.; Nakagawa, T.; Uno, T. New Method for the Evaluation of *in vitro* Dissolution Time and Disintegration Time. *Chem. Pharm. Bull.* **1982**, *30*, 1088–1090.

(26) Khan, F.; Li, M.; Schlindwein, W. Comparison of *in vitro* Dissolution Tests for Commercially Available Aspirin Tablets. *Dissolution Technol.* **2013**, *20*, 48–58.

(27) Mahalanobis, P. On the Generalized Distance in Statistics. *Proc Natl Inst Sci India Phys Sci.* **1936**, *2*, 49–55.

(28) Brereton, R. G.; Lloyd, G. R. Re-Evaluating the Role of the Mahalanobis Distance Measure. *J. Chemom.* **2016**, *30*, 134–143.

(29) Ma, M. C.; Wang, B. B. C.; Liu, J. P.; Tsong, Y. Assessment of Similarity between Dissolution Profiles. *J. Biopharm. Stat.* **2000**, *10*, 229–249.

(30) Tsong, Y.; Hammerstrom, T.; Sathe, P.; Shah, V. P. Statistical Assessment of Mean Differences between Two Dissolution Data Sets. *Ther. Innov. Regul. Sci.* **1996**, *30*, 1105–1112.

(31) Sathe, P.; Tsong, Y.; Shah, V. P. *In vitro* Dissolution Profile Comparison and IVIVR. Carbamazepine Case. *Adv Exp Med Biol* **1997**, *423*, 31–42.

(32) Chen, J. J.; Tsong, Y. Multiple-Time-Point Dissolution Specifications for a Sampling Acceptance Plan. *J. Biopharm. Stat.* **1997**, *7*, 259–270.

(33) Cardot, J.-M.; Roudier, B.; Schütz, H. Dissolution Comparisons Using a Multivariate Statistical Distance (MSD) Test and a Comparison of Various Approaches for Calculating the Measurements of Dissolution Profile Comparison. *AAPS J.* **2017**, *19*, 1091–1101.

(34) Varelas, C. G.; Dixon, D. G.; Steiner, C. A. Zero-Order Release from Biphasic Polymer Hydrogels. *J. Control. Release* **1995**, *34*, 185–192.

(35) Gibaldi, M.; Feldman, S. Establishment of Sink Conditions in Dissolution Rate Determinations. Theoretical Considerations and Application to Nondisintegrating Dosage Forms. *J. Pharm. Sci.* **1967**, *56*, 1238–1242.

(36) Wagner, J. G. Interpretation of Percent Dissolved-time Plots Derived from *in vitro* Testing of Conventional Tablets and Capsules. *J. Pharm. Sci.* **1969**, *58*, 1253–1257.

(37) Costa, F. O.; Sousa, J. J. S.; Pais, A. A. C. C.; Formosinho, S. J. Comparison of Dissolution Profiles of Ibuprofen Pellets. *J. Control. Release* **2003**, *89*, 199–212.

(38) Higuchi, T. Rate of Release of Medicaments from Ointment Bases Containing Drugs in Suspension. *J. Pharm. Sci.* **1961**, *50*, 874–875.

(39) Higuchi, T. Mechanism of Sustained-action Medication. Theoretical Analysis of Rate of Release of Solid Drugs Dispersed in Solid Matrices. *J. Pharm. Sci.* **1963**, *52*, 1145–1149.

(40) Higuchi, T.; Dayal, S.; Pitman, I. A. N. H. Effects of Solute-Solvent Complexation Reactions on Dissolution Kinetics : Testing of a Model by Using a Concentration Jump Technique. **1972**, *61*, 695–700.

(41) Siepmann, J.; Peppas, N. A. Higuchi Equation: Derivation, Applications, Use and Misuse. *Int. J. Pharm.* **2011**, *418*, 6–12.

(42) Tahara, K.; Yamamoto, K.; Nishihata, T. Application of Model-Independent and Model Analysis for the Investigation of Effect of Drug Solubility on Its Release Rate from Hydroxypropyl Methylcellulose Sustained Release Tablets. *Int. J. Pharm.* **1996**, *133*, 17–27.

(43) Korsmeyer, R. W.; Peppas, N. A. Macromolecular and Modeling Aspects of Swelling Controlled Systems. *Control. Release Deliv. Syst.* **1981**, 77–90.

(44) Korsmeyer, R. W.; Gurny, R.; Doelker, E.; Buri, P.; Peppas, N. A. Mechanisms of Solute Release from Porous Hydrophilic Polymers. *Int. J. Pharm.* **1983**, *15*, 25–35.

(45) Ritger, P. L.; Peppas, N. A. A Simple Equation for Description of Solute Release I. Fickian and Non-Fickian Release from Non-Swellable Devices in the Form of Slabs, Spheres, Cylinders or Discs. *J. Control. Release* **1987**, *5*, 23–36.

(46) Ritger, P. L.; Peppas, N. A. A Simple Equation for Description of Solute Release II. Fickian and Anomalous Release from Swellable Devices. *J. Control. Release* **1987**, *5*, 37–42.

(47) Peppas, N. A.; Sahlin, J. J. A Simple Equation for the Description of Solute Release. III. Coupling of Diffusion and Relaxation. *Int. J. Pharm.* **1989**, *57*, 169–172.

(48) Weibull, W. A Statistical Distribution Function of Wide Applicability. *J. Appl. Mech.* **1951**, *18*, 293–297.

(49) Langenbucher, F. Linearization of Dissolution Rate Curves by the Weibull Distribution. *J. Pharm. Pharmacol.* **1972**, *24*, 979–981.

(50) Yamaoka, K.; Nakagawa, T.; Uno, T. Application of Akaike's Information Criterion (AIC) in the Evaluation of Linear Pharmacokinetic Equations. *J. Pharmacokinet. Biopharm.* **1978**, *6*, 165–175.

Chapter 2

A computational procedure for analysis and comparison of dissolution profiles

The concepts and tools developed for the study of dissolution profiles are presented in this chapter. Firstly, the advantages of using R and the respective IDE, RStudio® are outlined. A general computational procedure is also proposed within the context established by the conceptual framework and by the relevant guidelines and regulations.

2.1. R and RStudio®

R is a freely available software[1] widely used by the scientific community for computational statistics, data manipulation and visualization. This open-source structure language was created by Ross Ihaka and Robert Gentleman at the University of Auckland in 1992[2].

R provides to the user a wide variety of packages and functions that allow performing statistical tests, including linear or non-linear statistical analysis, time series analysis, and classification or clustering of data with different characteristics. All these functionalities can be complemented with graphical representations for enhancing the interaction with the user[3].

Another advantage of R is that it is available for different operating systems, which has boosted the number of users. There are many large companies that use R routinely, ranging from big pharmaceuticals such as Pfizer, Bayer, and Roche to financial or social companies including Google and Facebook[2]. The number of users that share their work on the internet and provide technical support to other users is increasing worldwide.

R has also been used in the field of medicinal chemistry to develop several tools, including statistical algorithms and graphical frameworks[4]. These allow establishing one of the connections between medicinal chemistry and computational chemistry. R is also used for processing and interpretation of large data sets, being used, for example, in QSAR modelling[5]. In this work, R will be an essential tool for developing programs that

allow characterizing different dissolution profiles, based on several parameters and the implementation of the mathematical models described in the previous chapter.

RStudio® is an integrated development environment (IDE) for the R language, that makes its use straightforward. Basically, RStudio® is divided into four panels (see Figure 2.1). In panel 1, the lines of R code are written for constructing a script that will be read and processed in panel 2, corresponding to the terminal or console. Panel 3 displays the history of object values, comprising matrices and/or tables inserted. In panel 4 the graphics, of any form and including, for example, more complex structures such as dendrograms, are produced.

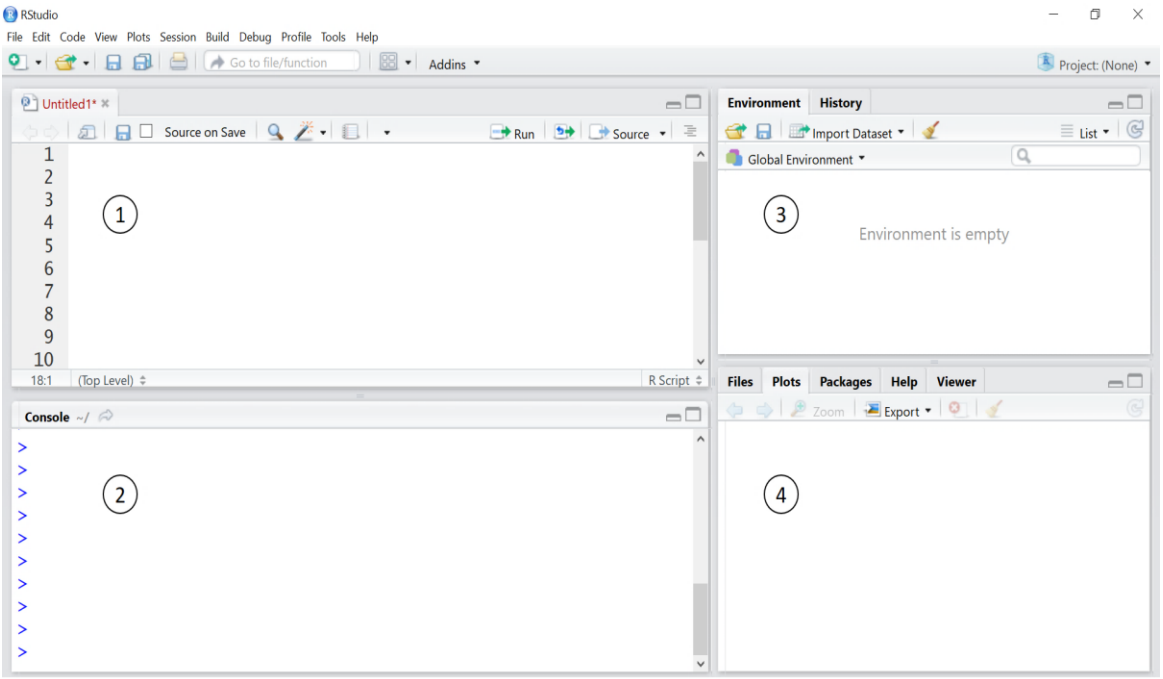

Figure 2.1 – Representative screenshot of RStudio® containing 4 different panels: the source panel, or code editor (1) the tabbed workspace and the history interface (2), the console (3) and (4) the panel that gives access to the user files, R packages, help support, and graphical visualization.

Details concerning program development are gathered in Appendices I and II. Appendix I presents some basic commands and more general aspects, while Appendix II focuses in the least-squares approaches.

2.2. Validation, analysis and development

2.2.1. Independent approaches

In what follows, the procedures and results for approaches independent of model, including fit factors, MDT and data visualization will be presented. The Mahalanobis Distance method will also be, specifically, introduced.

2.2.1.1. Fit factors, MDT and graphical visualization

Fit factors as described in the previous chapter, must be established following the principles and procedures contained in the relevant guidelines.

The developed script questions the user on some conditions that need to be fulfilled. Firstly, a question is presented to enter the number of dissolution tests performed for each formulation. If the value is lower than 12, the value required by the EMA guideline[6], a warning message will appear. This message allows the user to proceed with the calculations without meeting the requirements of the guideline or simply stop the analysis. In preliminary trials, it may be useful to obtain these results without performing the 12 assays, saving resources and time. There are still two questions about the highest value of relative standard deviation (RSD) or coefficient of variation (CV) for the first point and for the remaining points. If in the first points the value of RSD or CV is larger than 20%, the program is interrupted immediately assuming error. The same occurs if the value of RSD or CV in the following points is greater than 10%.

It is necessary to use a reference product which is compared with the various test drug products. Thus, after the questions the user is instructed on how to build an appropriate .csv file (Figure 2.2), since the program was developed with the purpose of recognizing input data in this format.

```
  Time Reference Test 1 Test 2 Test n
1 t1   ..        ..     ..     ..
2 ..   ..        ..     ..     ..
3 tn   ..        ..     ..     ..

Is this the format of your .csv file?

1: Yes
2: No

Selection:
```

Figure 2.2 – Base model for the input data.

It is intended that the file only contain final values, i.e., the mean values of all dissolution profiles for each test. The first column of the dataset is always ascribed to the time value, the second column, to the reference product, and the following columns to the test products to be compared with the reference. With this input requirement, it is warranted that the formulations to be compared possess profiles defined in the same time points.

The script is intended to run in its entire sequence. Initially, a question at a time where is needed to enter the number of tests performed and the values of RSD or CV requested. The program continues if the values fulfil these conditions. The base format of the input file is shown and, if the selection is 1, a window is automatically opened for the user to choose the .csv file containing the data to be studied. After the input, the program automatically checks if there are at least three time points different from zero, and calculates the fit factors for the formulations considering one mean value above 85%.

The data present in what follows was selected from previous studies conducted in our research group, and serve as an example of application. The first column contains the time of sampling collection, the second column the dissolution values for the reference, and in the following columns the dissolution values corresponding to the test drugs to be compared with the reference.

An illustration of the output is provided in Scheme 2.1. The first menu appears after inserting the file; it is possible to choose between four available options (1 for *Plot*, 2 for f_1, 3 for f_2 and 4 for *MDT*). This selection generates a result (blue lines) and also a new menu appears containing the previous options and a new one (5 for *Quit*). This new menu is repeated (green line) until the user makes the Selection: 5 for *Quit*. In the option *Plot* there is a possibility of record the produced graph, if the answer is *Yes* (1), a new menu is automatically generated, for selecting the format (PDF or PNG) and the name of the file to be saved. The graph is stored in the same directory as the initial .csv file.

This procedure possesses several advantages including the automation and optimization of the process. Another advantage is how the output is obtained. One of the major problems and challenges is to understand the results and interpret them. To make this easier, all results possess the same name of the input .csv file provided by the user. In the graphical representation, the legend is depicted automatically for each dissolution profile and the results of the fit factors are shown with the relation between the reference product and the pharmaceutical forms.

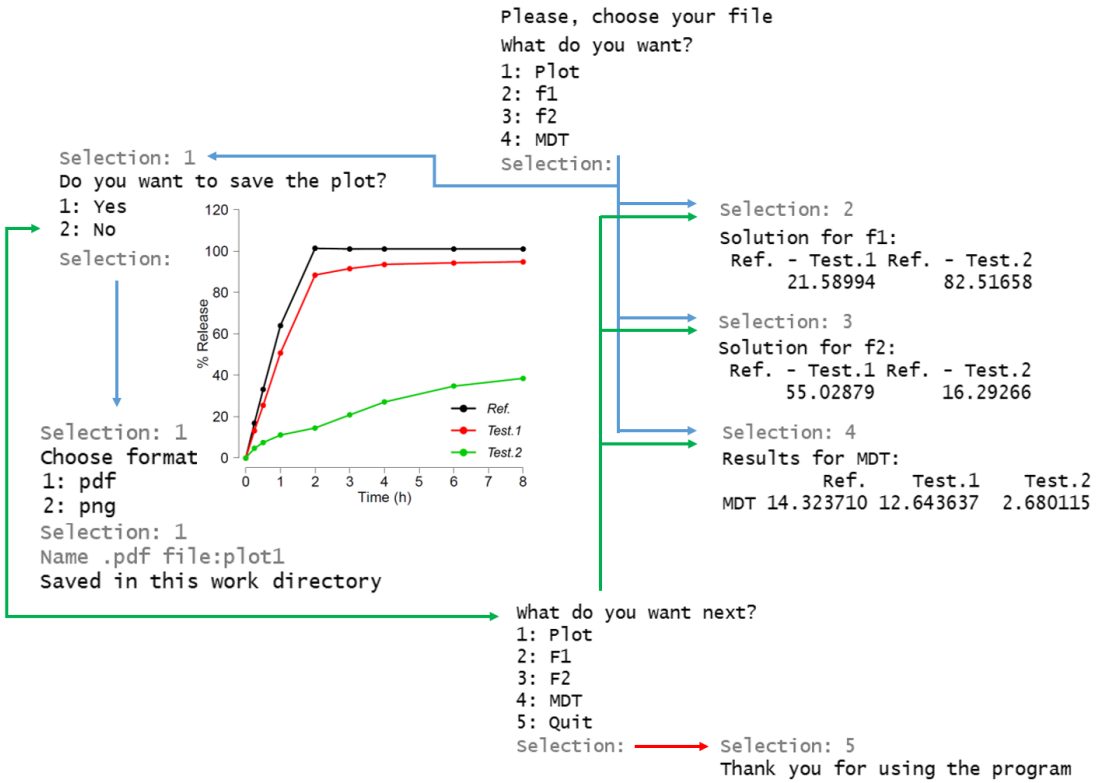

Scheme 2.1 – Schematic representation of the general operation of the program developed and the respective output. Blue lines refers to a single direction, green lines indicates repetition, and red line indicates exiting the program.

2.2.1.2. Mahalanobis Distance

For the more complex calculation of the Mahalanobis Distance (D_M), all dissolution values of each test are used. This calculation only compares two datasets at a time, that is, a .csv file for the reference and a .csv for the test product. The input must follow the model shown in Figure 2.3. If the answer is *Yes* (1) in this first step, two windows are automatically opened to select the .csv file for the reference and for the test product to calculate the Mahalanobis Distance. Note that it is arranged in a different way, compared to the input in Figure 2.2. This calculation does not use the averages for each time for all the tests, but instead uses each profile individually. The first column contains the test number or formulation number (chosen by the user in the .csv file). The subsequent columns contain the values of dissolution for each time and each test.

As the program proceeds, at a certain point the user must provide the upper limit of the desired confidence interval. This value represents the maximum tolerable difference between the two dissolution profiles under study, usually 90%, for taking them as equivalent, as explained in the previous chapter.

```
  Tablet t1 t2 t3 tn
1 1      .. .. .. ..
2 2      .. .. .. ..
3 3      .. .. .. ..
4 n      .. .. .. ..

Is this the format of your .csv files?

1: Yes
2: No

Selection:
```

Figure 2.3 – Base model for an input table for calculating Mahalanobis Distance.

The data presented in ref. 7[7] was used to perform the validation of this script. The output with the various results is represented in Figure 2.4. The parameter *n* corresponds to the number of tests, *p* is the number of time points for each of these tests, and *K* is a value used for intermediate calculations. These are followed by the Mahalanobis Distance (D_M), lower limit (D_M^l), the upper limit (D_M^u) and the tolerable difference between the two dissolution profiles ΔD_M. The last line of the output indicates whether there is (TRUE) or not (FALSE) similarity between the dissolution profiles under study, according to Equation (1.18).

```
Confidence interval:   90

Study of the Mahalanobis Distance
                          Values
n                         6
p                         8
K (scaling vector)        0.1125
Mahalanobis Distance (DM) 27.0542968045905
DM lower limit            20.2219091747326
DM upper limit            33.8866844344484
DM tolerable difference   19.7076173411869
Profile Similarity        FALSE
```

Figure 2.4 – Results obtained with the calculation of Mahalanobis Distance.

From literature, it is no easy to identify uses and applications of this distance in the drug dissolution. Nevertheless, it is considered that it may provide a useful measure to test the similarity between dissolution profiles. To the best of our knowledge there are no specific guidelines to clarify which dissolution interval must be used to put in practice this method. It is not established whether it is correct to use all data, or if there should be no more than one point above 85%, similarly to fit factors. However, there are some relatively recent contributions that use this metrics[8]. In these studies when all values are used the method becomes insensitive to detect all the differences, it has a low specificity

where can result in false positives. When the limit of 85% is imposed as a modification of the method it exhibits a higher sensitivity[8,9].

2.2.2. Dataset

The validation of the R scripts for a primary analysis of dissolution profiles and for the methods dependent of the model was performed using a dataset containing the dissolution profiles of different formulations, previously studied in our research group[10] (see Figure 2.5). Briefly, the data express the release profiles of solid dosage forms for oral administration based on nanostructured lipid carriers of olanzapine and simvastatin coated with different conventional polymers agents. The dissolution test was carried out for 8 hours with samples collected at 0.5, 1, 1.5, 2, 2.25, 2.5, 2.75, 3, 4, 5, 6, 7, 8 hours and an initial medium with pH 1.2 was exchanged for a medium with pH 6.8 at 2 hours. The pharmaceutical forms tested are represented by *F* followed by an identifying number. The formulations *F1* to *F8* contain nanostructured lipid carriers of olanzapine and the remaining nanoparticles loaded are with simvastatin. These will be relevant for the technical development in Chapter 5. Also presented are the release profiles of reference drugs: olanzapine (OL) and simvastatin (SV). The .csv file is arranged in order indicated in Figure 2.2.

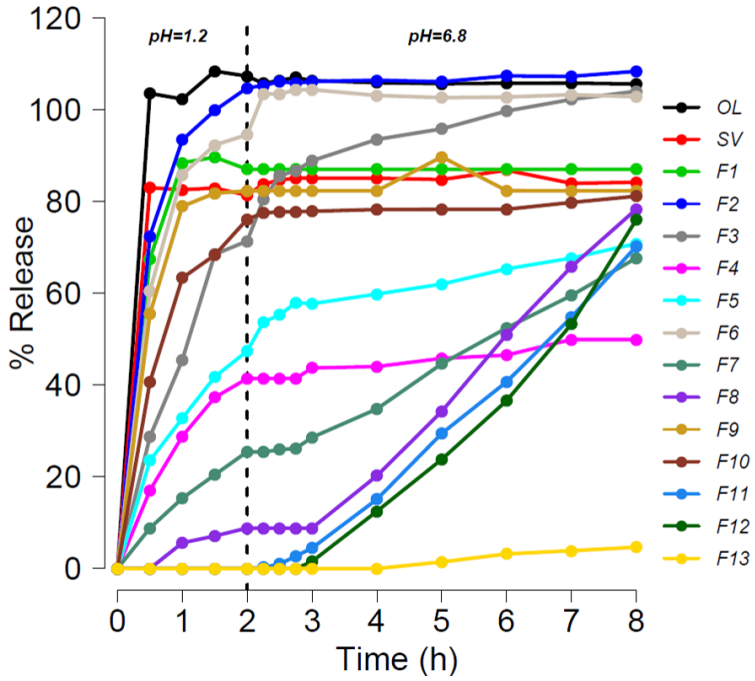

Figure 2.5 – *In vitro* release profiles of olanzapine (OL) and simvastatin (SV) commercial references and different formulations (1 to 13), used in the validation of the developed scripts. Dashed line at 2 h identifies the change in the dissolution medium at pH values from 1.2 to 6.8.

2.2.3. Similarity analysis

Taking advantage of the developed program represented in Scheme 2.1, the output referring to MDT and fit factors values were extracted and analysed. To elucidate about the EMA guideline in not using more than one value higher than 85%, a new calculation was performed without this condition. In this way, the script was changed to calculate fit factors for all dissolution values. The results following the guideline and for taking into account all dissolution points, without restrictions, are summarized in Tables 2.1 and 2.2.

The similarity study between the formulations and the respective references is a challenge since both components are of immediate dissolution. More problematic is the comparison for olanzapine, where only the first point is used for the comparison. For this reason, it is interesting to study EMA's requirement on the points to be used. Following the guideline, only formulation 9 is equivalent to the reference (SV), displaying a value of f_2 higher than 50 and a value of f_1 less than 15 (see Table 2.2). Without following the guideline, considering all dissolution points, a slight increasement of the calculated values is observed. For this reason, in *F10* (with all values) the value of f_1 can be considered a false positive. Other false positives appear when all points of formulation 2 are used to compare with olanzapine. From Figure 2.5 it is easy to check that the first point of *F2* is very distant from the first point of the reference, but in the final of each dissolution process, and as usual, the asymptotic value is approximately the same. In formulation 6, the value of f_1 considering all points is very different compared to 85% of the dissolution, which may indicate that the difference factor (f_1) may not be the ideal index for establishing the similarity between dissolution profiles.

The importance of using a limit required by guidelines for dissolution values is thus recognized, as it allows ensuring a precise and correct evaluation of similarity between the reference and test products.

Table 2.1 – Fit factors calculation for olanzapine (OL) with the corresponding formulations following the guideline (85% criterion) and calculated for all points (AP). Shaded values are accepted for each fit factor.

		OL–F1	***OL–F2***	***OL–F3***	***OL–F4***	***OL–F5***	***OL–F6***	***OL–F7***	***OL–F8***
f_2	**85%**	29.68	32.89	13.81	10.67	12.37	25.80	8.70	6.77
	AP	35.10	52.11	25.14	9.95	14.25	43.16	7.27	4.11
f_1	**85%**	34.79	30.01	72.29	83.56	77.27	41.61	91.49	100.00
	AP	18.90	4.37	23.61	61.57	49.43	8.17	68.37	77.73

Table 2.2 – Fit factors calculation for simvastatin (SV) with the corresponding formulations following the guideline (85% criterion) and calculated for all points (AP). Shaded values are accepted for each fit factor.

		SV–F9	***SV–F10***	***SV–F11***	***SV–F12***	***SV–F13***
f_2	**85%**	50.06	37.42	5.55	5.41	5.41
	AP	55.20	42.49	8.23	7.82	4.83
f_1	**85%**	6.83	17.47	99.32	100.00	100.00
	AP	5.33	12.64	80.00	81.37	98.80

The MDT values are interpreted by direct comparison with the value of the references, OL and SV. As shown in Table 2.3, for OL the formulations with the closest values are 1, 2 and 6. For SV, *F9* presents a more similar value to reference.

Table 2.3 – MDT values for references and for the different formulations.

Drug formulation								
OL	***F1***	***F2***	***F3***	***F4***	***F5***	***F6***	***F7***	***F8***
50.96	28.76	26.58	8.69	5.39	5.91	21.54	3.62	6.51

Drug formulation					
SV	***F9***	***F10***	***F11***	***F12***	***F13***
41.03	22.74	13.92	6.33	7.96	0.67

2.2.4. Derivative analysis

The derivative of a function represents the variation of this function between two points, when the difference between these points tends to zero that is, it is the slope of the line tangent to the function at point *x*. In practical terms, a high positive slope represents a large increase between two points on the graph and the opposite for a negative slope. If the slope is 0, there is no variation between the points.

Analysis of the first derivative in a dissolution profile is useful to provide information about the respective behavior. Burst release can be identified, but several collections are required in the initial state of the dissolution test for its detection. When present, the study of the first derivative allows evaluating the extent of the initial release, and identifying a regime change in which a stable release profile is reached.

The derivative also allows understanding if there are variations in a certain profile and detecting changes in the release regime. For example, it allows to identify in which part significant differences in the amount release occur. In *F10* (see Figure 2.6), when the

asymptotic limit is reached, the derivative does not detect more variations because all drug has been released. The use of the derivative study is also useful to signal if, in the course of dissolution assay, release stopped (null derivative), with a different subsequent behaviour. Generally, until reaching the plateau, there are changes in the derivative, once there is still drug to be released.

The other two formulations (*F4* and *F8*, see Figure 2.6) are a good example for observing regime changes in the course of dissolution profile. In these two cases, there is a period after the 2 hours of trial where there is no release, a consequence of changing the medium, imposing a different pH (1.2 to 6.8). Derivatives also help to identify changes in the release regime, which are usually accompanied by a visible change in the respective values.

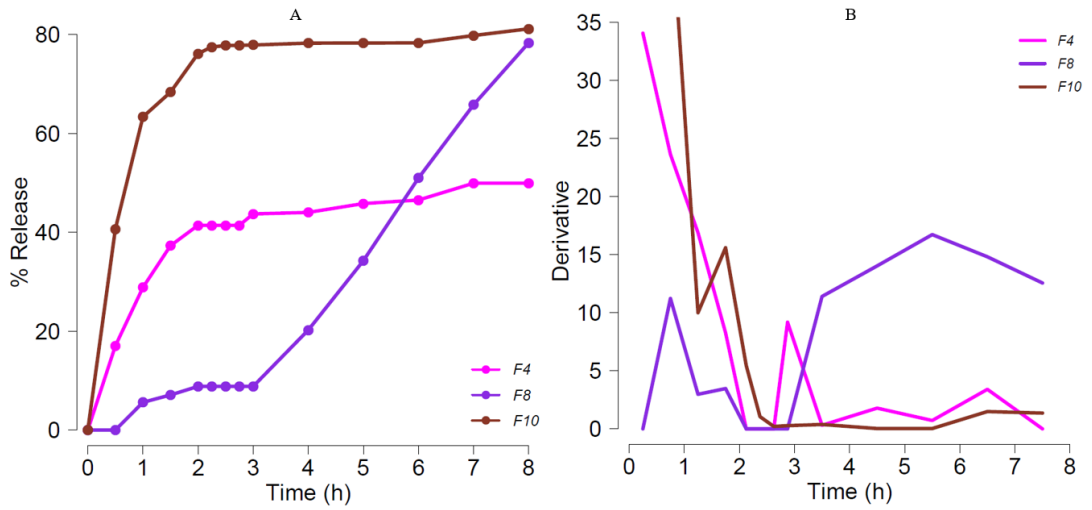

Figure 2.6 – Dissolution profiles for the formulations *F4*, *F8* and *F10* (A) and the graphical visualization of the first derivative of each formulation (B).

2.2.5. Model dependent approaches

2.2.5.1. The additional parameter

As discussed previously, an additional parameter, corresponding to the asymptotic value of the dissolved percentage can be assigned to the first order and Weibull models (Equations (1.20) and (1.23), respectively). In the following analysis, the impact of this additional parameter (c_2) on the first order and Weibull equations will be addressed. To carry out this study, the sum of squares of the residues in the two functions, with and without the parameter, for each dissolution profile, was calculated. The results are summarized in Table 2.4.

From Table 2.4, it is observed that the addition of the parameter in both models results, generally, in a smaller sum of squares. The Weibull function also generates smaller values for residues, without the parameter, than when compared to the first order function. This can be explained by the additional parameter in the Weibull model which improves the curve fitting to the dissolution points.

To better understand the impact of an additional parameter, formulation *F2* (Figure 2.7) was individually inspected. The results show that the additional parameter produces clearly a higher quality fit, especially if used in conjunction with the Weibull function.

Table 2.4 – Values of the sum of squares of residues with and without the additional (asymptotic dissolution) parameter.

	First order		**Weibull**	
	With c_2	Without c_2	With c_2	Without c_2
OL	22.30	470.48	19.32	466.99
SV	22.22	2819.85	15.29	15.30
F1	35.83	1628.78	7.64	234.01
F2	16.74	426.26	4.86	415.89
F3	73.09	95.42	72.02	82.80
F4	32.60	2069.59	30.23	11039.37
F5	62.38	1428.06	41.27	114.09
F6	56.66	145.29	52.42	141.44
F7	98.32	105.67	51.81	105.47
F9	65.42	2233.58	50.05	327.50
F10	19.15	2170.08	19.32	338.82

2.2.5.2. Lag time

The lag time is the time between the administration of the pharmaceutical dosage form containing the drug and the beginning of absorption[12]. Dissolution profiles of drugs often exhibit lag time. In some formulations, the existence of lag time may have a positive effect, in cases where a later release is intended.

When a lag time is apparent, a new parameter t_{lag} must be included in model dependent approaches. In the current work, a script that checks for the existence of a lag time and for the calculation of t_{lag} has been developed. The program reads all points for each dissolution test, and determines if points with $t > 0$ are nonzero. If any value is zero,

the existence of a lag time is probable. As a previous calculation, the linear equation of the two first points where the dissolution is detected is established. Through this equation, a linear interpolation is performed to find t_{lag}, which represents the last time point for which there is zero release. If this time value is negative, or if it is located before zero release time points, it is considered invalid and t_{lag} is equated, if possible, to the time just before the first instance where drug release is detected.

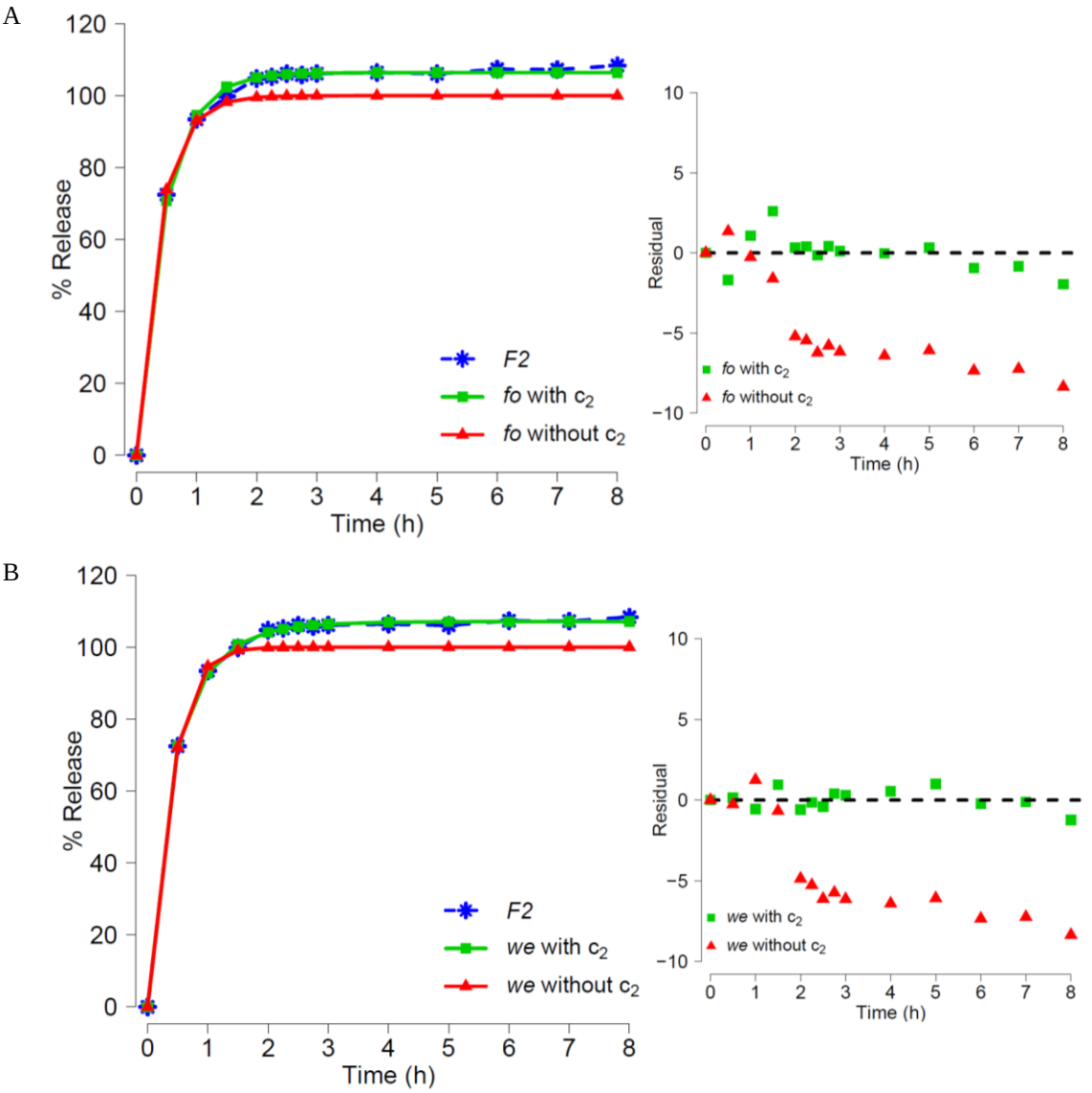

Figure 2.7 – (Left) The original points of *F2* and the curve fit with the first order (A) and Weibull (B) models, with (green squares) and without (red triangles) the additional parameter. (Right) The residual difference between the points of *F2* and the points of the fitting curve with (green squares) and without (red triangles) the parameter. The residuals represented by the triangles depart from zero, and do not show significant alternation, thus revealing a poor quality fit.

This parameter redefines the functions, changing the initial point for the time when the dissolution starts. As an example, the rearrangement for the Weibull equation can be described as

$$f(t) = c_2\left(1 - exp\left(-\frac{(t - t_{lag})}{c_1}\right)^{c_3}\right) \quad (2.1)$$

Figure 2.8 illustrates a situation in which lag time is present, in formulation *F12*. Lag time was determined, and the dissolution curve followed equation (2.1).

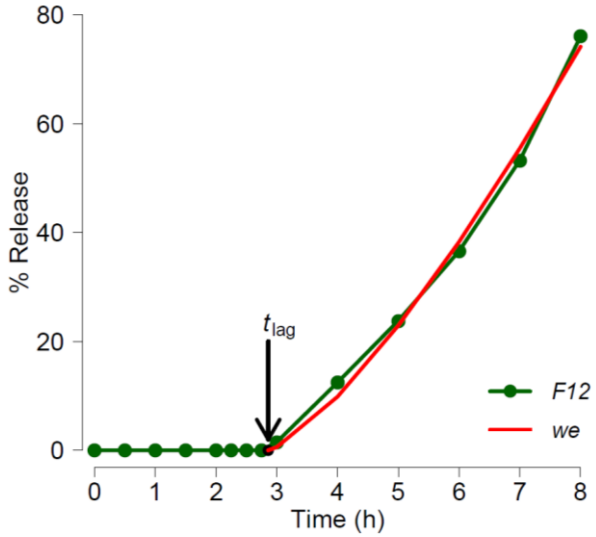

Figure 2.8 – Representation of a lag time formulation (*F12*) adjusted with the Weibull model. The parameter t_{lag} represents the time at which dissolution sets in.

2.2.5.3. Higuchi and Korsmeyer-Peppas models

For these two models, the curve fit is valid for the first 60% of the total release drug, where it is assumed that there is a one-dimensional diffusion under perfect sink conditions. These models are not useful for studying a profile with immediate release, or for establishing the whole release profile, including points above the 60% limit.

As such, these two models do not define the asymptotic release limit, because when time tends to infinity the percentage of drug released will also be infinite: they just predict the initial growth.

For the following analysis, formulation 5 (*F5*) will be studied. It is represented in Figure 2.9, already adjusted to these two models. Following Equations (1.21) and (1.22), constant c_1 is similar in both models and, correspondingly, c_2 does note appreciably depart from 0.5, which indicates a dissolution profile close to Fickian diffusion (see Table 2.5).

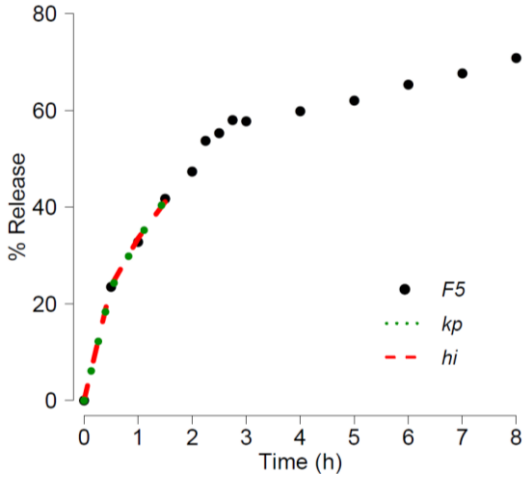

Figure 2.9 – *F5* fitted with the Higuchi (*hi*) model (red dashed line) and fitted with the Korsmeyer-Peppas (*kp*) (green dots).

Table 2.5 – Values of curve fitting for Higuchi (*hi*) and Korsmeyer-Peppas (*kp*) models.

	c_1	c_2
hi	33.51	–
kp	33.43	0.53

2.2.5.4. One *in vitro* test, two dissolution profiles

In vitro tests are essential in the preliminary study of any drug in order to predict the drug behavior in the body. In many dissolutions tests, the dissolution medium is switched, with a pH ranging from 1.2 to pH of 6.8 as in the example of the dataset studied. There are drugs which have different behaviors in each of the dissolution media and, in these cases, it is useful to divide the dissolution profile in two. To cover as an example, formulation 8 (see Figure 2.10) was used. Initially, there is a lag time, and then, upon 2 hours an exponential growth is observed. After the change of pH, there is no variation for one hour, and the release continued only after the third hour of dissolution. This dissolution does not appear to display a single mechanism, and this profile was divided into two, with each part studied individually. Note that the second function must be written taken into account the amount already dissolved, in the form of an additive constant, and the time already elapsed, this similarly to what was described for the lag time (see subsection 2.2.5.5).

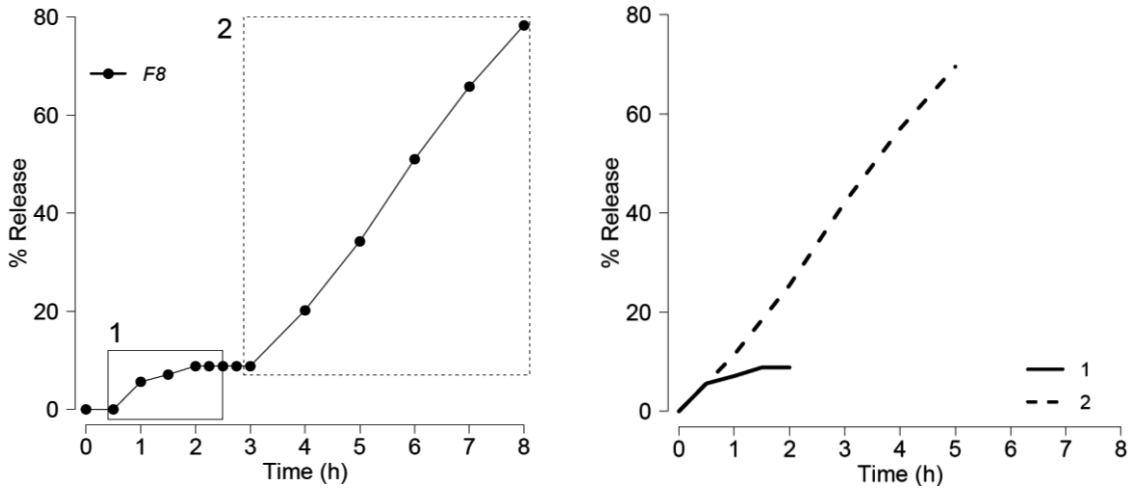

Figure 2.10 – (Left) The dissolution profile of *F8*. Between 2 and 3h there is a change in the regime of dissolution. Rectangle 1 divides the first part of the dissolution and the rectangle 2 represents the second part. (Right) The representation of each part.

2.2.5.5. Final output

After the analyses above, and the special study in each dissolution profile, it is necessary to select which of the models fits best the curve to the dissolution points. As detailed in the previous chapter, there are two indices to draw these conclusions: the adjusted coefficient of determination ($R^2_{adjusted}$) and Akaike's information criterion (AIC). It is also of interest to analyse the parameters for each model. It is important, for example, to see if the additional parameter, which represents the asymptotic limit in the first order function is close to the corresponding one from the Weibull function. The remaining parameters are useful for studying the behavior of the dissolution, the shape of the curve or to directly compare the various profiles with these parameters.

The study of the dissolution profiles for *F8*, depicted in Figure 2.10, is summarized in Table 2.6. To reach these results, a script was developed to study all the models for each dissolution profile, and in the final, it allows access to the output of all the calculated results. The user can see the values of each parameter as well as the values for each index.

By the analysis of the AIC and $R^2_{adjusted}$, it is simple to conclude that the first order model is the one that better fits the points in the first part, while the Weibull function is more adequate for the second part. This selection is explained by the high value of the adjusted coefficient of determination and the lowest value of AIC. The asymptotic limit for the first order and Weibull in the first part is approximately the same, which validates

the use of these functions. This is expected because, as previously stated, between 2 and 3 hours there is a regime change, and the asymptotic limit for the first part of the dissolution is well defined. In the second part, as the curve growth tends to infinity, the first order model is not as efficient as the Weibull function to set the asymptotic limit.

Table 2.6 – Parameters for several fitted models to formulation *F8*, and respective quality indicators.

		c_1	c_2	c_3	AIC	$R^2_{adjusted}$
zo	**1**	5.33	–	–	18.67	0.93886
	2	13.89	–	–	17.81	0.99843
hi	**1**	6.82	–	–	4.91	0.98818
	2	25.97	–	–	39.34	0.94440
kp	**1**	7.23	0.35	–	-1.24	0.99562
	2	12.48	1.08	–	15.81	0.99879
fo	**1**	1.75	9.20	–	-1.29	0.99567
	2	0.01	1474.68	–	20.79	0.99819
we	**1**	0.72	10.30	0.73	-0.95	0.99561
	2	5.52	119.70	1.38	6.09	0.99977

After achieving the value of the parameters for each model, the first order ($fo(t)$) and Weibull ($we(t)$) functions can be rewritten

$$fo(t) = 9.20(1 - \exp(-1.75\ t)) \tag{2.2}$$

$$we(t) = 119.70\left(1 - exp\left(-\frac{t}{5.52}\right)^{1.38}\right) \tag{2.3}$$

For interpretation, it is necessary to remember that the profile was divided into two parts, and then the initial concentration of the second part is not zero. When there are two or more dissolution parts, the concentration value of the last time of the previous part must be summed to the function of the next part of dissolution profile

$$we(t) = 119.70\left(1 - exp\left(-\frac{t - t_f}{5.52}\right)^{1.38}\right) + fo(t_f) \tag{2.4}$$

where t_f represents the last time used to calculate the final concentration in the first order function, and at same time represent the time where dissolution in the second part begins.

2.3. References

(1) RStudio www.rstudio.com/ (accessed Jul 10, 2018).

(2) Olszewski, A. Is R suitable enough for biostatisticians involved in Clinical Research & Evidence-Based Medicine? www.r-clinical-research.com/ (accessed Jul 10, 2018).

(3) The R Foundation. The R Project for Statistical Computing www.r-project.org/ (accessed Jul 10, 2018).

(4) Mente, S.; Kuhn, M. The Use of the R Language for Medicinal Chemistry Applications. *Curr. Top. Med. Chem.* **2012**, *12*, 1957–1964.

(5) Svetnik, V.; Liaw, A.; Tong, C.; Christopher Culberson, J.; Sheridan, R. P.; Feuston, B. P. Random Forest: A Classification and Regression Tool for Compound Classification and QSAR Modeling. *J. Chem. Inf. Comput. Sci.* **2003**, *43*, 1947–1958.

(6) Guideline on the investigation of bioequivalence. EMA Committee For Medicinal Products For Human Use (CHMP). London, UK, **2010**.

(7) Tsong, Y.; Hammerstrom, T.; Sathe, P.; Shah, V. P. Statistical Assessment of Mean Differences between Two Dissolution Data Sets. *Ther. Innov. Regul. Sci.* **1996**, *30*, 1105–1112.

(8) Yoshida, H.; Shibata, H.; Izutsu, K.-I.; Goda, Y. Comparison of Dissolution Similarity Assessment Methods for Products with Large Variations: f2 Statistics and Model-Independent Multivariate Confidence Region Procedure for Dissolution Profiles of Multiple Oral Products. *Biol. Pharm. Bull.* **2017**, *40*, 722–725.

(9) Mangas-Sanjuan, V.; Colon-Useche, S.; Gonzalez-Alvarez, I.; Bermejo, M.; Garcia-Arieta, A. Assessment of the Regulatory Methods for the Comparison of Highly Variable Dissolution Profiles. *AAPS J.* **2016**, *18*, 1550–1561.

(10) Mendes, M.; Soares, H. T.; Arnaut, L. G.; Sousa, J. J.; Pais, A. A. C. C.; Vitorino, C. Can Lipid Nanoparticles Improve Intestinal Absorption? *Int. J. Pharm.* **2016**, *515*, 69–83.

(11) Guideline on quality of oral modified release products. EMA Committee For Medicinal Products For Human Use (CHMP). London, UK, **2014**.

(12) Pozzi, F.; Furlani, P.; Gazzaniga, A.; Davis, S. S.; Wilding, I. R. The Time Clock System: A New Oral Dosage Form for Fast and Complete Release of Drug after a Predetermined Lag Time. *J. Control. Release* **1994**, *31*, 99–108.

Chapter 3

Oral films based on lipid nanoparticles for administration of olanzapine and simvastatin

In this chapter, the effect of encapsulation drugs, available in the market, into lipid nanoparticles for improving their therapeutic efficacy is addressed. The oral route of administration is explored, resorting to thin oral films, rather than using conventional tablets. This dosage form is relatively recent and has attracted great interest to researchers and pharmaceutical companies.

Oral films are essentially composed of a drug and a polymer matrix. The therapeutic strategy is to combine two complementary drugs: olanzapine and simvastatin. The polymer matrix to be exploited is hydroxypropyl methylcellulose (HPMC) which possesses specific characteristics that allow the controlled release of drugs. Four different grades of HPMC (100SR, 4000SR, 15000SR and 100000SR) are evaluated. The *in vitro* dissolution profiles extracted from the oral thin films produced are characterized and the mathematical models for drug release are addressed, based on the procedures described in the previous chapters.

3.1. Lipid nanoparticles

Nano-size particles have been extensively explored in the last decades for pharmaceutical and biomedical applications. Nanometric devices have evolved to solve problems related to unsatisfactory therapeutic responses of drugs that are already in the market. To circumvent a low bioavailability or the existence of too many adverse effects, colloidal systems pose an alternative to protect the drug, to slow down degradation, optimize targeting, reduce toxicity, control release and/or delivery the drug in the active site for improving the therapeutic efficacy[1].

Solid lipid nanoparticles (SLN) emerged in 1991 and are an alternative to the conventional colloidal systems, such as emulsions, liposomes, micro and polymeric nanoparticles[2]. SLNs possess several advantages including better physicochemical stability, ease of scaling-up production, low cost and reduction, or even absence of toxicity[2–4]. Additionally, SLNs enable the encapsulation of poorly soluble drugs, in a

stable solid matrix at room and body temperatures, thus allowing a controlled release of the drug[5,6]. Consequently, the therapeutic efficacy is enhanced as a result of changing the type of release with improved tolerability and targeting of the encapsulated drug[7].

SLNs display sizes ranging typically from 40 to 1000 nm and are composed of solid lipids (melting point ≥ 40°C, 0.1% – 30% w/w) which are in the solid state at room temperature and are stabilized by an aqueous solution of a surfactant (0.5% – 5% w/w) [8,9]. The solid lipids used for the preparation of SLNs can be fatty acids with hydrocarbon chains of different lengths, fatty acid esters, fatty alcohols, waxes, glycerides, or a mixture of mono-, di- and triglycerides[10,11]. The selection of the solid lipid depends on the solubility of the drug and the respective conditions, the drug loading capacity, the release behavior and the stability of the SLN.

However, SLNs have some limitations, such as low drug loading and drug expulsion during storage[12,13]. To overcome these issues, a second generation of lipid nanoparticles, the nanostructured lipid carriers (NLC), was designed. These consist of a matrix blending solid lipids and liquid lipids[9]. This matrix has a lower melting point than SLNs, is less organized and has more imperfections, which allow a higher exposure of the drug[14]. Diverse liquid lipids may be incorporated in the preparation of NLC, such as medium chain triglycerides, oleic acid, Transcutol® HP and Capryol® 90[15]. The selection of the liquid lipid, similarly to that of the solid lipid, is governed by the solubility of the drug.

According to the method of preparation and the composition of the lipid matrix, three types of NLC can be distinguished, depending on the amount of liquid lipid mixed in the solid lipid[14,16]. In type I, the matrix presents many imperfections, able to accommodate the drug, as a result of the small amounts of liquid lipid added. In type II, after the use of specific liquid lipids, recrystallization of the solid lipid, after homogenization, is avoided. Type III contains a mixture with a higher amount of liquid lipid, resulting in the formation of oily nano compartments, when the solid lipid precipitates. This process is especially advantageous for drugs that are more soluble in liquid lipid than in solid lipid, allowing to encapsulate a larger amount of drug in the nanoparticles. As a result, the drug loading capacity and the performance in the dissolution release process are improved[17].

3.1.1. Lipid nanoparticles production

Several methods have been proposed for producing lipid nanoparticles. The rationale behind the selection of the method is based on the use of a green method with sustainable excipients[14]. Different traditional physical methods with reasonable modifications in their methodology have been transposed for the controlled synthesis of nanoparticles. These include, for example, ultra-sonication, micro-emulsion and supercritical fluid technique, high-pressure homogenization, ultrafiltration, solvent emulsification-evaporation and others. These are the methods commonly used for the formulation of lipid nanoparticles[14].

In this work lipid nanoparticles were produced by the high-pressure homogenization (HPH) technique, which is described below.

3.1.1.1. High-Pressure Homogenization

HPH is widely applied as a simple and inexpensive process for the formation of nanoparticles, and is easily transposable to an industrial scale process[17]. Through this process emulsions with small sizes are obtained. Important characteristics such as the stability of the particles and reactivity are ensured with the provided nanoemulsions[18–20].

High-pressure homogenizers work through a pump that pushes a liquid with high pressure (100 – 2000 bar) through a restricted passage called the gap region (in the range of a few microns). The fluid accelerates on a very short distance to a very high speed (above 1000 km/h), leaves the gap region and enters the exit region flowing towards the impact ring. After passing through this region, the fluid exits through the outlet[20].

Nanoparticles can be produced using hot or cold HPH techniques. The former is explored in this work and the lipid is melted at approximately 10°C above the respective melting point (point at which the drug is dissolved). This molten lipid phase is dispersed in a previously heated surfactant solution, at the same temperature, through a high shear mixing device (Ultra-Turrax). The obtained pre-emulsion is then introduced into the high-pressure homogenizer at a temperature above the lipid melting point at a pressure ranging from 100 to 1500 bar for a predefined time. A nano-emulsion is obtained, leading to recrystallization of the lipid, after cooling, and the formation of lipid nanoparticles.

3.1.2. Therapeutic applications

Lipid nanoparticles have a great therapeutic potential, and a wide variety of drugs, including hydrophilic molecules, can be incorporated into NLC[16,21]. They can be

administered by various routes such as parenteral, transdermal or oral[22]. In this work, oral thin films (OTF) are developed, containing lipid nanoparticles as a differentiated dosage form for the oral route.

The oral route of administration is the most convenient and versatile route when compared to other alternatives, providing good compliance by the patients[23]. Currently, most of the marketed drugs are available in the oral delivery systems. However, the main disadvantages are the first pass effect in the liver, which decreases the bioavailability of the drug. Another problem is the variability in the absorption, because throughout the gastrointestinal tract there are numerous enzymes that can promote drug degradation or change their active form[24,25].

The reduction of particle size to a nano range allows overcoming these limitations, as well as increasing bioavailability, reducing the dosage and controlling the release of the drug. The adhesiveness of the nanoparticles allows a strong interaction with the intestinal wall, favouring absorption[26]. The ionic strength and the low pH on gastric environment may destabilize the lipid nanoparticles, leading to the formation of aggregates[27]. However, the pathway and uptake mechanism by gastrointestinal tract are still poorly understood. Three different pathways of uptake have been suggested: paracellular pathway, intracellular uptake and transport via the epithelial cells lining the intestinal mucosa, and a lymphatic uptake via the M-cells and the Peyer's patches[28].

The method for producing lipid nanoparticles, and their compositions also affect the absorption and stability of SLN/NLC. Bio-adhesion is also affected, depending on the surface properties (e.g. hydrophobicity and surface charge). The presence of lipids, promotes an increase in lymphatic absorption, and avoids the pre-systemic metabolism in the liver[29].

3.2. Oral thin films

Oral films can be defined as thin and flexible layer targeted for the rapid and local or systemic release of an API. The nature of these thin films allows increasing patient compliance. Thin films improve the onset of drug action and bioavailability, reduce the dose frequency and enhance the drug efficacy. An ideal thin film needs to have a fast disintegration as well as a fast dissolution rate or a long residence time at the site of administration. To avoid toxic and adverse effects, the excipients employed in the manufacturing of films should be biocompatible and biodegradable[30]. Various types of thin films have been designed, namely oral thin films, oral soluble films, oral strip or

orodispersible films[30]. These are composed of a water-soluble polymer film that hydrates, disintegrates and dissolves rapidly, when placed on the tongue or in the mouth cavity, without ingestion of water or chewing. In this process, the active compound can be absorbed sublingually or disintegrated and swallowed without irritation to the patient (if the granules have a size smaller than 200 μm)[31].

OTFs avoid problems associated in the swallowing process with a strong impact on children and in the geriatric population as well as on patients who generally cannot swallow tablets or capsules[32–34]. In fact, OTFs are an appealing and easy-to-administer form. Likewise, oral films can be very useful for bedridden and non-cooperative patients since they are easily administered and difficult to expel[35]. However, there are certain limitations with the age of the patient, once it is assumed that swallowing is only fully developed from the age of 12, and with the aging process, some dysfunctions may arise at this level. This problem results in a different dosage for each individual and adapted to each patient and situation. However, this therapeutic approach may be beneficial for drugs with a small therapeutic window and for drugs requiring precise dose adjustment in the early stages, allowing the development of customized drug therapeutic targets[36].

Another advantage is the fastness and the economically viable research process. Typically, a new drug takes 20 years to reach the market, with a significant investment in research and development (R&D). In most cases, the new drugs not guarantee the sufficient conditions to be approved in the final clinical trials, and that is why just 1 in 100000 new drugs have reached the market. The fact that any drug already in the market (API), can be incorporated into OTF, makes the respective investigation and investment a very attractive process.

The API may belong to numerous classes of drugs, such as antihistaminic, anti-diarrheal, anti-depressants, vasodilators, anti-asthmatic or anti-emetic[37]. In terms of composition, different classes of excipients can be included. Plasticizers, such as polyethylene glycol (PEG), glycerol and diethyl phthalate[38], provide OTFs with improved mechanical properties, such as tensile strength and percent elongation[39]. Often, to mask the bitter taste of the API are used flavours, like that of mint. The use of fructose, sorbitol and mannitol as sweetening agents are also commonly used to provide ease of disintegration on the buccal cavity[40].

Usually, films have an area ranging from 5 to 20 cm^2 and are ultra-thin having a size between 50 to 150 μm, where the drug is incorporated into the matrix form composed of a hydrophilic polymer[41]. The composition of a typical oral film is shown in Table 3.1.

Table 3.1 – General composition of an oral film[41].

Components	Concentration (%)
Active pharmaceutical ingredient	1 – 25
Hydrophilic polymer	40 – 50
Plasticizer	0 – 20
Flavours and sweetening agents	0 – 40

Some problems can occur during the manufacturing process. These may include the entrapment of air bubbles, insufficient uniformity of content, batch-to-batch variability, and other effects caused by organic solvents[35,42].

The polymer matrix may be composed of one or more polymers with different properties that modify the functionality. Control may exist in some characteristics depending on the polymer used or the concentration, such as mucoadhesiveness, disintegration time, drug loading capacity, mechanical strength, and elasticity. The properties of the polymers (e.g. molecular weight) are also important factor to be considered. A general rule is that, polymers with low molecular weight dissolve faster[43]. Cellulose-derived polymers including hydroxypropyl cellulose (HPC), methyl cellulose (MC), carboxymethyl cellulose (CMC) and hydroxypropyl methylcellulose (HPMC) are commonly used. These derivatives are commercially available and possess a wide range of attractive physicochemical properties.

3.2.1. Hydroxypropyl methylcellulose

HPMC (Figure 3.1) is one of the most widely used cellulose ether derivatives in the preparation of hydrophilic matrixes and polymers for oral controlled drug delivery systems[44]. HPMC is synthesized by the reaction of alkaline cellulose with methylene chloride and propylene oxide. The main characteristics are the ability to swell and the gelling properties, which by modulating the viscosity with different types and amounts of HPMC, different release profiles can be obtained.

HPMC is water soluble and a polymer of non-ionic nature and therefore chemically stable over a wide pH range, 3.00 – 11.00[45]. This is relevant for controlled release since a wide range of pH ensures the adequate release of active substances throughout the gastrointestinal tract. It is a non-hazardous polymer commonly used in the food industry, and described as non-irritating and non-toxic.

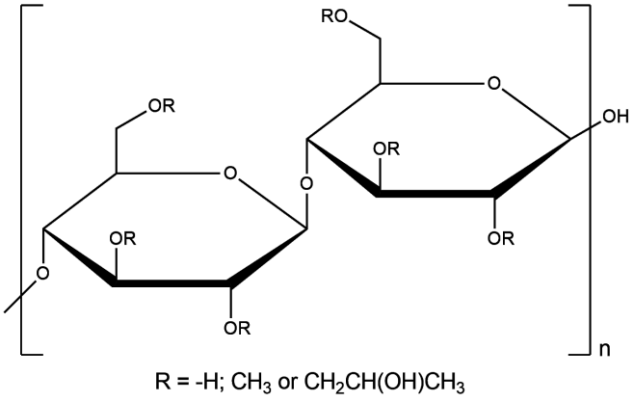

Figure 3.1 – Chemical structure of HPMC.

During manufacturing, the physicochemical properties of HPMC are strongly affected by the amount of methoxy groups, hydroxypropyl groups and by the molecular weight[46]. Various types of HPMC are commercially available depending on molecular weight, particle size, viscosity and the ratio between the methoxy (-OCH_3) and hydroxypropyl (-$OCH_2CH(OH)CH_3$) groups. The different types of HPMC are classified according to the content of the radicals: 2208, 2906 and 2910. In this code the first two characters indicate the percentage of substitution by methoxy groups and the last values represent the percentage by hydroxypropyl groups[47]. They can also be identified by letters (E, F, and K) according to Table 3.2.

Table 3.2 – Classification of HPMC derivatives containing different substituents. Classification and properties adapted by Dow®[48].

Products	Methoxyl group content (%)	Hydroxypropoxyl groups content (%)	HPMC substitution type
E	28.0 – 30.0	7.0 – 12.0	2910
F	27.0 – 30.0	4.0 – 7.5	2906
K	19.0 – 24.0	7.0 – 12.0	2208

Each content influences the ability of the matrix system to release the drug. This can be explained by the self-diffusion coefficient (SDC). HPMC with substitution of K type presents a lower value for SDC in water within the gelling layer, than the E and F types. This indicates that there is a higher resistance to water diffusion in the matrix system containing HPMC type K, with less water mobility in the gelling layer. The drug will also be more covered, and the release will be slower than with the substitution grades E and F. The presence of the hydroxypropyl groups contributes to the hydration ratio of

the polymer, in contrast to the methoxy groups, which are relatively hydrophobic. Thus, HPMC type K will rapidly form a gel layer to modulate the release by displaying a higher ratio of this substituent, promoting hydration. This gel layer is responsible to control the amount of drug released over time, according to the specific grade of HPMC.

A classification based on the controlled and sustained release (SR) is also considered for HPMC. Figure 3.2 presents a schematic illustration of the dissolution process of a hydrophilic matrix with HPMC of type SR. Firstly, there is a contact of the polymer with water and the formation of a gel layer begins; when complete, this stabilizes the dissolution of the drug. This step is very important for highly water-soluble drugs or excipients. The polymer is hydrated, and water goes into the pharmaceutical form. In the last step, the dissolution of the polymer is completed. This process occurs continuously, repeating this cycle, by dissolving an external layer by erosion, followed by an inner layer which will consequently be hydrated.

Figure 3.2 – Schematic illustration of the dissolution process of the matrix in the pharmaceutical form. (a) corresponds to the first stage of this process with an initial swelling; (b) reflects the hydration following by expansion and erosion (c and d); (e) refers to the final dissolution of the polymer. Adapted from ref. 45.

In order to modify the release behavior, it is important to take into account the balance between hydration and dissolution. Often, the initial contact with the polymer in the aqueous medium results in a rapid release of the drug to the surface, corresponding to the burst effect. Other factors may influence the release of a drug through this polymer, such as the amount of HPMC, the ratio between HPMC and the pharmaceutical form, particle size, viscosity and molecular weight. In general, an increase in the viscosity of the polymer improves the control on the release of the drug. In the same way, the higher the molecular weight of the polymer the lower the respective rate of release.

In this work, the incorporation of lipid nanoparticles encapsulating olanzapine and simvastatin in HPMC is performed. Four different grades of the polymer (100SR, 4000SR, 15000SR and 100000SR) described for the controlled release, were kindly provided by Shin-Etsu Chemical Co., Ltd. The properties of the manufacturer are described in Table 3.3.

Table 3.3 – Properties of different grades of the HPMC used in this work. The values of viscosity were obtained by 2% w/w aqueous solution at 20°C. Adapted from the product properties manual of Shin-Etsu Chemical Co., Ltd.

Grades		Viscosity (mPa.s)	Substitution type	Methoxy content (%)	Hydroxypropoxy content (%)
90SH	**100SR**	80 – 120	2208	22.0 – 24.0	8.5 – 10.5
	4000SR	3000 – 5600			
	15000SR	11250 – 21000			
	100000SR	75000 – 140000			

3.3. Problem and strategy

Olanzapine (OL) (Figure 3.3 A) belongs to the benzodiazepine class of drugs. These antipsychotic drugs potentiate the effect of the GABA (inhibitory neurotransmitter) through a chemical structure composed of a benzene ring fused with a diazepine ring. Olanzapine, a second-generation atypical antipsychotic, with a higher affinity for blocking dopaminergic (D_2) and serotonergic (5-HT_{2A}) receptors is mainly used for the treatment of schizophrenia. Beyond the large hepatic metabolism by cytochrome CYP450 1A2 (50-60% metabolized), prolonged use may result in some undesirable side effects[49]. Such as weight gain, headaches or drowsiness. Another adverse effect is dyslipidemia. Also, there is a higher risk of increasing the level of triglycerides and cholesterol in the low-density lipoproteins (LDL) and decreasing high-density lipoproteins (HDL), thus increasing the risk of cardiovascular problems. This recurring problem requires treatment with statins, namely simvastatin (SV)[50]. The latter (Figure 3.3 B) is an inactive lactone which is hepatically hydrolyzed to β-hydroxy acid (Figure 3.3 C). Once activated, the pro-drug, simvastatin acid (SVA) acts by inhibiting the action of the enzyme 3-hydroxy-3-methylglutaryl coenzyme A reductase[51]. This action will lead to the inhibition of cholesterol synthesis, reduction of triglyceride levels and an increase in HDL levels. The main properties of each drug are summarized in Table 3.4.

Upon the successful encapsulation of these OL and SV and incorporation of the resulting nanoparticles into the polymer for controlled release, it is intended to decrease the daily dose and the number of intakes. From the technological point of view, the nanoparticle production process is economically viable and easily up-scalable, as well as the production of oral thin films.

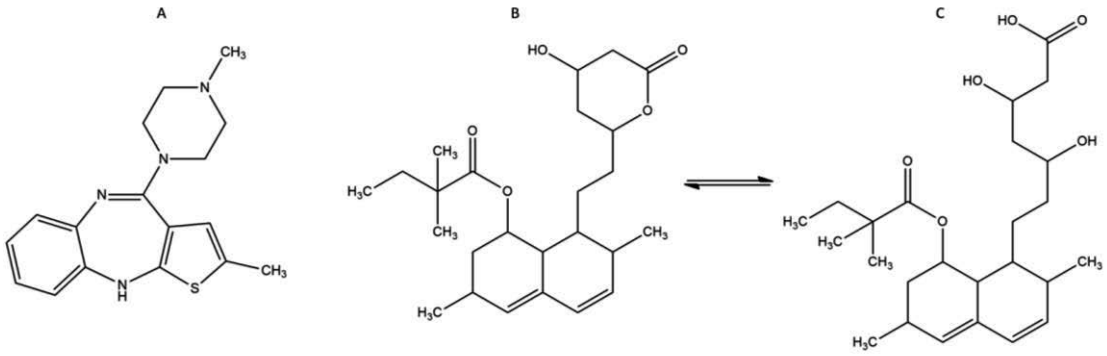

Figure 3.3 – Chemical structures of (A) olanzapine, (B) simvastatin and the prodrug (C) simvastatin in the respective acid form (β-hydroxy acid).

Table 3.4 – Physicochemical and pharmacokinetic properties of olanzapine and simvastatin. Values are obtained from the DrugBank database (available from *www.drugbank.ca*).

Drug	Olanzapine	Simvastatin
Molecular weight (g/mol)	312.43	418.57
Log P	2.8	4.7
Aqueous solubility (µg/mL)	3 – 5	30
Melting point (°C)	195	135 – 138
Daily oral dose (mg/day)	5 – 10	10 – 40
Half-life (h)	33	2
Bioavailability (%)	60	5

3.4. References

(1) Beija, M.; Salvayre, R.; Lauth-de Viguerie, N.; Marty, J.-D. Colloidal Systems for Drug Delivery: From Design to Therapy. *Trends Biotechnol.* **2012**, *30*, 485–496.

(2) Müller, R. H.; Mäder, K.; Gohla, S. Solid Lipid Nanoparticles (SLN) for Controlled Drug Delivery - A Review of the State of the Art. *Eur. J. Pharm. Biopharm.* **2000**, *50*, 161–177.

(3) Muchow, M.; Maincent, P.; Müller, R. H. Lipid Nanoparticles with a Solid Matrix (SLN®, NLC®, LDC®) for Oral Drug Delivery. *Drug Dev. Ind. Pharm.* **2008**, *34*, 1394–1405.

(4) Uner, M. Preparation, Characterization and Physico-Chemical Properties of Solid Lipid Nanoparticles (SLN) and Nanostructured Lipid Carriers (NLC): Their Benefits as Colloidal Drug Carrier Systems. *Pharmazie* **2006**, *61*, 375–386.

(5) Mukherjee, S.; Ray, S.; Thakur, R. S. Solid Lipid Nanoparticles: A Modern Formulation Approach in Drug Delivery System. *Indian J. Pharm. Sci.* **2009**, *71*, 349–358.

(6) Hu, L.; Tang, X.; Cui, F. Solid Lipid Nanoparticles (SLNs) to Improve Oral Bioavailability of Poorly Soluble Drugs. *J. Pharm. Pharmacol.* **2004**, *56*, 1527–1535.

(7) Manjunath, K.; Venkateswarlu, V. Pharmacokinetics, Tissue Distribution and Bioavailability of Nitrendipine Solid Lipid Nanoparticles after Intravenous and Intraduodenal Administration. *J. Drug Target.* **2006**, *14*, 632–645.

(8) Battaglia, L.; Gallarate, M. Lipid Nanoparticles: State of the Art, New Preparation Methods and Challenges in Drug Delivery. *Expert Opin. Drug Deliv.* **2012**, *9*, 497–508.

(9) Müller, R. H.; Petersen, R. D.; Hommoss, A.; Pardeike, J. Nanostructured Lipid Carriers (NLC) in Cosmetic Dermal Products. *Adv. Drug Deliv. Rev.* **2007**, *59*, 522–530.

(10) Mäder, K.; Mehnert, W. Solid Lipid Nanoparticles: Production, Characterization and Applications. *Adv. Drug Deliv. Rev.* **2001**, *47*, 165–196.

(11) Puglia, C.; Bonina, F. Lipid Nanoparticles as Novel Delivery Systems for Cosmetics and Dermal Pharmaceuticals. *Expert Opin. Drug Deliv.* **2012**, *9*, 429–441.

(12) Rawat, M.; Singh, D.; Saraf, S.; Saraf, S. Nanocarriers: Promising Vehicle for Bioactive Drugs. *Biol. Pharm. Bull.* **2006**, *29*, 1790–1798.

(13) Wissing, S. .; Kayser, O.; Müller, R. . Solid Lipid Nanoparticles for Parenteral Drug Delivery. *Adv. Drug Deliv. Rev.* **2004**, *56*, 1257–1272.

(14) Ganesan, P.; Narayanasamy, D. Lipid Nanoparticles: Different Preparation Techniques, Characterization, Hurdles, and Strategies for the Production of Solid Lipid Nanoparticles and Nanostructured Lipid Carriers for Oral Drug Delivery. *Sustain. Chem. Pharm.* **2017**, *6*, 37–56.

(15) Fang, C.-L.; Al-Suwayeh, S. A.; Fang, J.-Y. Nanostructured Lipid Carriers (NLCs) for Drug Delivery and Targeting. *Recent Pat. Nanotechnol.* **2013**, *7*, 41–55.

(16) Müller, R. H.; Radtke, M.; Wissing, S. A. Nanostructured Lipid Matrices for Improved Microencapsulation of Drugs. *Int. J. Pharm.* **2002**, *242*, 121–128.

(17) Muller, R. H.; Shegokar, R.; Keck, C. M. 20 Years of Lipid Nanoparticles (SLN and NLC): Present State of Development and Industrial Applications. *Curr. Drug Discov. Technol.* **2011**, *8*, 207–227.

(18) Schultz, S.; Wagner, G.; Urban, K.; Ulrich, J. High-Pressure Homogenization as a Process for Emulsion Formation. *Chem. Eng. Technol.* **2004**, *27*, 361–368.

(19) Qian, C.; McClements, D. J. Formation of Nanoemulsions Stabilized by Model Food-Grade Emulsifiers Using High-Pressure Homogenization: Factors Affecting Particle Size. *Food Hydrocoll.* **2011**, *25*, 1000–1008.

(20) Håkansson, A.; Trägårdh, C.; Bergenståhl, B. Dynamic Simulation of Emulsion Formation in a High Pressure Homogenizer. *Chem. Eng. Sci.* **2009**, *64*, 2915–2925.

(21) Natarajan, J.; Vvsr, K.; De, A. Nanostructured Lipid Carrier (NLC): A Promising Drug Delivery System. *Glob. J. Nanomedicine* **2017**, *1*, 555575.

(22) Yoon, G.; Park, J. W.; Yoon, I.-S. Solid Lipid Nanoparticles (SLNs) and Nanostructured Lipid Carriers (NLCs): Recent Advances in Drug Delivery. *J. Pharm. Investig.* **2013**, *43*, 353–362.

(23) Kerz, T.; Paret, G.; Herff, H. *Cardiac Arrest: The Science and Practice of Resuscitation Medicine*; **2007**.

(24) Gibaldi, M.; Boyes, R. N.; Feldman, S. Influence of First-pass Effect on Availability of Drugs on Oral Administration. *J. Pharm. Sci.* **1971**, *60*, 1338–1340.

(25) Rowland, M. Influence of Route of Administration on Drug Availability. *J. Pharm. Sci.* **1972**, *61*, 70–74.

(26) Florence, A. T. Issues in Oral Nanoparticle Drug Carrier Uptake and Targeting. *J. Drug Target.* **2004**, *12*, 65–70.

(27) Severino, P.; Andreani, T.; Macedo, A. S.; Fangueiro, J. F.; Santana, M. H. A.; Silva, A. M.; Souto, E. B. Current State-of-Art and New Trends on Lipid Nanoparticles (SLN and NLC) for Oral Drug Delivery. *J. Drug Deliv.* **2012**, *2012*, 1–10.

(28) Kreuter, J. Peroral Administration of Nanoparticles. *Adv. Drug Deliv. Rev.* **1991**, *7*, 71–86.

(29) Harde, H.; Das, M.; Jain, S. Solid Lipid Nanoparticles: An Oral Bioavailability Enhancer Vehicle. *Expert Opin. Drug Deliv.* **2011**, *8*, 1407–1424.

(30) Karki, S.; Kim, H.; Na, S. J.; Shin, D.; Jo, K.; Lee, J. Thin Films as an Emerging Platform for Drug Delivery. *Asian J. Pharm. Sci.* **2016**, *11*, 559–574.

(31) Kimura, S. I.; Uchida, S.; Kanada, K.; Namiki, N. Effect of Granule Properties on Rough Mouth Feel and Palatability of Orally Disintegrating Tablets. *Int. J. Pharm.* **2015**, *484*, 156–162.

(32) Guideline on Pharmaceutical Development of Medicines for Paediatric Use. EMA Committee For Medicinal Products For Human Use (CHMP). London, UK, **2013**.

(33) Reflection paper on the pharmaceutical development of medicines for use in the older population. EMA Committee For Medicinal Products For Human Use (CHMP). London, UK, **2017**.

(34) Castro, P. M.; Fonte, P.; Sousa, F.; Madureira, A. R.; Sarmento, B.; Pintado, M. E. Oral Films as Breakthrough Tools for Oral Delivery of Proteins/Peptides. *J. Control. Release* **2015**, *211*, 63–73.

(35) Dixit, R. P.; Puthli, S. P. Oral Strip Technology: Overview and Future Potential. *J. Control. Release* **2009**, *139*, 94–107.

(36) Borges, A. F.; Silva, C.; Coelho, J. F. J.; Simões, S. Oral Films: Current Status and Future Perspectives: I-Galenical Development and Quality Attributes. *J. Control. Release* **2015**, *206*, 1–19.

(37) Nagar, P.; Chauhan, I.; Mohd, Y. Insights into Polymers: Film Formers in Mouth Dissolving Films. *Drug Invent. Today* **2011**, *3*, 280–289.

(38) Bala, R.; Khanna, S.; Pawar, P.; Arora, S. Orally Dissolving Strips: A New Approach to Oral Drug Delivery System. *Int. J. Pharm. Investig.* **2013**, *3*, 67.

(39) Arya, A.; Chandra, A.; Sharma, V.; Pathak, K. Fast Dissolving Oral Films: An Innovative Drug Delivery System and Dosage Form. *Int. J. ChemTech Res.* **2010**, *2*, 576–583.

(40) Gavaskar, B.; Kumar, S. V.; Sharan, G.; Madhusudan Rao, Y. Overview on Fast Dissolving Films. *Int. J. Pharm. Pharm. Sci.* **2010**, *2*, 29–33.

(41) Irfan, M.; Rabel, S.; Bukhtar, Q.; Qadir, M. I.; Jabeen, F.; Khan, A. Orally Disintegrating Films: A Modern Expansion in Drug Delivery System. *Saudi Pharm. J.* **2016**, *24*, 537–546.

(42) Cilurzo, F.; Musazzi, U. M.; Franzé, S.; Selmin, F.; Minghetti, P. Orodispersible Dosage Forms: Biopharmaceutical Improvements and Regulatory Requirements. *Drug Discov. Today* **2018**, *23*, 251–259.

(43) Hoffmann, E. M.; Breitenbach, A.; Breitkreutz, J. Advances in Orodispersible Films for Drug Delivery. *Expert Opin. Drug Deliv.* **2011**, *8*, 299–316.

(44) Siepmann, J.; Peppas, N. A. Modeling of Drug Release from Delivery Systems Based on Hydroxypropyl Methylcellulose (HPMC). *Adv. Drug Deliv. Rev.* **2001**, *48*, 139–157.

(45) Ford, J. L. *Hydrophilic Matrix Tablets for Oral Controlled Release*; **2014**.

(46) Osorio, F. A.; Molina, P.; Matiacevich, S.; Enrione, J.; Skurtys, O. Characteristics of Hydroxy Propyl Methyl Cellulose (HPMC) Based Edible Film Developed for Blueberry Coatings. *Procedia Food Sci.* **2011**, *1*, 287–293.

(47) Etsu-Shin Chemical Co., L. *Methylcellulose USP Hypromellose USP*.

(48) Callaghan, J. T.; Bergstrom, R. F.; Ptak, L. R.; Beasley, C. M. Pharmacokinetic and Pharmacodynamic Profile. *Clin Pharmacokinet* **1999**, *37*, 177–193.

(49) Lieberman, J. A.; Stroup, S. T.; McEvoy, J. P.; Swartz, M. S.; Rosenheck, R. A.; Perkins, D. O.; Keefe, R. S. E.; Davis, S. M.; Davis, C. E.; Lebowitz, B. D.; et al. Effectiveness of Antipsychotic Drugs in Patients with Chronic Schizophrenia. *N. Engl. J. Med.* **2005**, *353*, 1209–1223.

(50) Ballantyne, C. M.; Olsson, A. G.; Cook, T. J.; Mercuri, M. F.; Pedersen, T. R.; Kjekshus, J. Influence of Low High-Density Lipoprotein Cholesterol and Elevated Triglyceride on Coronary Heart Disease Events and Response to Simvastatin Therapy in 4S. *Circulation* **2001**, *104*, 3046–3051.

(51) Stancu, C.; Sima, A. Statins: Mechanism of Action and Effects. *J. Cell. Mol. Med.* **2001**, *5*, 378–387.

Chapter 4

Materials and Methods

In what follows, all materials and methods employed for the preparation and characterization of lipid nanoparticles loaded with olanzapine and simvastatin are described. The procedures to prepare oral films and the respective *in vitro* evaluation, and the quantification of drugs through HPLC analysis are also presented.

4.1. Materials

Simvastatin was kindly provided by Bluepharma (Coimbra, Portugal). Olanzapine was purchased from Zhejiang Myjoy (Hangzhou, China). Glyceryl tripalmitate (tripalmitin, T8127, melting point 66°C), polysorbate (Tween 80), sodium chloride (NaCl, M=58.44 g/mol), poly(ethylene glycol) (PEG 400) and phosphoric acid (H_3PO_4) were provided by Sigma (St. Louis, MO, USA). Oleic acid was acquired from Fluka (St. Louis, MO, USA). Different grades of hydroxypropyl methylcellulose (HPMC) was a gift from Shin-Etsu (Japan). A sample of Polydimethylsiloxane (PDMS) was provided by the research group Structure, Energetics and Reactivity of the Department of Chemistry, University of Coimbra. PDMS preparation is done using the Sylgard 184 Silicone Elastomer Kit with the combination of silicone and curing agent at a ratio of 10:1[1]. Potassium chloride (KCl, M=74.56 g/mol), monopotassium phosphate (KH_2PO_4, M=136.09 g/mol) and potassium phosphate monobasic (KH_2PO_4, M=136.09 g/mol) were purchased from Panreac Quimica SA and hydroxide sodium (NaOH) came from Merck KGaA, Germany. Water was purified (Millipore) and filtered through a 0.2 µm nylon filter before use.

All other reagents and solvents were of analytical or High-Performance Liquid Chromatography (HPLC) grade.

4.2. Methods

4.2.1. Preparation of lipid nanoparticles

The loaded lipid nanoparticles (LLN) were prepared by the hot high-pressure homogenization (HPH) technique, following an optimized procedure, previously reported[2–4].

The LLN were prepared at 80°C, a temperature above the melting point of the solid lipid. First, the lipid phase was weighed (15% w/w) containing tripalmitin and oleic acid (at a ratio of 50:50); 5% (w/w) of olanzapine and the same amount of simvastatin was added. This molten lipid phase was then emulsified in an aqueous solution of Tween 80 (3% w/v, 200 mL) at the same temperature using an Ultra-Turrax for 1 min (Ystral GmbH D-7801, Dottingen, Germany).

The resulting pre-emulsion was processed through preheated high-pressure homogenization (HPH) (Emulsiflex-C3, Avestin, Inc, Ottawa, Canada) at a pressure of 1000 bar for 16 minutes and 40 seconds. At the end of this process the nanoparticles were stored at 4°C.

4.2.1.1. Characterization of the lipid nanoparticles

To control and evaluate the quality of lipid nanoparticles, several measurable parameters are required, including the particle size and morphology, polydispersity index, zeta potential, encapsulation efficiency, drug loading, and *in vitro* drug release. These parameters are crucial for establishing the biological performance and stability profile and are influenced by the composition of the formulations and the respective preparation method[5].

4.2.1.1.1. Particle size analysis

Particle size (PS) and polydispersity index (PI) are used for assessing the quality control of the lipid nanoparticles and for studying the stability profile of the formulations. Dynamic light scattering (DLS, also known as photon correlation spectroscopy (PCS)) allows measuring the size of the particles in the submicron region, varying from 0.3 nm to 10 μm. DLS evaluates the Brownian motion of particles through a laser beam of light and relates this movement to its size. A slower Brownian motion is associated to a larger particle. A greater diffusion of larger particles is reflected by the translational diffusion coefficient, used in the Stokes-Einstein equation. Through the correlation between the

light intensity and time, the mean size and the polydispersity index are automatically determined[6].

The PI is a dimensionless measure of the broadness of the size distribution, ranging from 0 to 1. A PI value lower than 0.25 is associated to a homogeneous size distribution. Values exceeding 0.25 correspond to heterogeneous size distribution, and those close to 1 are associated to particle aggregation[7].

PS and PI were assessed by a Zetasizer Nano ZS (Malvern Instruments, Malvern, UK). All the samples were previously diluted with ultrapurified water (1:100) to generate appropriate scattering intensity. Three replicate analyses were performed. The cumulants method was used to data analysis.

4.2.1.1.2. Zeta potential

Zeta potential (ZP) is a physical property associated to the stability of particles stability in a certain medium. The ZP value is determined by the sum of attractive and repulsive Van der Waals. A ZP value higher than |30| mV is usually considered appropriate to consider a dispersion as stable[7,8]. On the other hand, when ZP is close to zero, particles are prone to form aggregates.

The ZP was determined by electrophoretic light scattering (ELS) at 25°C using a Zetasizer Nano ZS (Malvern, Worcestershire, UK) apparatus. Samples were suitably diluted in ultrapurified water (1:100). Three replicate analyses were performed. The Helmholtz-Smoluchowsky equation was used for ZP calculation[6].

4.2.1.2. Drug loading and entrapment efficiency

Drug loading is the percentage of drug contained in the particles, for lipid mass, while the entrapment efficiency expresses the percentage of drug entrapped inside the nanoparticles. The drug loading (DL) and entrapment efficiency (EE) of lipid nanoparticles were determined by measuring the concentration of free drug in the aqueous phase of the dispersion of nanoparticles.

The entrapment efficiency (EE) and drug loading (DL) of nanoparticles were calculated according to the following equations[3], respectively

$$\%EE = \frac{(W_{total} - W_{free})}{W_{total}} \times 100\% \quad (4.1)$$

$$\%DL = \frac{(W_{total} - W_{free})}{W_{lipid}} \times 100\% \quad (4.2)$$

where W_{total} is the total amount of SV and OL determined, W_{free} is the amount of free drug determined in the aqueous phase after separation of the nanoparticles, and W_{lipid} is the amount of lipid in the nanoparticles.

To quantify the total amount of drugs, a specific volume of the LLN dispersion was suitably diluted in the mobile phase, and then heated at 60°C for 15 min in ultrasound waves. The dispersion was then centrifuged for 5 min at 12 000 rpm in a Minispin® (Eppendorf Ibérica S.L., Madrid, Spain). The supernatant was collected, filtered by a 0.22 µm membrane, and determined by high performance liquid chromatography (HPLC). For determination of the amount of free drug, the ultrafiltration-centrifugation method was used with a centrifugal filter unit (Amicon Ultra-4, Milipore, Germany) with a 100 kDa molecular weight cutoff. In this way, 500 µL of LLN was combined with the same volume of the mobile phase, placed in the inner chamber of the centrifuge filter unit and centrifuged at 3000g for 45 min at 4°C. The amount of free drug in the aqueous dispersion phase, collected in the outer chamber of the centrifugal filter after separation, was determined by HPLC.

4.2.2. Preparation and characterization of oral thin films

The oral thin films were prepared by mixing the LLN with different hydrogels previously prepared from hydroxypropyl methylcellulose (HPMC). Four different HPMC grades (100SR, 4000SR, 15000SR and 100000SR) at 2% (w/w) were tested for the preparation of hydrogels. For the two extremes of the HPMC grades (100SR and 100000SR) PEG 400 was also added in the same amount (2% w/w). This was performed to evaluate the effect of the presence of a plasticizer in the oral films. The two films containing plasticizer are denoted F100SR[P] and F100000SR[P]. Single HPMC or HPMC and plasticizer were mixed with hot ultrapurified water, in a bath at 80°C, under mechanical stirring (IKA® EUROSTAR POWER, IKA-Werke GmbH & Co. KG) during 1 hour at 250 rpm. The hydrogels were left over night at room temperature to gain the desired consistency.

The oral films were prepared through the mixture of LLN and an equivalent amount of hydrogel. Polydimethylsiloxane (PDMS) 1% w/w was added to the total mass of the above mixture, for reducing the presence of bubbles in the final formulation[9,10]. All

components were mixed under mechanical stirring for 30 min and the samples were centrifuged for 30 min at an acceleration of 3000g at 4°C.

For the formulations with HPMC, 20 g were placed in a backing layer (3 M Scotchpak 9748 fluoropolymer coated polyester film release, USA), with an area of 33 cm^2, followed by solvent evaporation in an oven at 40°C for 24 h. For the formulations containing plasticizer 30 g were placed in petri dish with 4.5 cm radius (63.58 cm^2), followed by solvent evaporation in an oven at 40°C for 36 h. The time in the oven was previously established as being ideal for the quantity and material where the formulation was placed. The final aspect of one oral film with and without plasticizer is shown in Figure 4.1.

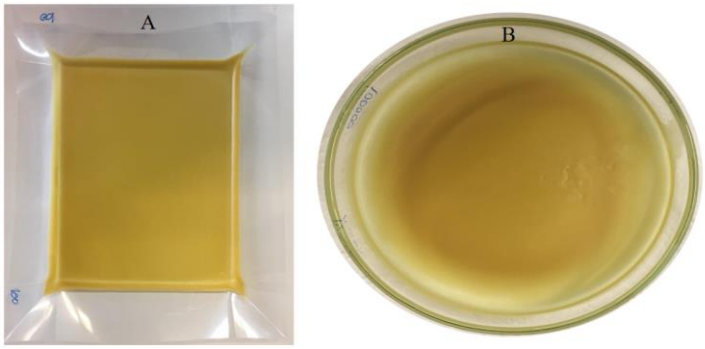

Figure 4.1 – Final aspect of oral film in the absence (A) and in the presence (B) of the plasticizer.

4.2.3. Mechanical properties

For evaluation of the mechanical properties of the films produced, a Texture Analyzer TA.XT Plus (Stable Micro Systems Ltd., Surrey, UK) was used. This device allows to analyse several textural features, such as the adhesive capacities of the different systems.

Six repetitions were performed. The data collection and calculations were performed using the instrument's own software, Texture Exponent 3.0.5.0.

4.2.3.1. Adhesive properties

The adhesion test was performed using probe P/10 (see Figure 4.2). Before the assay, 100 µL of ultrapurified water was placed during 2 min to ensure consistency of contact with the oral films.

From the measurements, several parameters can be obtained, such as adhesiveness, elongation to detachment and separation distance. The separation distance

is related to the energy needed to remove the patch from a defined surface, elucidated by elongation to detachment parameter. The area under the curve represents the energy of adhesion and the higher the value, the greater the work required to separate the adhesive probe. The adhesiveness is the work required to overcome the forces of attraction between the adhesive surface and the probe.

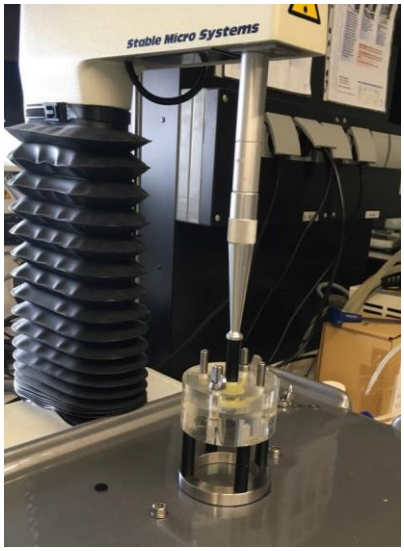

Figure 4.2 – TA.XT Plus Texture analyzer equipped with a mucoadhesive rig for the evaluation of adhesive properties with probe P/10.

4.2.4. Assay of OL and SV into oral films

For the quantification of OL and SV a pre-defined area of the films (1 cm^2) was cut and dissolved in 10 mL of mobile phase. For improving the extraction process the samples were placed on vortex mixing for 3 min and placed for 30 min in an ultrasonic bath at 60°C. At the end of the process the samples were placed on an orbital shaker for 12 hours. Finally, the samples were filtered (0.22 μm) and the drugs quantified by HPLC. Three assays were carried out for each film. Results are presented as mean ± standard deviation (SD).

4.2.5. *In vitro* release studies

Two *in vitro* tests were performed to simulate the route of an oral film in the body. The first test was performed for mimicking the mouth conditions with simulated saliva, and the second test was used for simulating the gastrointestinal tract conditions.

The first dissolution test was performed using USP apparatus 2 (paddles) and the second USP apparatus 1, the rotating basket (VK 7000 Dissolution Testing Station,

VanKel, USA). These consist of a metallic drive shaft connected to the paddles or to a cylindrical basket. The paddles or basket are positioned inside a vessel and the temperature of the vessel is kept constant using a water bath (for details see Chapter 1).

Dissolution profiles for the various oral films were obtained, and an area of 15.4 cm^2 was cut for films containing only HPMC and an area of 13.75 cm^2 was considered for films with HPMC and plasticizer.

Simulated saliva was composed of phosphate buffered saline (2.38 g Na_2HPO_4, 0.19 g KH_2PO_4 and 8.00 g NaCl per liter of ultrapurified water, adjusted to pH 6.8 with phosphoric acid)[11]. Each film sample was glued with double glue tape to a glass slide and placed on the bottom of the vessel so that the adhesive remained on the upper side of the glass slide. The dissolution study was performed using USP apparatus 2 method of dissolution at 37°C and 50 rpm using 300 mL of phosphate buffered saline, as the dissolution medium, for six trial runs. Samples corresponding to 900 µL were withdrawn at time intervals of 2.5, 5, 10, 15, 20 and 30 minutes, and an equivalent volume of dissolution medium was replaced. In the collected samples an equivalent volume of mobile phase was added and quantitated by HPLC, as described in section 4.2.7.

In order to simulate the conditions of fasted human gastrointestinal tract (GIT), the cut samples (see Figure 4.3) were placed in pH 1.2 (simulated gastric fluid without enzymes, USP XXV) for 2 h and, subsequently, in pH 6.8 (simulated intestinal fluid without enzymes, USP XXV) for 6 h at 37°C. Six runs were performed for each film, where each glass vessel contained 300 mL of medium and the baskets were set at a speed of 50 rpm. Samples (900 µL) were collected from the same point at 0.25, 0.5, 1, 2, 3, 4, 6 and 8 hours, and an equivalent volume of respective dissolution medium was replaced. For the collected samples an equivalent volume of mobile phase was added and quantitated by HPLC.

The dissolution profiles were obtained by representing the cumulative percentage of drug released as a function of time, and calculated by the following equation:

$$Release(\%) = \frac{(drug\ amount\ released)}{(total\ amount\ of\ drug\ in\ films)} \times 100 \qquad (4.3)$$

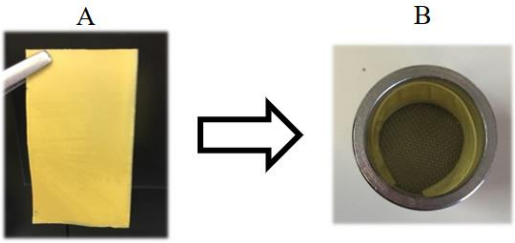

Figure 4.3 – Unfolded film (A) and film cut inside the basket (B).

4.2.6. Determination of pH

The pH of the relevant solutions was measured, using a digital pH meter Consort C3010 (Dias de Sousa, Portugal), previously calibrated using buffer solutions with pH of 4.00, 7.00 and 10.01.

4.2.7. HPLC determination of OL and SV

The quantification of drugs, OL and SV, was performed using a HPLC method previously validated[12]. Some alterations were made for producing an adequate method for the analysis.

A Shimadzu LC-2010HT apparatus equipped with a quaternary pump (LC-20AD), an autosampler unit (SIL-20AHT), a CTO-10AS oven, and a SPD-M2O4 detector was employed. The column used for the analysis was a RP18 (LiChroCART®, HPLC-Cartridge), with 5 µm particle size, 4.6 mm internal diameter, and 250 mm length. Chromatographic analysis was conducted in isocratic mode, and the mobile phase consisted of a mixture of ammonium acetate aqueous solution (0.02M): methanol: acetonitrile of 20:40:40 (v/v/v) at a constant flow rate of 1.1 mL/min. A run time of 15 min was established for separation of the three analytes, SVA, OL and SV. These were eluted at 4, 6 and 12 min, respectively. The detection was carried out at 230 nm, and an injection volume of 10 µL was used for all standards and samples. Individual stock solutions were first prepared. To obtain simvastatin acid a solution of simvastatin at a concentration of 2 mg/mL in methanol (HPLC) was prepared. An equivalent volume of a 0.02 M NaOH was added to the solution, which as placed in a bath of 60°C for 45 minutes. The solution was neutralized to pH = 7 with a solution of 1 M HCl. The stock solutions of OL and SV were prepared using 1 mg/mL of drugs in methanol (HPLC).

The results were processed using a Shimadzu LC-solution version 1.12 software.

4.3. References

(1) PDMS Mold Preparation Procedures http://www.digitaladdis.com/sk/PDMS_Mold_Preparation_Kassegne_MEMSLab.pdf (accessed Apr 15, 2016).

(2) Vitorino, C.; Almeida, J.; Gonçalves, L. M.; Almeida, A. J.; Sousa, J. J.; Pais, A. A. C. C. Co-Encapsulating Nanostructured Lipid Carriers for Transdermal Application: From Experimental Design to the Molecular Detail. *J. Control. Release* **2013**, *167*, 301–314.

(3) Vitorino, C.; Carvalho, F. A.; Almeida, A. J.; Sousa, J. J.; Pais, A. A. C. C. The Size of Solid Lipid Nanoparticles: An Interpretation from Experimental Design. *Colloids Surfaces B Biointerfaces* **2011**, *84*, 117–130.

(4) Mendes, M.; Soares, H. T.; Arnaut, L. G.; Sousa, J. J.; Pais, A. A. C. C.; Vitorino, C. Can Lipid Nanoparticles Improve Intestinal Absorption? *Int. J. Pharm.* **2016**, *515*, 69–83.

(5) Kathe, N.; Henriksen, B.; Chauhan, H. Physicochemical Characterization Techniques for Solid Lipid Nanoparticles: Principles and Limitations. *Drug Dev. Ind. Pharm.* **2014**, *40*, 1565–1575.

(6) Malvern Instruments Ltd. Dynamic Light Scattering: An Introduction in 30 Minutes. *DLS Tech. note* **2015**, *MRK656-01*, 1–8.

(7) Doktorovova, S.; Souto, E. B. Nanostructured Lipid Carrier-Based Hydrogel Formulations for Drug Delivery: A Comprehensive Review. *Expert Opin. Drug Deliv.* **2009**, *6*, 165–176.

(8) Clogston, J. D.; Patri, A. K. Zeta Potential Measurement. *Charact. nanoparticles Intend. drug Deliv.* **2011**, *1*, 63–70.

(9) Bergeron, V.; Cooper, P.; Fischer, C.; Giermanska-Kahn, J.; Langevin, D.; Pouchelon, A. Polydimethylsiloxane (PDMS)-Based Antifoams. *Colloids Surfaces A Physicochem. Eng. Asp.* **1997**, *122*, 103–120.

(10) Garrett, P. R. Defoaming: Antifoams and Mechanical Methods. *Curr. Opin. Colloid Interface Sci.* **2015**, *20*, 81–91.

(11) Gupta, M. M.; Patel Mitul, G.; Kedawat, M. Enhancement of Dissolution Rate of Rapidly Dissolving Oral Film of Meclizine Hydrochloride by Complexation of Meclizine Hydrochloride with β-Cyclodextrine. *J. Appl. Pharm. Sci.* **2011**, *1*, 150–153.

(12) Vitorino, C.; Sousa, J. J.; Pais, A. A. C. C. A Rapid Reversed-Phase HPLC Method for the Simultaneous Analysis of Olanzapine and Simvastatin in Dual Nanostructured Lipid Carriers. *Anal. Methods* **2013**, *5*, 5058–5064.

Chapter 5

Results and Discussion

Results on the production of particles and oral films are presented. Also included are the *in vitro* assays of the oral films in simulated saliva and in simulated conditions along the gastrointestinal tract. The computational approach involving the previously developed scripts is also employed and discussed.

5.1. Co-encapsulation lipid nanoparticles: up-scaling production and characterization

Preliminary studies concerning the scale-up procedure of the formulation were firstly carried out, so as to provide a reasonable batch size to support the further production of the films. For that, batches with different volumes, times and preparation procedures were studied and validated. A multiple 200 mL batches containing tripalmitin and oleic acid (15% w/w, at a ratio of 50:50), olanzapine and the same amount of simvastatin (5% w/w) and an aqueous solution of Tween 80 (3% w/v, 200 mL) was obtained after using an Ultra-Turrax for 1 min and preheated HPH for 16 minutes and 40 seconds. The same procedure method was employed in batches prepared, to assure the quality of the production of oral films and prevent errors associated to batch-to-batch variability. Thus, it was expected that the amount of the olanzapine (OL) and simvastatin (SV) would be the same in each film.

5.1.1. Lipid phase composition

The choice of tripalmitin and oleic acid is based on the previous studies[1]. The solubility of the different drugs in the lipids is detailed in Table 5.1. Both liquid and solid lipids were selected for ensuring maximal solubility of both drugs and increasing drug loading. Simvastatin solubility in tripalmitin is higher, when compared to that of olanzapine. To increase the co-encapsulation of the two drugs, oleic acid (used as lipid liquid) is added, once the solubility of olanzapine in this lipid is higher.

Table 5.1 – Solubility of simvastatin (SV) and olanzapine (OL) in the different lipids. Values are expressed as mean ± SD. Data reproduced from ref. 1.

Lipid	SV	OL
Tripalmitin (mg/g)	34.5 ± 4.1	< 12
Oleic Acid (mg/mL)	17.1 ± 0.2	177 ± 5

5.1.2. Characterization

To ensure the efficiency and quality of the procedure for producing nanoparticles, the polydispersity index (PI), particle size (PS) and zeta potential (ZP) were evaluated (see Table 5.2). The stability of loaded lipid nanoparticles (LLN) was also monitored after 30 days of production to assess the impact of the storage temperature.

High-pressure homogenization time, shear stress, cavitation forces, lipid ratio and surfactant concentration are some factors that can change the particle size. The values chosen for these parameters, considered as optimized to obtain a size in the nanoparticles region, are described in previous papers of the group[2]. In the present work, the particle size for the LLN produced is 149 nm, without significant variations after 30 days.

In what concerns the polydispersity index (PI), an ideal value will be lower than 0.1, although in literature a value lower than 0.3 is considered acceptable[3]. For the LLN produced, the PI values measured after production (0.153) and 30 days at 4°C (0.166) were considerably lower than those reported in the literature. In this way, the nanoparticles can be considered monodisperse and homogeneous, without formation of aggregates even after 30 days of storage.

A high value of zeta potential (> |30| mV) suggests the presence of a large repulsion between particles, indicating lower aggregation. In the case of the nanoparticles produced, despite the ZP values are slightly higher (towards positive values) than -30 mV, formulations can be generally considered suitable for the purpose of this study. Note that this aspect is not critical, since formulations will be further jellified.

Table 5.2 – Polydispersity index (PI), particle size (PS) and zeta potential (ZP) of LLN after 30 days of storage at 4°C. Results are expressed as mean ± SD, n=3.

	PI	PS (nm)	ZP (|mV|)
day 1	0.153 ± 0.027	149 ± 6.63	22.7 ± 3.45
day 30	0.166 ± 0.012	144 ± 3.20	24.7 ± 0.21

5.1.3. Drug loading and entrapment efficiency

The entrapment efficiency of SV and OL in the LLN, as described in the previous chapter, Equation (4.1), was determined by measuring the concentration of free drug in the aqueous phase of the nanoparticle dispersion. Equation (4.2) was used to calculate the total drug loading of nanoparticles.

Achieving a high drug loading is attractive in the way to improve the potential and performance of pharmaceutical products[4]. For lipophilic drugs, retention efficiency values between 90% and 98% are expected, whereas for hydrophilic compounds the loading capacity and the entrapment efficiency are lower[5]. There are several factors that can affect the drug loading in the lipid, specifically the properties of lipids in which the drugs will be solubilized. For drugs that are highly soluble in the molten lipid, a sufficient drug loading is warranted.

LLN presented an entrapment efficiency higher than 96% for both drugs and a drug loading of 5.2% and 4.9% for SV and OL, respectively (see Table 5.3). This supports their suitability to co-encapsulate OL and SV.

Table 5.3 – Entrapment efficiency (%EE) and drug loading (%DL) into co-encapsulate of OL and SV in the LLN. Results are expressed as mean ± SD, n=3.

	%EE	**% DL**
OL	96 ± 1.00	4.9 ± 0.2
SV	99 ± 0.97	5.2 ± 0.3

5.2. Oral films: pre-formulation studies

After characterization and evaluation of the quality of the nanoparticles loaded with OL and SV, hydroxypropyl methylcellulose (HPMC) was included in the formulations so as to provide suitable intermediate products for the manufacturing of final oral films. Several tests were then performed. HPMC powder 1% w/w and 1.5% w/w of HPMC were added directly to the LLN and left hydrated under stirring. The formation of clumps that led to the appearance of a heterogeneous dispersion, with HPMC quickly precipitating, was observed. The clumps were well visible when these formulations were casted to compose the oral films, which compromised the uniformity of the films. It was also tried to perform the mixture in a water bath but without significant improvements.

To overcome this problem, hydrogels containing 2% w/w of each HPMC grade were previously prepared in ultra-purified water at 80°C under mechanical stirring.

Subsequently, the hydrogels were mix with the LLN accordingly, yielding to a considerably homogeneous dispersion.

When the films were deposited and placed in the oven at 40ºC, a number of air bubbles emerged, and were visible by the end of the drying process. These can be explained by the presence of a surfactant and by the agitation process, during the blending of LLN with the hydrogel, introducing air in the oral films. Based on anti-foam properties of PDMS, 1% of this polymer was added to the total mass of the final formulation to produce oral film, resulting in a considerably reduction of air bubbles. Moreover, techniques such as ultrasonication, vacuum exposition and centrifugation were used in an attempt to remove the air bubbles. Independent tests were performed with each of these techniques. Better results were obtained when centrifugation was applied yielding to a bubble-free product.

The ratio of hydrogel to LLN was also assessed. Two LLN:hydrogel ratios, 50:50 and 75:25, were tested. By visual inspection, it was observed that the film with a lower amount of hydrogel (50:50 ratio), displayed higher uniformity and detached more easily than the film containing a lower percentage of hydrogel (75:25). The latter, also evidenced a loss in elasticity and resistance. This led to the selection of the proportion 50:50 as optimal to proceed with the studies.

Table 5.4 summarizes the composition of the final oral films. In the sections that follow, the impact of the incorporation of HPMC and plasticizer on the oral films will be sequentially inspected.

Table 5.4 – Composition (%) of formulations to prepare oral films. Each oral film contains the same amount of loaded lipid nanoparticles (LLN). (a) represents the percentage of HPMC polymer and plasticizer (PEG 400) added in the production of hydrogel.

Film code	LLN	HPMC[(a)]	PEG 400[(a)]	Water	PDMS
F100SR	50	2	–	47	1
F4000SR	50	2	–	47	1
F15000SR	50	2	–	47	1
F100000SR	50	2	–	47	1
F100SR[P]	50	2	2	45	1
F100000SR[P]	50	2	2	45	1

5.3. Oral films: impact of HPMC

5.3.1. Assay of OL and SV in oral films

As described in Chapter 4, oral films containing various grades of HPMC were produced under the same conditions. However, it is necessary to take into consideration the different molecular weights for each HPMC grade and, consequently, different viscosities, which can modify the consistency and net structure of the polymer.

Since the procedure method to prepare LLN batches was the same it was expected that all films would have the same amount of drug, Table 5.5 presents the amount of each drug in 1 cm^2 for each film. It is interesting to observe that, for both drugs, the film with the higher molecular weight polymer (F100000SR) yielded the highest amount of OL and SV. Conversely, F100SR contains the lowest amount of both drugs per square centimetre. Complementary parameters such as thickness were also analysed (see Table 5.6). A higher thickness of F100000SR may also contribute to a larger amount of drug per area. For the films that present a higher amount of both drugs (F4000SR and F100000SR), the percentage of OL and SV in each millimetre (ratio between thickness (mm) and quantity (mg/cm^2)) is slightly higher in F4000SR than F100000SR.

Table 5.5 – Amount of olanzapine (OL) and simvastatin (SV) per square centimeter (mg/cm^2) for the oral films produced with different polymers (F100SR, F4000SR, F15000SR and 100000SR). Results are expressed as mean ± SD, n=3.

OL (mg/cm^2)			
F100SR	**F4000SR**	**F15000SR**	**F100000SR**
0.832 ± 0.025	0.903 ± 0.017	0.856 ± 0.016	0.986 ± 0.018
SV (mg/cm^2)			
F100SR	**F4000SR**	**F15000SR**	**F100000SR**
0.941 ± 0.020	1.127 ± 0.026	1.045 ± 0.007	1.184 ± 0.015

Table 5.6 – Thickness (µm) of oral films produced with various polymers measured at different points. Results are expressed as mean ± SD, n=3.

F100SR	**F4000SR**	**F15000SR**	**F100000SR**
47 ± 7	46 ± 2	49 ± 4	50 ± 5

These results are compatible with the difficulties during the manufacturing process of oral films already reported. A batch-to-batch variability may also affect the consistency in the results obtained by the assay of OL and SV in oral films.

These *in vitro* assays are an important approach for establishing the release of a drug in a compartment on the human body. However, in future work, complementary studies to estimate the absorption percentage of each drug, and to adjust the producing method of LLN to daily dose, will be produced.

5.3.2. Adhesive properties

The use of lipid nanoparticles to produce oral films, increases bioavailability and improves drug delivery, due to reduction of particle size. Oral films should reveal good adhesive properties so as (i) to be retained in the mouth and (ii) to improve the distribution of drug throughout the gastrointestinal tract (GIT).

The adhesive properties of each polymer are summarized in Table 5.7. Films can be ordered by increasing adhesiveness as F15000SR < F4000SR < F100000SR < F100SR. Interestingly, the molecular weight of the polymer was not the dominant property in governing the adhesive properties. The 100SR polymer led to better results of adhesiveness as well as energy of adhesion, while the polymer that provided a larger distance to the separation of the film to the probe was 4000SR.

Table 5.7 – Adhesiveness (g), energy of adhesion (g.sec) and distance to separation (mm) for different oral films. Results are expressed as mean ± SD, n=6.

	Adhesiveness (g)	**Energy of Adhesion (g.sec)**	**Distance to separation (mm)**
F100SR	253 ± 62.7	8.55 ± 5.93	1.70 ± 0.35
F4000SR	95.2 ± 77.6	7.26 ± 2.97	2.37 ± 0.56
F15000SR	56.7 ± 26.8	2.72 ± 0.83	1.43 ± 0.84
F100000SR	155 ± 61.8	5.32 ± 0.68	1.03 ± 0.46

5.3.3. *In vitro* release studies

In vitro release studies are an important tool for quality control purposes as well as for prediction of the *in vivo* performance of drug delivery systems. These have become essential in for drug development, being adopted in the United State Pharmacopeia (USP). Release studies provide preliminary information for describing the characteristics of the drug formulation and are capable of discriminating the final products in terms of release controlling mechanism. *In vitro* release studies should simulate *in vivo* conditions that, in this case, is intended to discriminate physiological conditions in the buccal cavity and on the gastrointestinal tract. Several parameters can be adapted to improve the quality of the

assay, such as volume, composition and viscosity of the simulated medium, the presence of enzymes and motility. In this study, two distinct *in vitro* studies are performed for (i) simulating conditions in the mouth during 30 minutes with simulated saliva at pH 6.8, as a medium, and (ii) discriminating the conditions along the GIT, in which the medium was switched after 2 hours of the test from pH 1.2 to pH 6.8. Two different release profiles corresponding to OL and SV were considered. The latter, represents the addition between the amount detected of inactive drug and the active form (simvastatin acid).

In vitro tests were initially performed with the HPMC films without plasticizer, in the simulated saliva medium at pH 6.8. The resulting dissolution profiles for OL and SV are shown in Figure 5.1. It is observed that within 30 minutes of the assay, no more than 10% of each drug is released in the formulations under study. In this period of time, the films do not disintegrate, resulting in a solid matrix that is easily disrupted with the touch. Unexpectedly, film F100SR was the one that determined a higher control of the release of both drugs in this medium. The HPMC that offered a lower control in the release of olanzapine was 4000SR and, for simvastatin, both 4000SR and 100000SR did not provided this control. With this assay, it was observed that these oral films were not absorbed sublingually. In the next step, absorption along the GIT are evaluated.

In this, each oral film was introduced in a solution at pH 1.2, in the first 2 hours, and switched to pH = 6.8 for the remaining 6 hours of the assay. The dissolution values used as a reference for OL and SV were the same as those referenced in Chapter 2 in section 2.2.2. From the analysis of Figure 5.2, it is simple to realize that there is no significant effect of any type of HPMC on the olanzapine release control. With the exception of the F15000SR film, all the others displayed a complete release, close to 100%. It should be noted that in all polymers, OL was only released within the first 2 hours (pH = 1.2) without significant changes for the remainder of the assay. Olanzapine displays a pKa = 7.24 (constant by *DrugBank*[6]), and in the stomach (acidic pH), the drug is in the ionized form, possessing charge and a high polarity, which makes difficult diffusion through the plasma membrane. In turn, at a basic and neutral pH, as in the intestine, some OL is in the non-ionized form, which allows the respective absorption. As such, with the films under study, it is considered that OL is released and subsequently absorbed along the gastrointestinal tract. Observing the dissolution profiles it is difficult to infer on which polymer better controls the release of OL. By magnifying the release data in the first two hours of the assay, a separation between the films with two polymers with lower molecular mass and the other two (F15000SR and F100000SR) is easily

observable. At 15 and 30 minutes time points, the differences between these films were approximately 20%, on percentage released, and in the following points the release value was close to the asymptotic value of 100%, except for the F15000SR film, for which no more than 80% of the OL content was released.

The dissolution profiles of simvastatin in the oral films contrast with those of olanzapine (see Figure 5.3). In the reference profile of SV, the drug is immediately released. In the oral films tested, the presence of the polymer seems delaying the release of drug. In some way, HPMC polymer protects SV from contact with acid pH, and the release starts at pH 6.8. For F100SR, in the first two hours, a small amount of drug was released: this is probably due to the fact that this is the polymer with the lower molecular weight. These are interesting results, because, since SV is only released in a basic medium (intestine) becoming available for absorption. Since SV is a prodrug, it is carried along the portal vein to the liver to be metabolized.

The interactions between the drugs and the HPMC polymer can affect the ability of HPMC to hydrate. In this situation, the gel layer becomes more fragile and less able to resist under erosional stress[7]. In this way, the properties of each drug, such as the respective dimension or molecular weight, can affect the erosion rate and consequently, the amount released over time. Thus, it is suggested that the interactions between HPMC and SV are stronger than those with OL. Taking into account the chemical structure of each drug (see Figure 3.3), the number of donor and electron acceptor groups is the same for OL and SV, but SVA has one more acceptor bond[8–10]. In future work, further insigths on the interactions between these drugs and HPMC will be provided, resorting to computational approaches.

In what pertains to SV, there is a direct relationship between the molecular weight of the polymer and the control on drug release. The least controlling film was the one containing the 100SR polymer, corresponding to a drug release of 30%. The other polymers followed the order of the respective molecular weight: 4000SR, 15000SR and 100000SR. Surprisingly, F100SR released approximately the double than the other films polymers. Despite the low amount of drug dissolved, it is expected that, in the human body, more drug is released once the residence time in the intestine exceeds 6 hours.

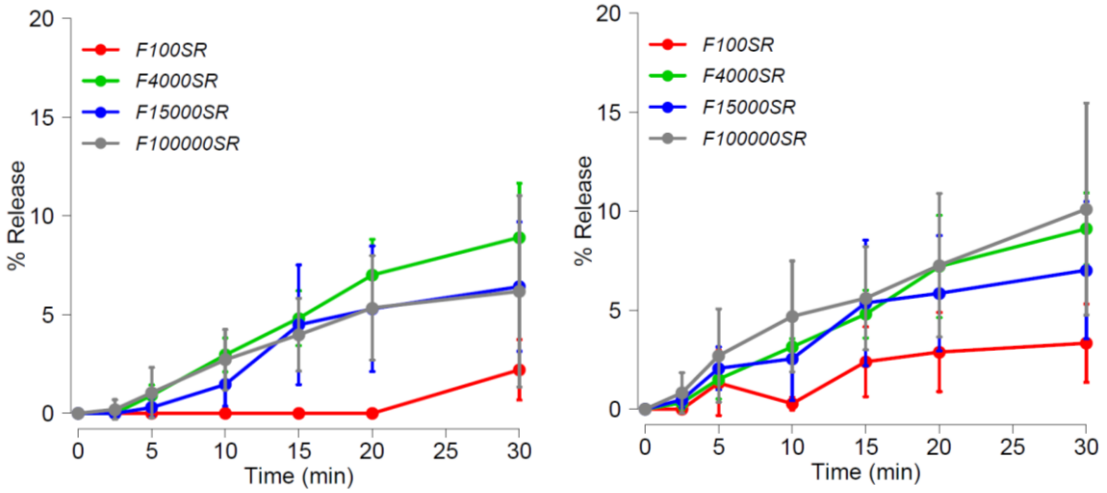

Figure 5.1 – Dissolution profiles of (left) olanzapine (OL), and (right) simvastatin (SV) for the oral films under study. The assays were performed with simulated saliva medium at pH = 6.8 over 30 minutes (mean ± SD, n=6).

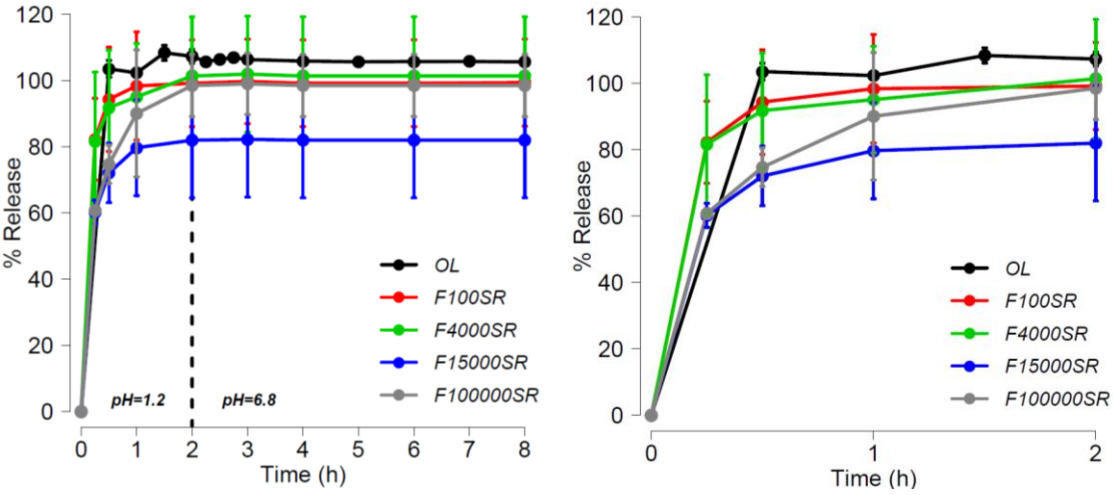

Figure 5.2 – Release profiles of olanzapine in films containing different polymers along the simulated GIT (mean ± SD, n=6). The assays were performed in the first two hours at a pH of 1.2, switched to pH = 6.8, and compared with the reference drug product. On the right, the release of the first two hours of assay is enlarged.

5.4. Oral films: impact of plasticizer

5.4.1. Assay of OL and SV in oral films

Films combining the plasticizer PEG 400 in the same weight percentage as the HPMC polymers, in the hydrogels, were also studied. The polymers 100SR and 100000SR were selected because they possess lower and higher molecular masses. The quantity assay of OL and SV and the film thickness are described in Tables 5.8 and 5.9, respectively.

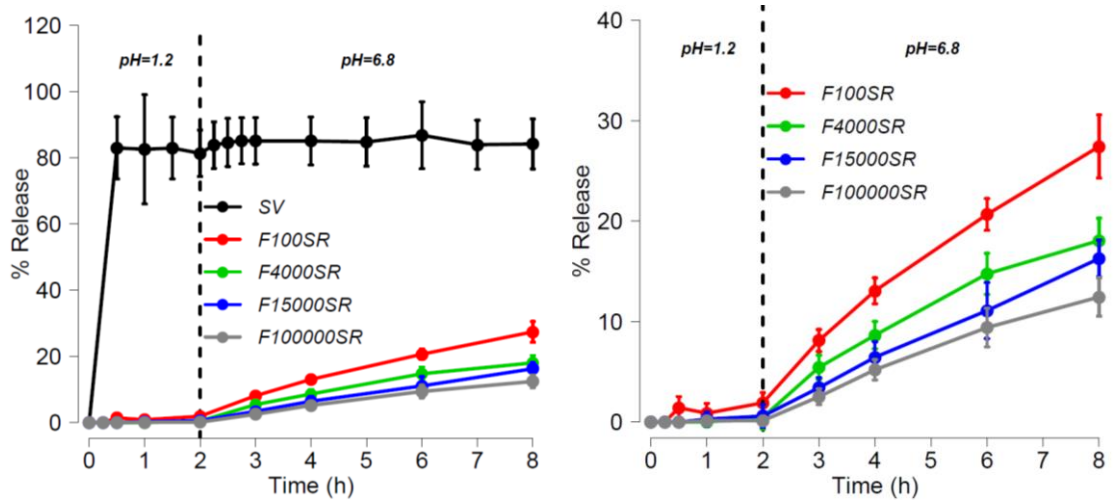

Figure 5.3 – Release of simvastatin in films with different polymers along the GIT (mean ± SD, n=6). The assays were performed in the first two hours at a pH of 1.2 and then switched to pH = 6.8. On the right, dissolution profiles without reference drug product.

The final thickness of the films with PEG 400 is approximately the same, slightly lower for films without plasticizer. In the dosing assays of films containing plasticizer, the amount of drug per square centimeter is approximately two times higher than the films without plasticizer. These results cannot be directly compared, since the ratio of the final formulation deposited per area in each material is different, higher in the backing layer. However, it is interesting to highlight the changes of the preparation of oral films, including the addition of plasticizer and exchange of deposition material. In the petri dish, the final film was detached slightly better than in the backing layer. In fact, the incorporation of PEG 400 in films was already reported due to the ease removal from the mould[11]. Indeed, when a plasticizer is added to a polymer, the glass transition temperature decreases, which makes the final film more malleable and flexible[12,13]. PEG 400 possesses has particularity of increasing the permeation of the water vapor across the polymer, and in this way, the solvent evaporates more easily[14]. Proportionally, more pores are opened to the passage of humidity and this explain why the incorporation of the plasticizer leads to a more effective drug extraction process, and to the increase of the drug amount per square centimeter. Coherently, the same trend was observed by Barhate et al.[15] when PEG 400 was used. In this way, the addition of plasticizer decreases the retention of drugs in the matrix, improving the total amount released. This must be addressed in detail in future work.

Table 5.8 – Amount of olanzapine (OL) and simvastatin (SV) per square centimeter (mg/cm^2) for the oral films F100SR and F100000SR with PEG 400 as plasticizer [P]. Results are expressed as mean ± SD, n=3.

OL (mg/cm^2)	
F100SR[P]	**F100000SR[P]**
1.558 ± 0.223	1.582 ± 0.203
SV (mg/cm^2)	
F100SR[P]	**F100000SR[P]**
1.661 ± 0.227	2.089 ± 0.243

Table 5.9 – Thickness (µm) of F100SR and F100000SR oral films produced with PEG 400 as plasticizer [P], measured at different points. Results are expressed as mean ± SD, n=3.

F100SR[P]	**F100000SR[P]**
44 ± 1	46 ± 1

5.4.2. Adhesive properties

The adhesive properties of the films containing the plasticizer were also inspected and compared with the films in the absence of plasticizer. The results are summarized in Table 5.10. The addition of plasticizer increased substantially the energy of adhesion, especially for F100SR[P]. However, the adhesiveness and distance to separation decreased with the addition of plasticizer.

Table 5.10 – Adhesiveness (g), energy of adhesion (g.sec) and distance to separation (mm) for oral films produced with plasticizer and compared to correspondent oral films in the absence of plasticizer. Results are expressed as mean ± SD, n=6.

	Adhesiveness (g)	**Energy of Adhesion (g.sec)**	**Distance to separation (mm)**
F100SR	253 ± 62.7	8.55 ± 5.93	1.70 ± 0.35
F100SR[P]	173 ± 48.8	91.8 ± 35.4	0.11 ± 0.01
F100000SR	155 ± 61.8	5.32 ± 0.68	1.03 ± 0.46
F100000SR[P]	25.5 ± 17.4	36.0 ± 24.2	0.04 ± 0.01

5.4.3. *In vitro* release studies

The dissolution profiles of OL and SV into the oral cavity and in the simulated GIT conditions for the films, in which plasticizer (PEG 400) was added to HPMC for the

formation of the hydrogel, were also addressed. Figure 5.4 shows the drug release profiles in the assay with simulated saliva medium. The results for the films with plasticizer, represented by [P], were identical for OL and SV, registering a higher control on drug release in F100000SR[P]. The reverse occurred when the films without plasticizer were compared: the final drug amount released from F100SR was identical to that of F100000SR[P]. In the assays performed to simulate the passage in the GIT, the release of drugs in the films containing plasticizer followed the same order, in terms of polymer used, as that of the films in the absence of plasticizer (see Figures 5.5 and 5.6). F100SR[P] is the one that less controls the release of SV, allowing, however, almost doubling the release of SV in F100SR. These results can be explained by the fact that in the presence of plasticizer, more pores are opened, increasing the exposition of matrix to erosion. In summary, from these results it can be concluded that the addition of plasticizer increases SV release for the film containing the polymer with lower molecular weight, i.e. the release is less controlled. For F100000SR[P], a higher control in the SV release is observed.

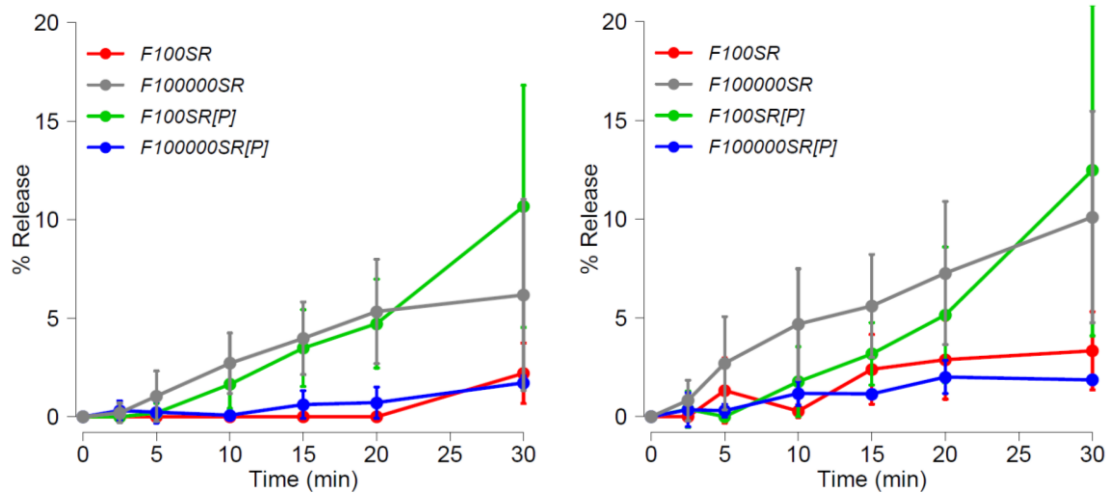

Figure 5.4 – Dissolution profiles of (left) olanzapine (OL), and of (right) simvastatin (SV) in simulated saliva medium at pH=6.8 over 30 minutes (mean ± SD, n=6). The films with plasticizer are identified with [P] after the polymer grade. Films in the absence of plasticizer are also shown for comparison purposes.

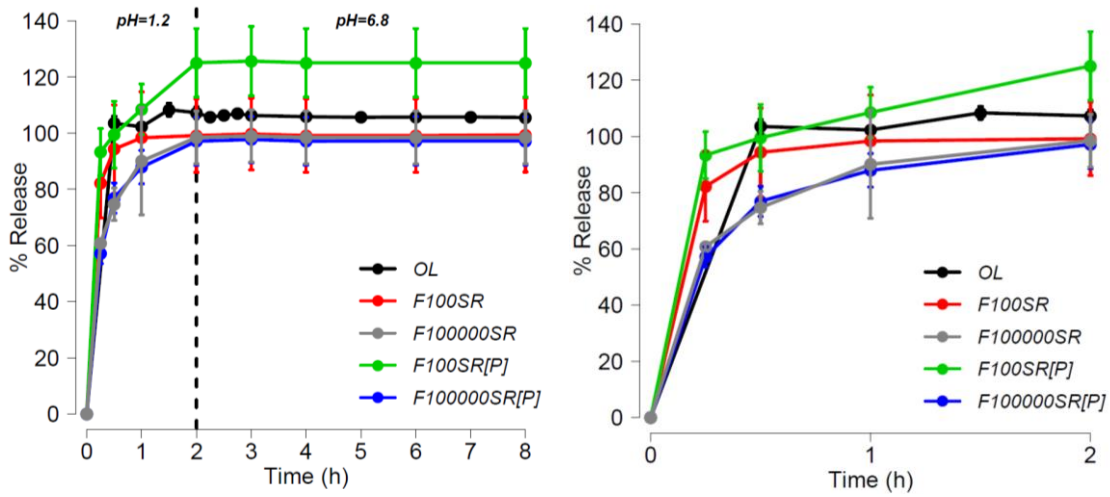

Figure 5.5 – Release of olanzapine in films in which HPMC polymers are blended with plasticizer ([P]) and in the absence of PEG 400 along the simulated GIT (mean ± SD, n=6). The assays were performed in the first two hours at a pH of 1.2, switched to pH = 6.8, and compared with the reference drug product. On the right, the release of the first two hours of assay is enlarged.

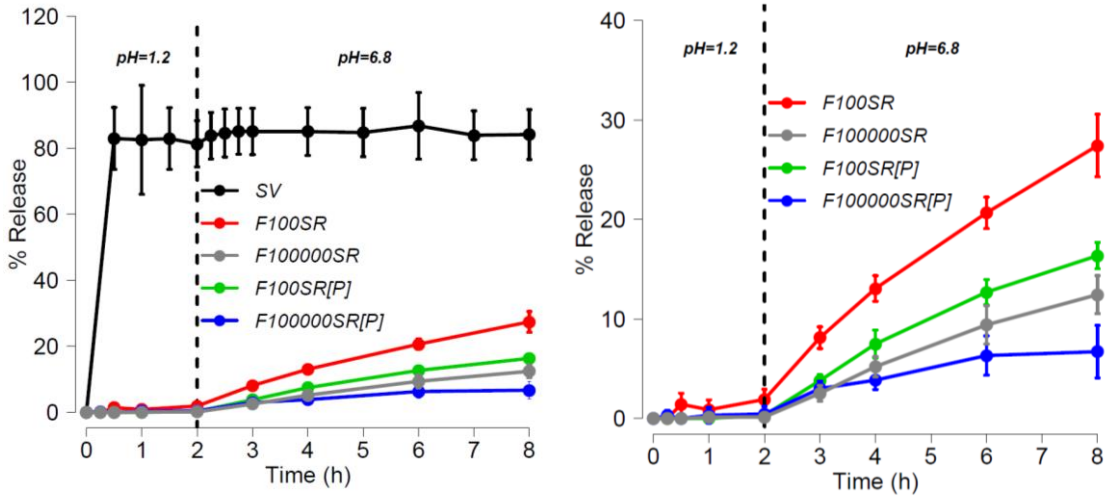

Figure 5.6 – Release of simvastatin in films containing polymers blended with plasticizer ([P]) and in the absence of PEG 400 along the simulated GIT (mean ± SD, n=6). The assays were performed in the first two hours at a pH of 1.2 and then switched to pH = 6.8. On the right, dissolution profiles obtained are enlarged.

5.5. Computational approach

In what follows, the dissolution profiles will be analyzed resorting to the approaches and scripts developed.

5.5.1. Independent approaches

Calculations of fit factors were performed for the dissolution profiles obtained from the *in vitro* assays of films, in the presence/absence of plasticizer, along the gastrointestinal tract. These factors cannot be measured for the reference values of OL and SV previously applied, because the time points are different from the sampling times of the *in vitro* assay of the oral films.

The parameter f_2 was calculated between all dissolution profiles of OL for the films containing the different polymers and considering the effect of introducing the plasticizer. The similarity factors for different releases are presented in Table 5.11. Two calculations were carried out, one complies the requirements of the EMA guideline, and the other considers all dissolution points. From the results it can be seen that, when the limit required by the guideline was employed, a more precise and similarity values were obtained, avoiding false positives and false negatives. At the same time, the similarity between films F100SR[P] and F100SR, and between F100000SR[P] and F100000SR for OL was confirmed.

From the f_2 calculated, the SV profiles were similar to each other. The f_1 was calculated, and the respective values are presented in Table 5.12. It can be observed that f_1 varies according to the reference values used, as represented by Equation (1.5). Assuming a dissolution profile of the oral film as a reference, it was possible to identify differences from the remaining films. The film which displayed the smallest sum of f_1 in each row of Table 5.12, was the film that, overall, less differs from the others. The sum of each column allows to identify the most similar film when it is used as the test product and the other films as reference. This provided an estimate of similarity, and can be considered as the mean value for the dissolution profiles under study. F100SR[P] and F15000SR[P] present lower sums when they are used as a reference and as test product, respectively. The lowest value of f_1 is located in the intersection of the row and the column of the respective films. This validates the smaller difference between the SV release profiles.

The MDT calculation of the dissolution profiles for OL and SV is shown in Table 5.13. In OL two groups are identified, one with films F100SR, F4000SR and F100SR [P] and the other by films F15000SR, F100000SR and F100000SR [P]. The closest values of MDT in the first group explains the similarity presented in Table 5.11. In the second group similarity occurs between the same polymers grades. It is also interesting to evaluate the consistency of results between these two different methods. For SV, there

are two very close MDT values, corresponding to the films F15000SR and F100SR[P]. From Table 5.12, the lowest value of f_1 corresponds to the comparison between the films F100SR [P] and F15000SR. Thus, similar MDT values represent the smaller differences between two dissolution profiles, and can be confirmed by f_1.

Table 5.11 – Similarity of OL dissolution profiles for oral films in the *in vitro* GIT simulation assay. Similarity factor as calculated according to the EMA guideline (85%) and for all points (AP). Key: S = Similar; NS = Not Similar.

		F4000SR	**F15000SR**	**F100000SR**	**F100SR[P]**	**F100000SR[P]**
F100SR	**85%**	S	NS	NS	S	NS
	AP	S	NS	NS	NS	NS
F4000SR	**85%**	–	NS	NS	S	NS
	AP	–	NS	S	NS	NS
F15000SR	**85%**	–	–	S	NS	S
	AP	–	–	NS	NS	NS
F100000SR	**85%**	–	–	–	NS	S
	AP	–	–	–	NS	S
F100SR[P]	**85%**	–	–	–	–	NS
	AP	–	–	–	–	NS

Table 5.12 – Calculation of the difference factor of SV dissolution profiles in the oral films, in the *in vitro* GIT simulation assay. *R* corresponds to the films used as reference (R_t) in the calculation of f_1 and *T* refers to the films established as test (T_t). In the last column and last row, the sum of the respective row and column is presented.

R \ *T*	**F100SR**	**F4000SR**	**F15000SR**	**F100000SR**	**F100SR[P]**	**F100000SR[P]**	*sum*
F100SR	–	35.52	48.12	59.38	44.65	72.29	259.96
F4000SR	55.08	–	21.27	37.52	14.16	58.37	186.39
F15000SR	92.76	26.43	–	87.27	96.04	71.00	373.50
F100000SR	146.19	59.56	27.72	–	37.09	38.34	308.90
F100SR[P]	80.65	16.49	9.05	27.22	–	52.13	185.54
F100000SR[P]	253.45	131.95	84.97	54.60	101.17	–	626.14
sum	628.14	269.96	191.13	265.98	293.10	292.12	

Table 5.13 – MDT values for the dissolution profiles of OL and SV in the films under study.

	F100SR	F4000SR	F15000SR	F100000SR	F100SR[P]	F100000SR[P]
OL	34.85	33.64	23.37	21.31	36.40	19.86
SV	3.10	2.31	2.02	1.60	2.03	1.03

5.5.2. Model dependent approaches

The mathematical models briefly summarized in Table 5.14 are some of the expressions used to fit points of dissolution to a curve, as explained in more detail in Chapter 1, section 1.2.2.

Table 5.14 – Release models tested.

Zero order	$c_1 t$
Higuchi	$c_1\sqrt{t}$
Korsmeyer-Peppas	$c_1 t^{c_2}$
First order	$c_2(1-\exp(-c_1 t))$
Weibull	$c_2\left(1-exp\left(-\frac{t}{c_1}\right)^{c_3}\right)$

The dissolution profiles obtained in the *in vitro* assay along GIT in films with the polymers under study, and in the presence/absence of plasticizer, were firstly studied, as an example for testing first order and Weibull models (see Table 5.15). Curve fitting with Higuchi and Korsmeyer-Peppas models are not used because the percent release is generally higher than 60% at the first release point. Presumably, the zero order model is not useful for studying these type of dissolution profiles, since they are characterized as displaying a very rapid release when dissolution starts, stabilizing after two hours. A low quality fit would, thus, be produced. The Weibull model is the one that better fits the points of dissolution in all oral films studied, as confirmed from the analysis of AIC and $R^2_{adjusted}$. The additional normalization parameter (c_2) does not impose a significant difference between the models, indicating that both first order and Weilbull models are establishing the same asymptotic limit.

Table 5.15 – Parameters for first order and Weibull models, AIC and $R^2_{adjusted}$ values for release profiles of olanzapine.

Function	Formulation	c_1	c_2	c_3	AIC	$R^2_{adjusted}$
fo	**F100SR**	6.97	99.00	–	16.54	0.9997
we		0.12	99.29	0.75	-4.01	0.99997
fo	**F4000SR**	6.40	100.02	–	39.94	0.9964
we		0.08	101.84	0.45	23.13	0.9995
fo	**F15000SR**	5.06	81.49	–	28.21	0.9986
we		0.17	82.12	0.69	-6.52	0.99997
fo	**F100000SR**	3.35	97.66	–	42.61	0.9953
we		0.28	99.15	0.68	24.95	0.9994
fo	**F100SR[P]**	4.80	121.85	–	58.00	0.9825
we		0.15	128.20	0.39	44.27	0.9965
fo	**F100000SR[P]**	3.32	96.47	–	36.86	0.9974
we		0.29	97.54	0.74	22.39	0.9995

The existence of lag time must be taken into account in the release profiles of SV. The t_{lag} parameter needs to be added to models, as exemplified with the Weibull model – Equation (2.1). Table 5.16 presents the results of each parameter for each model and the values for the selection indexes (AIC and $R^2_{adjusted}$). Once again, Weibull model was the one that best fitted the curve to the dissolution points in all oral films.

F100SR[P] was used as an example of application for the developed program directed to the prediction of the lag time. The comparison between the points and the best model to fit them (i.e. Weibull model) is presented in Figure 5.7. A small amount of SV was detected in 2 hours of the test, and this causes $t = 1$ to be the point prior to the start of the dissolution, i.e., where $f(t = 1) = 0$. The intersection with the time axis, performing the linear interpolation of the first two points in which SV was detected, is 1.91 h. Thus, as the time point 1.91 h exceeds than 1 h, $f(t = 1.91) = 0$ can be assumed. The fitted curve of the Weibull model begins before $t = 2$, as shown in Figure 5.7.

Table 5.16 – Parameters for release models under study, AIC and $R^2_{adjusted}$ values for release profiles of simvastatin.

Function	Formulation	c_1	c_2	c_3	AIC	$R^2_{adjusted}$
zo	**F100SR**	3.44	–	–	30.31	0.9813
hi		7.41	–	–	48.31	0.9220
kp		2.30	1.23	–	26.74	0.9905
fo		0.003	1051.63	–	32.57	0.9865
we		5.32	31.06	1.94	21.15	0.9953
zo	**F4000SR**	2.87	–	–	29.64	0.8438
hi		6.88	–	–	22.20	0.9901
kp		5.20	0.70	–	4.53	0.9980
fo		0.001	2639.70	–	31.88	0.9654
we		4.75	25.10	1.00	-7.08	0.9994
zo	**F15000SR**	2.00	–	–	23.35	0.9717
hi		4.24	–	–	39.50	0.9042
kp		1.01	1.39	–	10.70	0.9952
fo		0.003	732.03	–	25.59	0.9863
we		6.43	21.90	1.90	6.13	0.9972
zo	**F100000SR**	1.58	–	–	21.15	0.9646
hi		3.34	–	–	35.77	0.9017
kp		0.83	1.36	–	14.88	0.9881
fo		0.003	587.42	–	23.32	0.9822
we		4.89	13.22	2.34	2.12	0.9972
zo	**F100SR[P]**	2.53	–	–	24.60	0.8518
hi		6.01	–	–	24.70	0.9829
kp		4.03	0.79	–	1.70	0.9982
fo		0.001	2481.53	–	26.95	0.9642
we		4.62	21.94	1.13	-24.15	0.9999
zo	**F100000SR[P]**	0.90	–	–	13.56	0.9628
hi		1.96	–	–	25.95	0.9253
kp		0.75	1.10	–	15.04	0.9685
fo		0.01	172.59	–	15.60	0.9696
we		4.08	6.73	2.60	3.76	0.9915

The developed computational approach proves to be a useful tool for adjusting the dissolution profiles that display lag time, as those obtained with SV.

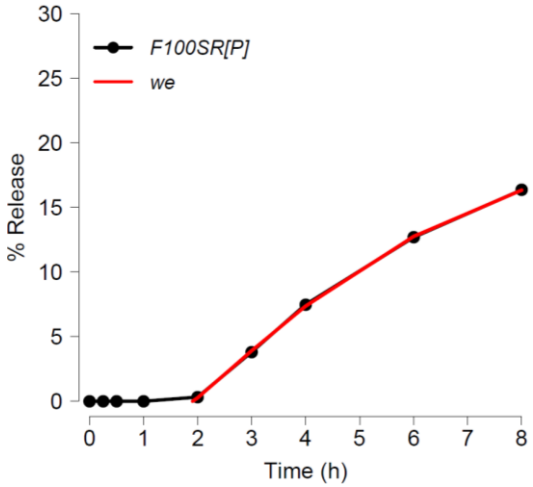

Figure 5.7 – Representation of dissolution profile for F100SR[P] and the respective fit using the Weibull model, considering the lag time.

5.6. References

(1) Vitorino, C. S. P. Lipid Nanoparticles Permeation Enhancement for Transdermal Drug Delivery, University of Coimbra - Faculty of Pharmacy, 2013.

(2) Vitorino, C.; Almeida, J.; Gonçalves, L. M.; Almeida, A. J.; Sousa, J. J.; Pais, A. A. C. C. Co-Encapsulating Nanostructured Lipid Carriers for Transdermal Application: From Experimental Design to the Molecular Detail. *J. Control. Release* **2013**, *167*, 301–314.

(3) Iqbal, M. A.; Md, S.; Sahni, J. K.; Baboota, S.; Dang, S.; Ali, J. Nanostructured Lipid Carriers System: Recent Advances in Drug Delivery. *J. Drug Target.* **2012**, *20*, 813–830.

(4) Müller, R. H.; Maaßen, S.; Weyhers, H.; Mehnert, W. Phagocytic Uptake and Cytotoxicity of Solid Lipid Nanoparticles (SLN) Sterically Stabilized with Poloxamine 908 and Poloxamer 407. *J. Drug Target.* **1996**, *4*, 161–170.

(5) Müller, R. H.; Mäder, K.; Gohla, S. Solid Lipid Nanoparticles (SLN) for Controlled Drug Delivery - A Review of the State of the Art. *Eur. J. Pharm. Biopharm.* **2000**, *50*, 161–177.

(6) Olanzapine, https://www.drugbank.ca/drugs/DB00334, (accessed Aug 20, 2018).

(7) Viridén, A.; Wittgren, B.; Larsson, A. The Consequence of the Chemical Composition of HPMC in Matrix Tablets on the Release Behaviour of Model Drug Substances Having Different Solubility. *Eur. J. Pharm. Biopharm.* **2011**, *77*, 99–110.

(8) Olanzapine, https://pubchem.ncbi.nlm.nih.gov/compound/olanzapine#section=Chemical-and-Physical-Properties, (accessed Aug 29, 2018).

(9) Simvastatin, https://pubchem.ncbi.nlm.nih.gov/compound/simvastatin#section=Chemical-and-Physical-Properties, (accessed Aug 29, 2018).

(10) Acetyl Simvastatin, https://pubchem.ncbi.nlm.nih.gov/compound/11812557#section=Chemical-and-Physical-Properties, (accessed Aug 29, 2018).

(11) Febriyenti; Noor, A. M.; Baie, S. B. B. Mechanical Properties and Water Vapour Permeability of Film from Haruan (Channa Striatus) and Fusidic Acid Spray for Wound Dressing and Wound Healing. *Pak. J. Pharm. Sci.* **2010**, *23*, 155–159.

(12) Sevgi Güngör, M. S. E. and Y. Ö. *Plasticizers in Transdermal Drug Delivery Systems, Recent Advances in Plasticizers, Dr. Mohammad Luqman (Ed.)*; 2012.

(13) Liew, K. Bin; Tan, Y. T. F.; Peh, K. K. Effect of Polymer, Plasticizer and Filler on Orally Disintegrating Film. *Drug Dev. Ind. Pharm.* **2014**, *40*, 110–119.

(14) Johnson, K.; Hathaway, R.; Leung, P.; Franz, R. Effect of Triacetin and Polyethylene Glycol 400 on Some Physical Properties of Hydroxypropyl Methylcellulose Free Films. *Int. J. Pharm.* **1991**, *73*, 197–208.

(15) Barhate, S. D.; Patel, M. M.; Sharma, A. S.; Nerkar, P.; Shankhpal, G. Formulation and Evaluation of Transdermal Drug Delivery System of Carvedilol. *J. Pharm. Res.* **2009**, *2*, 663–665.

Chapter 6

Concluding remarks

The work described in this dissertation contains the development of a computational platform for the general treatment of dissolution profiles, including strategies for addressing specific situations, followed by the development of oral films, comprising the respective evaluation and *in vitro* analysis.

In the computational section, programming in R language was used and explored resorting to RStudio®. Several scripts were developed to respond to the needs and difficulties in the study of dissolution profiles. Firstly, an integrated program was developed for the study of independent approaches following the EMA guideline in the calculation of fit factors (f_1 and f_2), MDT and for data visualization. A schematic representation of the operation mode of the script was proposed. The adequate interactivity between the user and the developed program, the automation and optimization of the analyses were ensured, facilitating the interpretation of the procedures and results. The presentation and the appearance of the output was one of the main goals in the course of this work. In the developed scripts the output is presented in a simple manner, in which all parameters and results are duly described.

For the calculation of the Mahalanobis Distance, a complete script was also developed for defining the confidence interval that will allow inferring on the similarity between the profiles under study.

The interpretation of the derivative value was focused on the detection of regime changes in the release of drugs. This analysis allows identifying significant changes in the amount of drug released, including the detection of burst release, lag time, or in which conditions an asymptotic value is defined.

The addition of the normalization parameter (c_2) to set up an asymptotic amount release, in the first order and in Weibull models, resulted in an improvement of the fit quality. This was demonstrated by a decrease in the sum values of the squares for the model containing this parameter. A script to check the presence of lag time was also developed, with adaption of the selected fit model. This program calculates the lag time value through simple linear interpolation, but an alternative is also proposed for cases in

which the first approach is not valid. Higuchi and Korsmeyer-Peppas models have also been explored for addressing the profile, up to 60% of the total released drug.

In the case wherein a regime change in the release is denoted, thus resulting in two or more dissolution patterns, models considering the fitting tailored to each situation were explored.

The adjusted coefficient of determination and the Akaike information criterion demonstrated to be an important tool for comparing models with a different number of parameters, and have been introduced in the general script. In general, Weibull is the model that better fits the experimental points in a dissolution curve.

In the experimental counterpart of this dissertation, lipid nanoparticles co-loaded with olanzapine and simvastatin conformed to desirable values concerning polydispersity index, particle size and zeta potential. They have also shown an adequate entrapment efficiency and drug loading, which validates the selection of lipids employed for co-encapsulation, meeting suitable critical quality attributes for oral administration.

The use of hydrogels, obtained from different HPMC grades, revealed interesting properties to produce the oral films, and the blending of the hydrogel with LLN resulted in a homogenous formulation. The impact of plasticizer on oral films was also studied, with the incorporation of PEG 400 in the hydrogel.

In general, all films revealed adhesive properties, which is beneficial to further promote a closer interaction with the intestinal epithelium, and favor drugs absorption.

According to the *in vitro* dissolution tests, different degrees of interaction between the drugs and the HPMC polymer were observed. In the simulated saliva test, within 30 minutes no more than 10% of each drug was released. In the test with the simulated conditions of human gastrointestinal tract, each drug presented different release behaviors in the presence of HPMC. For the release of olanzapine, there is no relevant effect from the HPMC grade, in which only at the 1 hour point of the assay some differences can be observed. The presence of HPMC delays the release of simvastatin in the acid medium (pH = 1.2). In these dissolution profiles, the HPMC grade with lower molecular weight releases a larger amount of SV than the polymer with higher molecular weight, presenting a lower control in drug release. The results were consistent with the addition of plasticizer, accompanied by an improvement of the quality in final oral films. The plasticizer improved the final aspect of the oral films, increasing their flexibility and adhesive properties, and the extent of drug release.

Thus, from a technological point of view, the more promising film is the one produced with lower molecular weight polymer, and plasticizer.

The computational approach demonstrates to be an important tool to characterize the dissolution profiles obtained with the oral films, easily producing coherent results for the analysis and rationalization of the systems under study.

Appendices

Appendix I

R programming

R is a versatile and powerful open-source programming language for statistical computing and data visualization. R is free (*freeware*) and involves is a large community of programmers responsible for developing numerous packages, and users that provide help in various formats. The increasing number of packages and libraries directed to specific areas and tasks is also a very attractive feature.

RStudio® is free and open-source integrated development environment (IDE) for R. A command line based environment is available for typing the commands rather of using the mouse and the menus. R commands can be stored in a single file as a script. The latter usually have names with the extension ".R" (e.g. *fitfactors.R*). The lines of code written in the script can be processed line-by-line or by selecting part of code using *Ctrl + ENTER* or *CTRL+SHIFT + S* for running the whole script.

Script development

Some important commands for script development will be presented.

The beginning

Command `rm(list = ls())` removes all objects stored in the current workspace, i.e., cleans R memory.

Before starting a program it is important to create a folder to be used as the working directory, from which R will import datasets and in which it will save the resulting data files or graphics. Command `> setwd("working directory")` allows accessing the working directory.

Some basic R commands

There are several types of objects in R, including vectors, matrices, dataframes, lists, functions, among others. These are used to generate and store information provided by the user for further manipulation. In the following example an object consisting of

several numeric elements is generated as a vector. In this case, the dataset time is defined with the values 0, 0.25, 0.5, 1, 2, 3, 4, 6, 8.

```
> time <- c(0, 0.25, 0.5, 1, 2, 3, 4, 6, 8)
```

The operator <- command is used to assign the numeric elements to an object (in this case time). The c() function is used for concatenate the numeric elements into a vector. For instance, the third element of vector time can be accessed using

```
> time [3]
```

in this case, the value in position 3 is 0.5.

To analyse and manipulate larger datasets, the latter cab be imported from the input files with different formats. In this work the data corresponding to the dissolution profiles are stored in .csv files and can be imported using

```
> dissolution <- read.csv ("name of file.csv")
```

this .csv file must be included in the working directory to be directly imported.

The data can be easily manipulated. It is possible to sort the data in each row or column-by-column, as well as to calculate statistical parameters. Some R commands allows selecting part of a data set or using the entire data set.

The which() function was widely used in the developed scripts. As the name implies, this command will ask, for which values are greater or less than a certain value, and gives the TRUE indices in the corresponding object. This is an important command specifically to follow the EMA bioequivalence guideline, in which no more than an average dissolution value of more than 85% may be used for the formulations, in the fit factors calculation,

```
> max85 <- min(c(which(dissolution [,2]>=85))
```

this command indicates in which position of column 2 ([,2]) of the dissolution data is the first value greater than 85, i.e., it is the first position of the minimum (min).

For datasets with multiple columns, corresponding to several dissolution essays, it is necessary to calculate the same function simultaneously for all columns, using

```
> for(i in 1:n) {commands}
```

this means that for each value of i that is comprised between 1 and n, commands will be calculated. In the first round i will be equal to 1, in the second i = 2, and so on, until i = n. To save the calculated results of a for loop it is necessary to create an empty object (vector()) to store the calculated values.

```
> max85<-vector()
```

The for loop can be used to do the same calculation with the which() function for all columns in the dataset (ncol(dissolution)).

```
> for(i in 1:ncol(dissolution)) {
> max85[i]<- min(c(which(dissolution [,i]>=85))
> }
```

There are situations that require performing a particular function or give information to the user only if some condition is met. R provides the if() function, followed by else, if the first condition is invalid (FALSE). The basic structure of if() is as follows

```
> if(condition){commands}
```

within the brackets exists a logical condition that will produce a TRUE or FALSE and the command inside the curly braces is executed if the previous condition is TRUE.

```
> if (max85[1] == max85[2]) {
> print("Length of vectors is equal")
> } else {print("Length of vectors is different")
> }
```

in the latter case, if the values are equal, i.e., if the condition = TRUE the first command is performed. If the condition = FALSE the command in else will be performed.

Plots

The most used plotting function in R is the function plot(x, y, ...). It is possible to add a tittle to a plot with the option main = "tittle". Similarly, xlab = " " and ylab = " " can be used to assign labels to the x-axis and y-axis, respectively. The plot type can be changed with the argument type = " ", to represent the plot with lines ("l"), circular points ("p") or both ("o"). The default colour is black, but it can be modified using col argument. To draw a new sequence of points in the plot at the specified coordinates, the generic function points(x, y,...) can be used in the same way as the plot() function. The legend() function can be used to add legends to plots. It is possible to choose the position, size and font of the text, insert lines, circular points, or boxes in the legend with the respective colours.

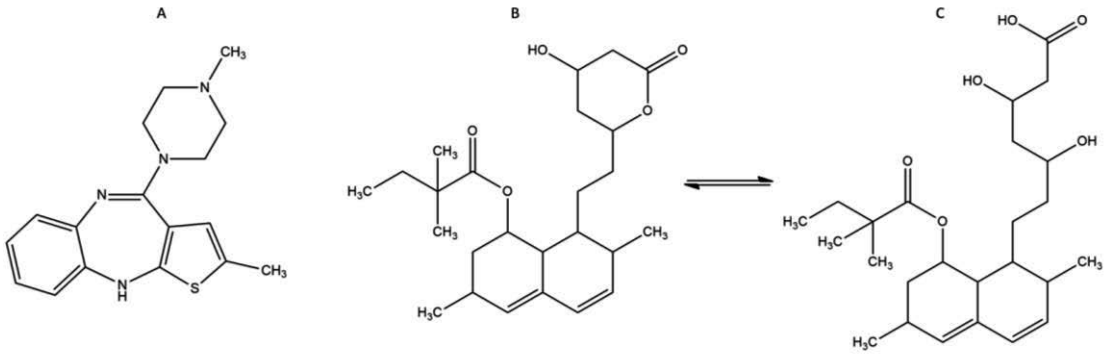

Figure 3.3 – Chemical structures of (A) olanzapine, (B) simvastatin and the prodrug (C) simvastatin in the respective acid form (β-hydroxy acid).

Table 3.4 – Physicochemical and pharmacokinetic properties of olanzapine and simvastatin. Values are obtained from the DrugBank database (available from *www.drugbank.ca*).

Drug	Olanzapine	Simvastatin
Molecular weight (g/mol)	312.43	418.57
Log P	2.8	4.7
Aqueous solubility (µg/mL)	3 – 5	30
Melting point (°C)	195	135 – 138
Daily oral dose (mg/day)	5 – 10	10 – 40
Half-life (h)	33	2
Bioavailability (%)	60	5

3.4. References

(1) Beija, M.; Salvayre, R.; Lauth-de Viguerie, N.; Marty, J.-D. Colloidal Systems for Drug Delivery: From Design to Therapy. *Trends Biotechnol.* **2012**, *30*, 485–496.

(2) Müller, R. H.; Mäder, K.; Gohla, S. Solid Lipid Nanoparticles (SLN) for Controlled Drug Delivery - A Review of the State of the Art. *Eur. J. Pharm. Biopharm.* **2000**, *50*, 161–177.

(3) Muchow, M.; Maincent, P.; Müller, R. H. Lipid Nanoparticles with a Solid Matrix (SLN®, NLC®, LDC®) for Oral Drug Delivery. *Drug Dev. Ind. Pharm.* **2008**, *34*, 1394–1405.

(4) Uner, M. Preparation, Characterization and Physico-Chemical Properties of Solid Lipid Nanoparticles (SLN) and Nanostructured Lipid Carriers (NLC): Their Benefits as Colloidal Drug Carrier Systems. *Pharmazie* **2006**, *61*, 375–386.

(5) Mukherjee, S.; Ray, S.; Thakur, R. S. Solid Lipid Nanoparticles: A Modern Formulation Approach in Drug Delivery System. *Indian J. Pharm. Sci.* **2009**, *71*, 349–358.

Appendix II

To fit a dataset, mathematical optimization techniques such as linear models, or nonlinear models through the least squares method are used. It is intended to minimize the sum of the squares of the differences between the estimated values and the original points (residuals). The smaller the residuals the better is the fit model.

It is necessary to consider for a simple linear regression a response variable (y) and the predictor variable (x), considering the formula

$$y = \alpha + \beta x_i + u_i$$

where α is a constant independent of x, β is the dependent parameter of x and u represents the error associated with the model.

By the least squares method, it is possible to estimate the values for α and β and thus estimate the model that best fit the data set. This method minimizes the sum of the squares of the residuals minimizing the difference in the final estimate, i.e., minimizes $\sum_{i=1}^{n} u_i^2$.

For multiple regression, each parameter has a different weight relative to y. The calculation function is similar to the linear regression

$$y = \alpha + \beta_1 x_i + \cdots + \beta_n x_i + u_i$$

To estimate the coefficients, the same method used in simple linear regression is adopted. For the least squares approach it is intended to minimize

$$\sum_{i=1}^{n} (y - \alpha - \beta_1 x_i + \cdots + \beta_n x_i)^2$$

Thus, the sum of squares can be minimized by

$$\beta = (x'x)^{-1}x'y$$

Fitting mathematical models in R

R provides some useful functions to calculate the parameters of each mathematical model, allowing to analyse and conclude on which model describes better the dissolution profile under study.

For the study of linear equations it is sufficient to write lm(formula), for linear model, and insert between the brackets the object formula. This is a simple type of linear regression that uses an independent variable to predict the outcome of a dependent

variable. The formula argument follows a specific format. In this case of linear regression dissolution[, 2] is the dependent variable and time is the independent variable.

For the example of a zero-order dissolution profile (zo), has simply to issue

```
> zo <- lm(dissolution[,2] ~ time)
```

To see the result of the linear regression simply type zo or write summary(zo). summary() is a function used to summarize the results of various functions. To directly obtain the slope of the curve (slope)

```
> slope<-summary(zo)$coefficients[2]
```

From the summary() function, further information can be obtained, including t-test, F-test, R-squared, residual, and significance values.

When the points are not arranged in a practically linear form, the linear regression adjustment becomes useless. When the points are widely scattered, the points are adjusted with a nonlinear function. The nonlinear function that better fit a dissolution model is generally the Weibull model, as illustrated before.

In nonlinear regression it is necessary to specify a function with a set of parameters to fit the data and give the program a set of initial values to estimate these final parameters. The simplest way to estimate these parameters is to use the nls() function, a nonlinear least squares approach. There are several algorithms for solving least squares. The default of the nls() function is the Gauss-Newton algorithm. This algorithm will look for minima of the function and interactively finds the minimum sum of the squares. To fit the Weibull model (we) in R, Equation (1.23) will be applied to the formula into the nls()

```
> we <- nls(dissolution[,2] ~ A*(1-exp(-(time/B)^C)), start = list(A=100, B=100, C=1))
```

For solving the function, the user must give initial values to the parameters. These initial parameters must be within the context of the approximation, otherwise, the function cannot reach the final value of the parameter. An alternative is to apply the logarithm to the functions, in order to predict some parameters. In other cases it is possible to increase the number of interactions of the model for increasing the convergence.

However, as mentioned earlier, R has a large community of users who, among other advantages, disseminate their work and make R packages available to other users. A package of great interest in the course of this work is minpack.lm. To install the package and put it in R's memory

```
> install.packages("minpack.lm")
```

```
> require("minpack.lm")
```

This package applies the Levenberg-Marquardt algorithm which is also useful for solving nonlinear least-squares problems. This method looks for the local minimum of the function instead of the global minimum and, in this way, converges more quickly.

Thus, if the nls() function does not converge there is an alternative, the nlsLM() function,

```
> we_pack <- nlsLM(dissolution[,2] ~ A*(1-exp(-(time/B)^C)), start = list(A=100, B=100, C=1))
```